

#6005

J.F.

24-1391

**LABORATORY DRAINAGE QUALITY FROM
MAFIC-INTRUSIVE, TUFFACEOUS-SEDIMENTARY,
AND WEATHERED WASTE ROCKS**

Final Report on Contract JSP012002
to the
U. S. Bureau of Land Management
Salt Lake City Office

30 June 2002

Kim A. Lapakko
David A. Antonson
Andrea Johnson
John Folman

Minnesota Department of Natural Resources
Division of Lands and Minerals
500 Lafayette Road
St. Paul, MN 55155-4045

#6005

**LABORATORY DRAINAGE QUALITY FROM
MAFIC-INTRUSIVE, TUFFACEOUS-SEDIMENTARY,
AND WEATHERED WASTE ROCKS**

Final Report on Contract JSP012002
to the
U. S. Bureau of Land Management
Salt Lake City Office

30 June 2002

Kim A. Lapakko
David A. Antonson
Andrea Johnson
John Folman

Minnesota Department of Natural Resources
Division of Lands and Minerals
500 Lafayette Road
St. Paul, MN 55155-4045

Table of Contents

List of Tables	i
List of Figures	i
List of Appendices	ii
Executive Summary	iii
1. Introduction	1
2. Objectives	3
3. Background on Mine Waste Dissolution	4
3.1. Mine Waste Dissolution	4
3.1.1. Acid Generation	4
3.1.2. Acid Neutralization	6
3.1.3. Trace Metal Release by Trace Metal Sulfide Oxidation	6
3.1.4. Key Solid-Phase Factors Controlling Mineral Oxidation and Dissolution	7
3.2. Previous Work	8
4. Methods	9
4.1. Materials	9
4.1.1. Mafic-Intrusive and Tuffaceous-Sedimentary Samples	9
4.1.2. Low NP Tuffaceous-Sedimentary Samples	10
4.1.3. USGS AML Weathered Waste Rock Sample	11
4.2. Dissolution Test Methods	12
4.2.1. ASTM Method D5744-96	12
4.2.2. MN DNR Method	12
4.2.3. ASTM and MN DNR Method Modifications	13
4.3. Analyses	13
4.3.1. Solid-Phase Analyses	13
4.3.2. Aqueous-Phase Analyses	14
4.4. Calculations	15
4.4.1. Potentials for Acid Production and Neutralization	15
4.4.2. Estimation of Minimum Mineral Availability for Reaction	16
4.4.3. Chemical Mass Release and Release Rates	16
5. Results	17
5.1. Introduction	17
5.2. Mafic-Intrusive Samples	18
5.2.1. Solid-Phase Analyses	18
5.2.2. Drainage Quality Results for the MN DNR Method	19
5.2.3. Extent of Sample Dissolution	21
5.3. Tuffaceous-Sedimentary Samples	21
5.3.1. Three Initial Samples	21
5.3.1.1. Solid-Phase Analyses	21
5.3.1.2. Drainage Quality Results for the MN DNR Method	22
5.3.1.3. Extent of Sample Dissolution	23
5.3.2. Six Low NP Tuffaceous-Sedimentary Samples	24

5.3.2.1.	Introduction	24
5.3.2.2.	Results	24
5.3.2.2.1.	Solid-phase Analyses	24
5.3.2.2.2.	Dissolution Test Results	25
5.4.	USGS AML Weathered Waste Rock Sample	27
5.4.1.	Solid-Phase Analyses	27
5.4.2.	Drainage Quality Results for the MN DNR Method	28
5.4.3.	Extent of Sample Dissolution	29
5.5.	Assessment of Dissolution Test Methods	29
5.5.1	Comparison of MN DNR and ASTM Methods	30
5.5.2.	Replication of MN DNR Method	31
6.	Summary	32
7.	Acknowledgments	34
8.	References	35

List of Tables

1.	AP and NP of mafic-intrusive and tuffaceous-sedimentary samples collected in 2000	41
2.	Particle size distribution of rock samples	42
3.	Whole rock chemistry of rock samples	44
4.	Trace metal analysis of rock samples	46
5.	Mineralogical composition of rock samples	50
6.	Sulfide and carbonate mineral liberation	52
7.	Estimation of minimum available AP (S^{2-}) and NP $[(Ca+Mg)CO_3]$	53
8.	Drainage quality summary	54
9.	Sulfate, calcium, and magnesium release rates	56
10.	Initial and final AP and NP $[(Ca+Mg)CO_3]$ of rock samples	57
11.	Estimated additional dissolution time to deplete carbonate minerals	59
12.	Summary of drainage from low NP tuffaceous-sedimentary samples at week 20	60
13.	Comparison of rates for MN DNR and ASTM D5744-96 method	61
14.	Comparison of ASTM and MN DNR method water retention	62

List of Figures

1.	Schematic of humidity cell for ASTM and MN DNR method	63
2.	MN DNR method drainage quality from 6.20% sulfide mafic-intrusive rock	64
3.	MN DNR method drainage quality from 6.45% sulfide mafic-intrusive rock	65
4.	MN DNR method drainage quality from 6.90% sulfide mafic-intrusive rock	66
5.	MN DNR method drainage quality from 6.90% sulfide mafic-intrusive rock	67
6.	ASTM method drainage quality from 6.90% sulfide mafic-intrusive rock	68
7.	MN DNR method drainage quality from 7.29% sulfide mafic-intrusive rock	69
8.	MN DNR method drainage quality from 7.39% sulfide mafic-intrusive rock	70
9.	MN DNR method drainage quality from 8.05% sulfide mafic-intrusive rock	71
10.	MN DNR method drainage quality from 8.55% sulfide mafic-intrusive rock	72
11.	MN DNR method drainage quality from 1.30% sulfide tuffaceous-sedimentary rock	73
12.	MN DNR method drainage quality from 1.36% sulfide tuffaceous-sedimentary rock	74
13.	MN DNR method drainage quality from 3.75% sulfide tuffaceous-sedimentary rock	75
14.	MN DNR method drainage quality from 3.75% sulfide tuffaceous-sedimentary rock	76
15.	ASTM method drainage quality from 3.75% sulfide tuffaceous-sedimentary rock	77
16.	SEM photomicrograph of 1.30% S_T low NP tuffaceous-sedimentary leached sample	78
17.	MN DNR method drainage quality from 12.99% sulfide USGS rock	79
18.	ASTM method drainage quality from 12.99% sulfide USGS rock	80
19.	Sulfate release rate vs. solid-phase percent sulfur	81

List of Appendices

1. Solids composition
2. Laboratory methods (temperature, humidity, air flow, water retention)
3. Drainage quality tables
4. Cumulative mass release tables
5. Calculation of rates of sulfate, calcium, and magnesium release
6. Quality assurance
7. Solids composition, laboratory methods, drainage quality, cumulative mass release, and release rates for low neutralization potential tuffaceous-sedimentary samples

EXECUTIVE SUMMARY

Generation of acidic drainage is the primary water quality concern associated with mine wastes, and release of heavy metals with neutral drainage is a secondary concern. Whereas drainage from some mine wastes is highly acidic with toxic concentrations of trace metals, other drainages are environmentally innocuous. In order to tailor mine waste management plans to the potential for adverse impacts on natural waters, the quality of drainage must be known. Prediction of mine waste drainage quality is necessary to develop mine waste management plans for proposed mines, for which no empirical data exist. This prediction may also be necessary for abandoned mine wastes, because the present drainage quality may not reflect the potential for long-term impacts.

Mine waste drainage quality is a function of mine waste composition, among other factors. Effects of compositional variations can best be assessed by conducting dissolution tests on a variety of well-characterized samples from a specific rock type (lithology). Based on the relationship between mine waste composition and drainage quality determined, environmentally sound mine waste management plans can be developed for the individual lithologies encountered in mineral resource development.

Mine wastes containing iron sulfides and moderate amounts of calcium and magnesium carbonates will generate neutral drainage as long as the calcium and magnesium carbonates are present and dissolving at a rate which exceeds that of acid production. If the dissolution rate for these carbonates decreases below that of acid production or the available carbonates are depleted or rendered unreactive, drainage will acidify if reactive iron sulfides remain. The time required for depletion may be quite long, in particular from the perspective of gathering accurate information for permitting a mine. Consequently, mine waste management and permitting decisions may be based on the erroneous assumption that the neutral drainage observed in short-term dissolution tests simulates that which will be generated in the field over a longer time period.

In the present study, seven mafic-intrusive and three tuffaceous-sedimentary waste rock samples were obtained from an open-pit metal mine, and one weathered waste rock sample was collected from an abandoned mine site in a carbonate-hosted deposit containing base metal sulfides (referred to as the US Geological Survey Abandoned Mine Land (USGS AML) sample). The mafic-intrusive and tuffaceous-sedimentary samples, all of which contained pyrite, were selected due to their relatively high content of calcium and magnesium carbonate minerals. The samples were characterized for particle size, chemistry, and mineralogy and subjected to dissolution testing.

The acid production potential of the samples was determined based on their sulfide content ($AP(S^{2-})$) and their acid neutralization potential based on the sum of their calcium carbonate and magnesium carbonate contents ($NP[(Ca+Mg)CO_3]$). The net NP (net NP = $NP[(Ca+Mg)CO_3] - AP(S^{2-})$) of all but one of the samples was less than zero, indicating an excess of acid producing potential. The respective net NP ranges for the mafic-intrusive and tuffaceous-sedimentary rocks were -216 to -79 and -38 to 22 g $CaCO_3$ equivalent $(kg\ rock)^{-1}$, and the net NP for the USGS AML sample was -280 g $CaCO_3$ equivalent $(kg\ rock)^{-1}$.

Although the AP(S²⁻) of the samples exceeded their NP[(Ca+Mg)CO₃], none of the samples produced acidic drainage during the 168 (mafic-intrusive, tuffaceous-sedimentary) or 158 weeks (USGS AML) of dissolution testing. Several cells were terminated after 102 weeks, leaving five mafic-intrusive, one tuffaceous-sedimentary, and the USGS AML samples in operation. The typical pH of drainage from the mafic-intrusive and tuffaceous-sedimentary rocks ranged from 7.8 to 8.2, while that from the USGS AML sample ranged from 7.9 to 8.2. Whereas the AP(S²⁻) of the samples exceeded the NP[(Ca+Mg)CO₃], drainage did not acidify because 52 to 86 percent of the (NP[(Ca+Mg)CO₃]) remained at the end of the period of record. (This does not consider terminated samples.)

If dissolution testing continued it is possible, if not likely, that the available calcium and magnesium carbonates would be depleted or rendered unreactive while reactive iron sulfides remained, at which time the drainage would acidify. If half of the initial NP[(Ca+Mg)CO₃] were available for reaction, an additional one to thirteen years of laboratory dissolution would be required prior to generation of acidic drainage. Thus, although it appears that drainages from most of these samples will acidify, this can not be concluded with certainty based on the data generated to date.

It should be noted that if management decisions for proposed or abandoned mine wastes were based on the existing drainage pH data (which is well within limits often required for discharges), potentially acid-producing mine waste could be erroneously classified. Inadequate reclamation of wastes from new mines could easily lead to adverse impacts on water quality. Similarly, the abandoned mine waste sample did not produce acidic drainage during the dissolution test, and it is likely that the drainage from this rock in the field was neutral for 75 to 100 years. Based on its field behavior alone, rigorous remediation measures would probably not be prescribed. However, its net NP was -280 g CaCO₃ equivalent (kg rock)⁻¹, suggesting that the rock had a high potential to produce acidic drainage for decades. Thus, in the absence of characterization and long-term predictive testing, a mine waste which could adversely impact drainage quality might be left unremediated, while financial resources were expended toward reclaiming less reactive mine wastes.

Testing of a new set of tuffaceous-sedimentary samples with NP[(Ca+Mg)CO₃] values ranging from 5.1 to 19 g CaCO₃ equivalent (kg rock)⁻¹ indicated that 0 to 31% of the NP[(Ca+Mg)CO₃] dissolved to maintain drainage pH of at least 6.0. SEM examination of a rock sample collected after dissolution tests were terminated indicated that some of the unavailable ferroan dolomite was largely included within rock particles. Portions exposed to drainage dissolved over the course of 40 weeks of testing, and it appeared this dissolution extended along the dolomite into the interior of the rock particle over time. It suggests that the dissolution of the ferroan dolomite slowed over time, as a result of decreased accessibility of acid to the carbonate mineral.

The original set of tuffaceous-sedimentary samples produced acid roughly 7 to 40 times slower than the new samples. Consequently, assuming similar modes of ferroan dolomite occurrence, availability of the ferroan dolomite in the original samples to maintain pH of at least 6.0 would be expected to exceed that observed for the new samples. The finer particle size of the original samples would also tend to increase this availability.

Elevated concentrations of some metals were observed in drainages from all samples. Initial drainages from the mafic-intrusive and tuffaceous-sedimentary samples contained elevated concentrations of manganese, antimony, arsenic and zinc; typical ranges of these solutes were 1-10, 0.02-0.06, 0.004-0.01, and 0.02-0.08 mg/L, respectively. The mafic-intrusive rock tended to produce higher concentrations of manganese, antimony and arsenic, while zinc concentrations from the two rock types were similar. Concentrations of these elements decreased over time. After 152 weeks manganese concentrations typically ranged from <0.002 to 0.08 mg/L, with a value of 0.26 mg/L observed for one mafic-intrusive sample. (Solid-phase manganese concentrations typically ranged from 0.05 to 0.15% MnO.) Antimony, arsenic and zinc concentrations typically decreased below detection limits after about 36 weeks. The approximate range of arsenic concentrations in the solids was 200 to 2000 parts per million (ppm), with concentrations in the mafic-intrusive rocks roughly four to eight times those in the tuffaceous-sedimentary rocks. Typical solid-phase concentrations of antimony and zinc were approximately 20 to 50 ppm and 20 to 70 ppm, respectively.

The USGS AML sample initially produced drainage with elevated concentrations of manganese (50 mg/L), zinc (~20 mg/L), antimony (~0.5 mg/L) and lead (~0.3 mg/L). Concentrations of all these elements decreased over time. Approximate concentrations after 152 weeks were 0.6, 0.05, 0.005 and 0.005 mg/L, respectively.

1. INTRODUCTION

Tailings and waste rock, as well as the mine itself, are components of metal mining operations which remain long after mining has ceased. These remnants may be, relatively speaking, chemically inert and therefore environmentally innocuous. On the other hand, mining wastes may adversely affect water quality long after mining has ceased. For example, acidic drainage was observed in 1977 at a Norwegian mine which had been abandoned in 1833 (Iversen and Johannessen 1987). Acidic drainage from mining areas has impacted thousand of miles of streams in the United States (U.S. Bureau of Mines 1985). Remediation of these problems can cost from tens to hundreds of millions of dollars (Biggs 1989).

As discussed by Lapakko (1990), governmental agencies have developed regulations to reduce the potential for problematic mine waste drainage and the associated financial liability. Plans for closure and post-closure care of mine wastes are an important aspect of these rules and must be submitted prior to mine development. This approach allows the costs of mine waste reclamation to be considered along with other mining costs in the assessment of mineral recovery economics.

In order to develop effective, efficient, and economical pre-development waste rock management plans, it is necessary to estimate the quality of drainage generated by the lithologies excavated in order to access the ore. Mitigation techniques can then be scaled to the estimated potential for adverse impact. Existing data on a waste rock of similar composition, generated by similar mining methods, and exposed to similar environmental conditions for an extended time provide the best indicator of drainage quality.

Since these data are rarely available, it is necessary to use other means of drainage quality prediction, such as compositional characterization and/or dissolution testing. Dissolution testing, however, can be expensive and may take several years to complete. In order to provide a less expensive and time consuming method of predicting waste rock drainage quality, the U.S. Bureau of Mines Salt Lake City Research Center (USBM) initiated a program to develop a mathematical model to predict the quality of drainage from discrete rock types (individual lithologies; White and Jeffers 1994; White et al. 1994; Lin 1996; Guard 1997; Lin et al. 1997). Such a tool will assist regulatory agencies, mining companies, and the public in assessing potential water quality impacts of waste rock drainage.

Whereas literature values can provide dissolution rates for modeling individual, isolated minerals present in a given lithology, empirical data are needed to provide rates describing their dissolution within the specific rock matrix. Distinct to each lithology are the grain size, surface morphology, and extent of liberation of the individual minerals. Within each lithology the interaction with other minerals and their dissolution products will also be unique. Thus, dissolution testing on individual lithologies is a necessary step in developing the mathematical model for predicting the quality of drainage from individual lithologies. This dissolution testing will also provide, on a primary level, empirical data on drainage quality and dissolution rates for the lithologies tested.

As the number of lithologies subjected to dissolution testing increases, the integrity of the mathematical modeling output will increase, as will the catalog of empirical data available to assist prediction of drainage quality from similar lithologies. The Duluth Complex is one lithology which

has been subjected to several dissolution studies in both laboratory and field (Lapakko 1988, 1994; Lapakko and Antonson 1994). In this rock type virtually all of the sulfur minerals occur as sulfides.

The present study examines the solid-phase characterization and dissolution of 17 waste rock samples: seven mafic-intrusive samples, three tuffaceous-sedimentary samples, six low neutralization potential tuffaceous-sedimentary samples and one waste rock sample which had been weathered in the environment for 75 to 100 years. All samples tested were subjected to accelerated weathering using the Minnesota Department of Natural Resources (MN DNR) method (Lapakko and White 2000), which is a modification of ASTM D5744-96 (ASTM 2000). In addition, one sample from each of the three rock types was also subjected to the ASTM method. Previous reports presented earlier stages of results on these three rock types (Lapakko 1998c, 1999c; Lapakko and Antonson 2000a).

2. OBJECTIVES

The original objectives of the project are as follows.

1. Describe the temporal variation of drainage quality, particularly pH, for the mafic-intrusive, tuffaceous-sedimentary, and weathered waste rock lithologies.
2. Determine the rates of sulfate, calcium, and magnesium release from the eleven samples.
3. Relate the drainage pH and rates of release to the solid-phase composition of the eleven samples.
4. Estimate the dissolution time required for acidification of drainages from the aforementioned rock samples.

Based on the initial 72 weeks of drainage, Lapakko and Antonson (2000a) estimated that 300 to 1500 weeks of additional dissolution were required to deplete all calcium and magnesium carbonate minerals present. It is possible, if not likely, that less than 100% of these minerals are available to dissolve and maintain drainage pH above 6.0.

To gain more timely insight on the calcium and magnesium carbonate availability and better estimate the additional dissolution time required for drainage acidification, six additional samples were collected, characterized (particle size distribution, chemistry) and subjected to dissolution testing. The objectives of this experiment were as follows.

1. Determine the availability of calcium and magnesium carbonate minerals to dissolve and maintain drainage pH above 6.0.
2. Determine the ability of non-carbonate host rock minerals to neutralize acid generated by pyrite in the samples.

Two objectives of a separate phase of the cooperative BLM/MN DNR study are assessment of the intralaboratory replication of ASTM method D 5744-96 and a modification of this method (MN DNR method). These two objectives are discussed only briefly in the present report and are presented in more detail elsewhere (Lapakko et al. 2002a).

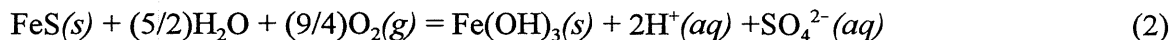
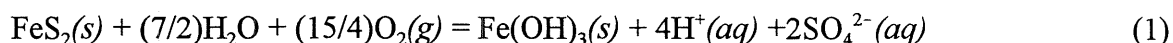
3. BACKGROUND

3.1. Mine Waste Dissolution

3.1.1. Acid Generation

Reactions involving acid production, acid neutralization, and trace metal release influence mine drainage quality. The following focuses on reactions which identify key solid phases. Detailed discussion of aqueous geochemistry fundamentals and geochemistry of acid mine drainage is presented by Nordstrom (1999), Nordstrom and Alpers (1999), Smith (1999) and Smith and Huyck (1999).

There are three general types of acid release from mine wastes: iron sulfide oxidation, dissolution of soluble iron sulfate minerals, and the dissolution of less soluble sulfate minerals of the alunite/jarosite series. The oxidation of iron sulfide minerals such as pyrite and pyrrhotite is responsible for the majority of mine-waste acid production (Stumm and Morgan 1981). Equations 1 and 2 are commonly published reactions representing pyrite and pyrrhotite oxidation by oxygen (after Stumm and Morgan 1981; Nelson 1978). These reactions depict the ultimate iron product as a ferric hydroxide precipitate, although the intermediate formation of aqueous ferric hydroxyl species (e.g. $\text{Fe}(\text{OH})_2(\text{aq})$, $\text{Fe}(\text{OH})_3(\text{aq})$) will also result in acid production.



The rate of oxidation and attendant acid production is dependent on solid-phase compositional variables. Oxidation rates vary among sulfide minerals, and it is often reported that reactivity decreases in the order marcasite > pyrrhotite > pyrite (e.g. Kwong and Ferguson 1990). However, different reactivity rankings have been reported by other authors and may be a function of reaction conditions (Jambor 1994, Plumlee 1999). For a given sulfide mineral, the oxidation rate increases with the reactive surface area available. It also varies with the crystal form of the mineral. For example, the oxidation of framboidal pyrite is reported to be much more rapid than that of euhedral pyrite.

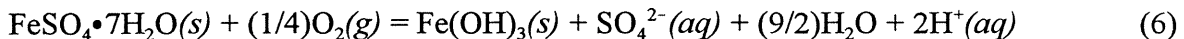
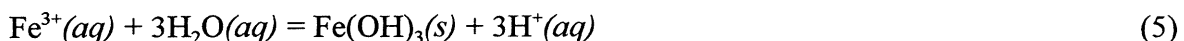
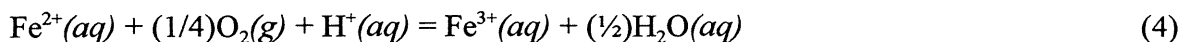
The rate of sulfide mineral oxidation also increases as pH decreases into a range conducive to bacterial mediation of ferrous iron oxidation. Nordstrom (1982) reported that as "pH decreases to 4.5, ferric iron becomes more soluble and begins to act as an oxidizing agent." As pH further decreases, bacterial oxidation of ferrous iron becomes the rate limiting step in the oxidation of pyrite by ferric iron (Singer and Stumm 1970), which is the only significant oxidizing agent in this pH range (Nordstrom 1982; Singer and Stumm 1970; Kleinmann et al. 1981). Lapakko and Antonson (1994) reported that oxidation of pyrrhotite in the pH range of 3.5 to 4.05 was roughly six to seven times that in the range of 5.35 to 6.1, and attributed the higher rate to bacterial oxidation. Data presented by Nordstrom and Alpers (1999) suggest that the bacterially mediated rate of pyrite oxidation by

ferric iron is roughly two to three orders of magnitude faster than the abiotic oxidation by oxygen at pH 2.

These weathering reactions produce acidic, iron- and sulfate-rich aqueous water which can 1) contact sulfide minerals and accelerate their oxidation, 2) evaporate partially or totally to precipitate hydrated iron-sulfate and other minerals, and/or 3) contact host rock minerals which react to neutralize some or all of the acid. Acidic flow which is not neutralized within the mine waste will exit as acid rock drainage (ARD).

Hydrated iron-sulfate and trace-metal sulfate minerals precipitate during the evaporation of acidic, metal- and sulfate-rich water within mine waste materials and store (for potential subsequent release) acid and metals released by sulfide mineral oxidation. The more common hydrated iron-sulfate minerals that occur as efflorescent salts on the surfaces of weathering pyrite include melanterite, rozenite, szomolnokite, romerite and copiapite ($\text{FeSO}_4 \cdot 7\text{H}_2\text{O}$, $\text{FeSO}_4 \cdot 4\text{H}_2\text{O}$, $\text{FeSO}_4 \cdot \text{H}_2\text{O}$, $\text{Fe}^{2+}\text{Fe}_2^{3+}(\text{SO}_4)_4 \cdot 14\text{H}_2\text{O}$, and $\text{Fe}^{2+}\text{Fe}_4^{3+}(\text{SO}_4)_6(\text{OH})_2 \cdot 20\text{H}_2\text{O}$, respectively; Alpers et al., 1994). According to Nordstrom (1982) and Cravotta (1994), these efflorescent salts are highly soluble and provide an instantaneous source of acidic water upon dissolution and hydrolysis. They are partially responsible for increased acidity and metals loadings in the receiving environment during rainstorm events. Their cumulative storage and incremental release may help explain the lag from mine waste placement to AMD formation particularly in arid climates.

As an example, equations 3, 4 and 5 summarize the step-wise dissolution of melanterite. The net result of equations 3 through 5 is summarized in equation 6, which shows a net production of two moles of acid for each mole of melanterite dissolved. Cravotta (1994) showed that a similar aqueous dissolution of romerite produced six moles of acid for each mole of romerite dissolved.



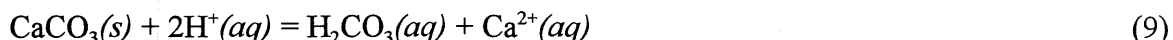
The alunite-jarosite mineral group consists of sulfate minerals which are less soluble than the efflorescent sulfate salts. According to Nordstrom (1982), the evaporative concentration of efflorescent iron sulfates leads to the precipitation of the more common iron minerals such as goethite and jarosite. Similar reaction of efflorescent aluminum sulfates will produce alunite. Alpers et al. 1994 reported that jarosite is slightly soluble and can, therefore, contribute acid according to equation 7. For example, preliminary leach studies on natural and synthetic jarosites conducted by the USBM showed a drop in pH from 6 in the deionized water leachant to 3 or 4 after contact with the jarosites. It should be noted, however, that these minerals are variable in both composition and reactivity. For

example, Alpers (2000) speculated that a pure jarosite or hydronium jarosite may buffer pH in the range of 1.5 to 3.



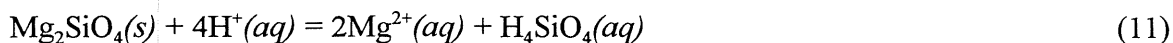
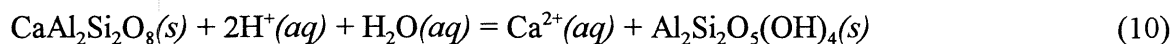
3.1.2. Acid Neutralization

The balance between the rates of acid production by iron-sulfide mineral oxidation and host rock mineral neutralization will determine the acidity of mine waste drainage. The most effective minerals for neutralizing acid are those containing calcium carbonate and magnesium carbonate, including calcite, magnesite, dolomite, and ankerite (CaCO_3 , MgCO_3 , $\text{CaMg}(\text{CO}_3)_2$, and $\text{CaFe}(\text{CO}_3)_2$, respectively). Equation 8 represents the dominant acid-neutralizing reaction of calcite (CaCO_3) above pH 6.4, while equation 9 is the dominant reaction below pH 6.4 (Drever, 1988):



Whereas calcite dissolves rapidly, rates of magnesium carbonate and calcium-magnesium carbonate (i.e. magnesite and dolomite) dissolution are substantially slower (Rauch and White 1977; Busenberg and Plummer 1986). Additionally, iron carbonates do not provide for net acid neutralization under oxidizing conditions, due to oxidation of the ferrous iron released, subsequent precipitation of ferric hydroxide, and the consequent acid production (reactions 4, 5).

Dissolution of silicates such as plagioclase-feldspar minerals (e.g. anorthite in equation 10, Busenberg and Clemency 1976) and olivine (e.g. forsterite in equation 11, Hem 1970) can also neutralize acid. However, their rates of dissolution and consequent acid neutralization are slow relative to the carbonate minerals (Nesbitt and Jambor 1998). Their effectiveness increases with increasing mineral content and decreasing grain size (Morin and Hutt 1994). Nonetheless, their dissolution can maintain neutral conditions only if the rate of acid production is quite slow (Lapakko et al. 1997).



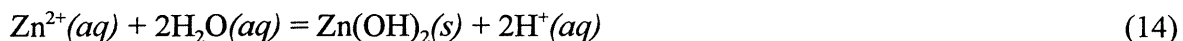
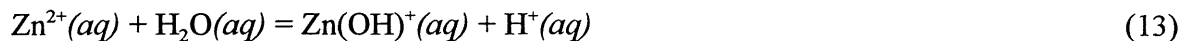
3.1.3. Trace Metal Release by Trace Metal Sulfide Oxidation

Trace metals are metals which occur at low average concentrations in the earth's crust but can be present at elevated levels in mineralized areas. Trace metals commonly occur as sulfide minerals, the oxidation of which releases the trace metal from the highly insoluble sulfide phase (e.g. reaction 12). Once released to solution, there are several types of reactions that can influence the migration and

fate of these minerals. Smith and Huyck (1999) present a series of diagrams for the generalized relative mobility of elements under different environmental conditions, for use as an initial estimate of metal behavior in surficial environments. At a regional scale, generalizations frequently can be used to estimate broad trends in metal mobility. However, as the scale becomes increasingly finer, estimating metal behavior generally becomes increasingly difficult (Smith and Huyck 1999).

In general, metals may remain in solution or be removed in secondary phases. For removal from solution, trace metals may precipitate as oxides, hydroxides, or carbonates; be adsorbed by surfaces such as iron oxyhydroxides (Smith 1999); or coprecipitate with other solid phases. In acidic solutions trace metal removal is limited, and elevated trace metal concentrations are often associated with these solutions. However, circumneutral drainages can also contain elevated concentrations of trace metals such as nickel, copper, cobalt (Lapakko 1993), zinc, manganese (Smith and Huyck 1999), molybdenum (Brown 1989), arsenic, and antimony (Lapakko 1991). Concentrations of molybdenum, arsenic, and antimony in particular can be elevated even as pH increases above 7.

Oxidation of arsenic and antimony sulfides can produce acid, as can oxidation of the iron sulfide fraction of mixed sulfide minerals such as chalcopyrite (Plumlee 1999). Other trace metal sulfide oxidation will produce acid if and only if the metal released hydrolyzes (reaction 13) or precipitates as a hydroxide, oxide, or carbonate (reaction 14). For most trace metals this will occur only at pH levels above 6, and as pH decreases below this level the secondary phases will dissolve. Consequently, they do not generally contribute to acid production observed at lower pH levels.



3.1.4. Key Solid-Phase Factors Controlling Mineral Oxidation and Dissolution

Whereas the acid-producing and acid-neutralizing mineral contents, and the balance of these contents, influences mine waste drainage quality, there are several subtle mineralogical factors which are also influential. Individual minerals may be entirely liberated from the rock matrix, occur interstitial to other minerals (partially liberated), or as inclusions within other minerals. The extent of liberation affects availability for reaction. For example, acid-producing or acid-neutralizing minerals included within minerals such as quartz will be essentially unavailable for reaction.

Oxidation of sulfide minerals and dissolution of carbonate minerals are surface reactions and, therefore, the rates of these reactions are dependent on the reactive surface area. Reactivity decreases as mineral surfaces are covered with coating, such as iron oxyhydroxides, while the concentration of lattice defects tends to increase reactivity. Mineral surface area is dependent on the extent to which

the mineral is liberated from the rock matrix, mineral grain size, and the “roughness” of the mineral surface.

3.2. Previous Work

The dissolution of mafic-intrusive, tuffaceous-sedimentary, and abandoned mine land waste rocks was reported by Lapakko (1998c, 1999c). The present report is part of a larger project which examined the dissolution of siltite-argillite rocks (Lapakko 1998a, 1999a), Archean greenstone rocks (Lapakko et al. 2002b), and a single sample of Duluth Complex gabbro in multiple tests (Lapakko 1998b, 1999b; Lapakko and Antonson 2000b; Lapakko et al. 2002a). The project also assessed two dissolution test methods (Lapakko 1998b, 1999b; Lapakko and Antonson 2000b; Lapakko and White 2000; White and Lapakko 2000; Lapakko et al. 2002a). The results of these phases of the project are not discussed in the present report.

4. METHODS

4.1. Materials

The current study originated with eleven waste rock samples that were characterized and subjected to dissolution testing for 102 to 168 weeks. Ten of the samples, seven mafic-intrusive and three tuffaceous-sedimentary rocks, were segregated from a “sulfide-carbonate mixed waste” bulk sample from an open-pit metal mine. The eleventh sample is a carbonate-hosted, base-metal-sulfide bearing waste rock from a 75 to 100-year old abandoned metal mine waste rock dump, and was provided by the United States Geological Survey (USGS, Smith 1998). This sample will be referred to as the USGS abandoned mine land (USGS AML) sample. Six additional tuffaceous-sedimentary samples with low neutralization potentials were collected and subjected to dissolution testing for 20 (five samples) or 40 weeks (one sample).

4.1.1. Mafic-Intrusive and Tuffaceous-Sedimentary Samples

The seven mafic-intrusive and three tuffaceous-sedimentary samples were segregated from a run-of-mine (ROM) bulk sample of “sulfide-carbonate mixed waste.” The sample was collected from the face of a 20-foot-high mine bench where the mixed waste was exposed. To facilitate collection of a bulk sample that would meet the desired range of sulfide-sulfur and carbonate-carbon content for the study, four grab samples were collected from the “sulfide-carbonate mixed waste” and blended into a composite sample for preliminary chemical characterization. Chemical analyses of the blended grab samples showed that the mixed waste exhibited the following percentage ranges: $1.59 \leq C_{\text{tot}} \leq 1.89$, $6.24 \leq \text{CO}_3 \leq 7.00$, and $4.77 \leq \text{S}^{2-} \leq 5.61$. Based on these values, an area of mixed waste exposed in the bench face was delineated, and the bulk sample was collected. The final bulk sample was placed into two 55-gallon drums and shipped to the mine metallurgical laboratory for sizing, crushing, splitting, and preliminary mineral characterization.

The bulk sample was passed through a 1.5-inch screen to obtain two fractions. The minus 1.5-inch fraction was returned to the 55-gallon drums and sent to the USGS to become a standard reference material. The plus 1.5-inch fraction was washed to clean the sample surfaces of very-fine mine waste material that had accumulated during excavation and had obscured surface mineralogy and texture. An unintended consequence of this rinsing was removal of oxidation products which had accumulated on the rock surfaces.

The plus 1.5-inch fraction was visually sorted into piles of similar rock types. Guidance for the visual sorting was based on the fact that the mixed waste bulk sample was initially classified in the field to be approximately 50% gray, sulfidic, fine-grained, mafic-intrusive rock, and 50% black, carbonaceous and silicified tuffaceous-sedimentary rock. The initial visual sorting emphasized gross mineralogical and textural differences and produced five separate piles. Three of the piles were characterized as mafic intrusive rock that varied from massive, homogeneous material with abundant disseminated pyrite, to fractured material with densely-spaced fracture-filling quartz and pyrite veinlets. The other two piles consisted of dark-gray to black, sparsely pyritic sedimentary rock that

varied from thin-bedded, carbonaceous material to fractured, silicified material with fracture-filling quartz veinlets. More rigorous sorting of the five piles, based on a binocular-microscope examination, produced ten samples; seven were mafic intrusive rocks with varying ranges of pyrite and carbonate content, and three were dark-gray to black, silicified tuffaceous sedimentary rocks with little or no pyrite or carbonate visually detectable.

The ten samples (designated as numbers M-1 through M-10) were then each stage-crushed to 100% passing 0.25 inch. Subsequently, each crushed sample was split by rotary splitter into more than 12 aliquots of 0.25 kg each. Twelve aliquots from each of the ten samples comprised three 1-kg humidity-cell charges. After the 12 aliquots were collected, a portion of leftover material (about 0.25 kg) from the rotary splitting of each sample was pulverized by ring and puck to 80% passing 150 mesh (100 micron) for chemical analyses. The balance of leftover split material was re-combined and bagged as “reject”. The 12 aliquots and “reject” comprising each sample were placed in plastic 5-gallon buckets and shipped to the MN DNR in Hibbing, MN. As-received sample masses ranged from 6 to 14.5 kg. Upon receipt at MN DNR, the “reject” portion of each sample was submitted for screen-fraction analysis at Lerch Brothers, Inc. in Hibbing, MN.

4.1.2. Six Low NP Tuffaceous-Sedimentary Samples

In September 2000, additional mafic-intrusive and tuffaceous-sedimentary samples were collected to assess the availability of calcium and magnesium carbonate minerals to neutralize acid and to assess acid neutralization by non-carbonate minerals. The seven original mafic-intrusive samples (M1 through M7) run being tested had NP[(Ca+Mg)CO₃] values of 41 to 112 g CaCO₃ equivalent (kg rock)⁻¹ and CO₂ contents of 2.15% to 5.85%. The tuffaceous-sedimentary samples run previously had NP[(Ca+Mg)CO₃] values of 37 to 77 g CaCO₃ equivalent (kg rock)⁻¹ and CO₂ contents of 1.92% to 4.05%.

All samples were generating typical drainage pH values ranging from 7.9 to 8.2 after 72 weeks of dissolution, indicating that acid neutralizing carbonate minerals (calcium and magnesium carbonates) had not been depleted. Based on release of calcium and magnesium with the drainages, calcium and magnesium carbonate depletion from the mafic-intrusive and tuffaceous-sedimentary samples ranged from 9 to 21% and 8 to 11%, respectively. If all calcium and magnesium carbonates present are available for reaction, an estimated additional 300 to 1500 weeks of dissolution would be required before they were depleted (Lapakko and Antonson 2000). To gain more timely insight on the calcium and magnesium carbonate availability and neutralization by non-carbonate host rock minerals, additional samples were collected for testing.

Seventeen additional samples (four mafic-intrusive and thirteen tuffaceous-sedimentary) were collected to augment experimentation on the mafic-intrusive and tuffaceous-sedimentary rock dissolution testing (Table 1). The objective of sample collection was to obtain samples with modest amounts of neutralization potential, for example 1 to 20 g CaCO₃ equivalent (kg rock)⁻¹. The tuffaceous-sedimentary samples consisted of dark gray to black, thin-bedded tuffaceous silty limestone that has been moderately to strongly altered (i.e., carbonized, decalcified, and silicified),

and contains disseminated pyrite and quartz veinlets. The mafic-intrusive samples were strongly altered fine-grained mafic-intrusive rocks (i.e., propylitized, argillized, and sulfidized) that are in intrusive contact with the tuffaceous-sedimentary rocks.

The seventeen samples were collected in 5-gallon buckets from mine waste exposed in 20-foot high benches in an open pit metal mine. During sampling, an attempt was made to collect up to “fist”-sized fragments of relatively fresh rock by chipping away the weathered portions. Samples were collected by lithologic type (i.e., tuffaceous-sedimentary or mafic-intrusive) in the vicinity of bench blast holes that generally assayed less than 3.5% and 6.0% sulfide sulfur and carbonate carbon, respectively. However, the four mafic-intrusive samples were collected from the vicinity of three blast holes containing from 2.6% to 3.5% sulfide sulfur, and from 1.3% to 3.7% carbonate carbon. Three of the thirteen tuffaceous-sedimentary samples (sample number’s 370-372) were collected from the vicinity of one blast hole containing 2.1% sulfide sulfur and 0.19% carbonate carbon. Six of the tuffaceous-sedimentary rocks, were selected for additional dissolution testing.

The samples were stage crushed, at Lerch Brothers Inc., to -0.64-cm to limit generation of fines. The process entailed screening the “fist”-sized rock samples to -0.64 cm and three crushing steps (large jaw crusher set at 1.92 cm, small jaw crusher set at 0.95 cm, roll crusher set at 0.64 cm). After each of the first two crushing steps, the -0.64 cm fraction was collected and the oversize was passed to the next crushing phase. Five 250-gram samples and one 300-gram sample were split from each bulk sample. The five 250-gram samples were stored in sealed plastic bags until filling the cells. The 300-gram split was pulped for subsequent analysis.

4.1.3. USGS Abandoned Mine Land (USGS AML) Weathered Waste Rock Sample

Broken waste rock fragments ranging in size from 2 by 3 to 3 by 5 inches, selected from a 75 to 100-year old abandoned metal-mine waste rock dump, comprise the USGS AML sample. A sample of approximately 25 kg was collected and shipped to the MN DNR in a 5-gallon bucket. Because of the 75 to 100 years of exposure on the dump, some of the individual sample fragments exhibited oxidation rims up to 1/8 inch thick. It was not possible to remove this oxidation rim during sample preparation. The sample is dominated by a coarsely crystalline matrix of dolomite that contains dispersed iron and base-metal sulfides. Iron sulfide as pyrite occurs in pods and some fracture fillings. Occasional visible grains of galena (PbS) and sphalerite (ZnS) comprise the base-metal sulfides. Some secondary calcite is also present.

Six hand specimens were selected from the USGS AML sample population for gross mineralogical and petrologic examination. The remainder of the sample was stage-crushed to 100% passing 0.25 inch. The crushed USGS AML sample was subsequently blended with three passes through a Jones Splitter containing 0.75-inch chutes. After blending, the sample was split into aliquots of about 0.25 kg. Four of these aliquots were randomly selected from the sample-aliquot population to make up the USGS AML sample’s 1-kg humidity-cell charge.

4.2. Dissolution Test Methods

4.2.1. ASTM Method D5744-96 (ASTM 2000)

Three samples were subjected to accelerated-weathering tests conducted according to ASTM Standard Method D5744-96. Four 0.25-kg aliquots (each in sealable plastic bags) comprising each sample were used to load individual humidity cells; this was done to minimize sample stratification and consequent fluid "channeling" in the cell. A 16-cell array identical to that illustrated by figure 1 in the standard method (ASTM 2000) was used, although not all cells were occupied. The final 16-cell-array included a sample from the mafic-intrusive (M-2) and tuffaceous-sedimentary rock types (M-8), as well as the USGS AML sample.

Samples were rinsed with three 500-mL rinses at week 0 (see section 4.2.3., Modifications of the ASTM Protocol), and subsequent weekly cycles consisted of the following:

- Tuesday - previous week's leachant (from 500-mL addition on Monday) collected and weighed; each humidity cell weighed to determine amount of interstitial water present in the waste rock sample after the leach (assumes no loss of rock due to dissolution or solids loss); three-day dry-air period initiated (same time each cycle) - NOTE: start of dry-air period begins the new week (i.e. week 1).
- Friday - dry-air period ends; each humidity cell weighed to determine evaporation rate of interstitial water; three-day wet-air period initiated (same time each cycle).
- Monday - wet-air period ends; each humidity cell weighed to determine gain/loss of interstitial water; 500-mL drip rinse initiated.
- Tuesday - previous week's leachant collected and weighed; each humidity cell weighed to determine amount of interstitial water present in the waste rock sample after the rinse; three-day dry-air period initiated; start of new week (i.e., week 2).

Initially air-flow rates ($L \text{ min}^{-1}$), temperature, and relative-humidity readings were taken once daily for each cell during the three-day dry-air period; these readings were also taken once daily for each cell on Friday and the following Monday during the wet-air period. Subsequently, air flow rates were measured before initiation of both the dry- and wet-air cycles, and temperature and relative humidity were measured at the beginning and end of both cycles.

4.2.2. MN DNR Method

An accelerated-weathering test method similar to ASTM Method D5744-96 has been designated as the MN DNR method (Lapakko and White 2000). The MN DNR method uses the same humidity-cell diameter (although about 3 cm shorter, Figure 1), waste rock charge, rinse volume and rinse application method as described in ASTM D5744-96. However, instead of subjecting the humidity

cell apparatus to the humid- and dry-air flow through the cell, the cells were stored in a controlled temperature and humidity room between weekly rinses.

The cells were weighed to determine the water retained after the rinse (Tuesday), on the fourth day of the cycle (Friday, concurrent with the switch of ASTM cells from wet to dry air cycle), and before the rinse (Monday, Appendix 2). It should be noted that the relative humidity readings were from the room itself. The humidity within the cells was probably near 100%, since the water retained in the cells was fairly constant during the weekly cycles (i.e. water did not evaporate).

4.2.3. ASTM and MN DNR Method Modifications

Three samples were subjected to humidity cell testing using the “Modified Humidity Cell” designated as ASTM Standard Method D5744-96 (ASTM 2000) and all eleven were subjected to the MN DNR method. The only departure from the standard-method protocol was the volume of de-ionized water used for the initial rinses (week 0). Instead of a single 500-mL rinse, each sample was rinsed with three 500-mL rinses (totaling 1.5 L) to flush residual sulfate salts produced by natural weathering prior to sample collection. The same initial-rinse technique (1.5 L vs 0.5 L week-0 rinse) was used in the MN DNR method.

The three-rinse procedure at week 0 consisted of an initial 500-mL drip rinse to wet the 1-kg sample, a 500-mL flooded rinse to saturate the sample (after sample flooding, leachant contacted sample for about five minutes prior to draining), and a final 500-mL rinse to complete the rinse. Recovered volumes from each of the three rinses were weighed, and composited. Samples (approximately 60 mL) from the composite were filtered, preserved and submitted for analyses. The flow-weighted average concentrations were determined for the three rinses and were reported as data for week zero in drainage quality tables.

4.3. Analyses

4.3.1. Solid-Phase Analyses

The original seven mafic-intrusive samples, three tuffaceous-sedimentary samples, and USGS AML sample were analyzed for particle size distribution, solid-phase chemistry, and mineralogy. Particle size distribution was determined using ASTM E 276-93 (ASTM 2000) by Lerch Brothers Inc. Dry sieving was used for the -100 fraction, since there was little difference between results of dry- and wet-sieving (Table 2).

The rock samples were analyzed for sulfur, sulfate (sulfide was determined by difference), and evolved carbon dioxide by ACTLABS in Tucson, AZ using ASTM E-1915-97 (ASTM 2000). A 10 percent hydrochloric acid solution was used to solubilize the carbonate minerals, and the carbonate present was quantified as the difference between total carbon in the initial sample and that in the residue. The remaining solid-phase constituents were determined by ACTLABS in Ancaster, ON. Whole rock constituents were determined using a lithium tetraborate fusion modified from ASTM

E886-94 (ASTM 2000) and analysis by inductively coupled plasma-atomic emission spectroscopy (ICP-AES) using a Thermo Jarrell-Ash ENVIRO II ICP. Concentrations of Ag, Cd, Cu, Ni, Pb, Zn, and Bi were determined using a total digestion method modified from Crock et al. (1983), with analysis by ICP-AES. Other trace elements were determined using instrumental neutron activation analysis (Hoffman 1992). Mineral content and degree of liberation of sulfide and carbonate minerals were determined using x-ray diffraction, optical microscopy, and SEM by Barry Frey of Midland Research (Nashwauk, MN) and Louis Mattson of Mineralogical Consulting Service (Pengilly, MN) (Appendix 1, Attachment A1.1). Optical microscope and SEM photos were taken on selected samples to demonstrate features commonly observed in the rock samples (Appendix 1, Photos A1.1. - A1.14.).

The low neutralization potential tuffaceous-sedimentary samples were analyzed for particle size distribution and chemistry only, using the methods described above. One tuffaceous-sedimentary sample, leached for forty weeks, was also analyzed. Scanning electron microscope and energy dispersive spectrometry (SEM and EDS) analyses were conducted by P.L. McSwiggen of the University of Minnesota Department of Geology using a JEOL 8900 Electron Probe Microanalyzer.

4.3.2. Aqueous-Phase Analyses

Water samples were analyzed for specific conductance, pH, alkalinity, acidity, and Eh at the MN DNR in Hibbing, MN. Specific conductance was analyzed using a Myron L conductivity meter. An Orion SA720 meter, equipped with a Ross combination pH electrode (8165), was used for pH analyses. Alkalinity (for pH \geq 6.3) and acidity were determined using standard titration techniques for endpoints of 4.5 and 8.3, respectively (APHA et al. 1992). Eh readings were taken using a Beckman model 11 meter with an Orion electrode (9678BN) over the initial 58 (mafic-intrusive and tuffaceous-sedimentary rocks) or 48 weeks (USGS AML sample). Due to funding limitations and resultant time constraints, it was decided to eliminate these measurements. These readings were considered to be of lower priority since 1) readings over time and among samples were fairly constant; 2) with the sampling and analysis scheme used, samples were exposed to the atmosphere for roughly 24 hours, which would affect Eh; and 3) Eh had not been incorporated into modeling efforts at the University of Utah.

Composite samples from rinses at week 0 and samples from weeks 1 and 4 of two mafic-intrusive (M-1, M-3) and one tuffaceous-sedimentary (M-8) sample were analyzed by inductively coupled plasma mass spectrometry (ICP-MS, Perkin Elmer mode-SCIEX-Elan 5000) at the University of Minnesota Department of Geology (Minneapolis, MN) to identify trace elements released. Based on these scans (Appendix 3), trace elements were selected for subsequent determination at the Minnesota Department of Agriculture (St. Paul, MN). Prior to 23 August 1999 (week 55 for mafic-intrusive and tuffaceous-sedimentary samples and week 45 for the USGS sample), metals were determined with a Varian 400 SPECTRAA; a Zeeman GFAA furnace was attached for low concentrations. Subsequent analyses were conducted using inductively coupled plasma mass spectrometry (ICP-MS, Hewlett Packard HP4500 Series, model #G1820A). Sulfate concentrations exceeding five mg/L were

determined using a Technicon AA2 automated colorimeter. Lower concentrations were determined using a Dionex ion chromatograph and, after 10 November 1998, a Lachat QuickChem 8000.

4.4. Calculations

4.4.1. Potentials for Acid Production and Neutralization

Chemical data can be used to determine maximum potentials for acid production and neutralization in g CaCO₃ equivalent (kg rock)⁻¹. Assuming all sulfur is present as iron sulfide yields the maximum potential for acid production (AP(S_T), equation 15). Assuming the carbon dioxide (CO₂) is associated with calcium and magnesium yields the maximum potential for acid neutralization (NP(CO₂), equation 16). However, there are sulfur-bearing minerals which do not contribute to acid production (e.g. barite, BaSO₄, gypsum, CaSO₄ and, in general, trace metal sulfides) and carbonate minerals which do not contribute to acid neutralization (e.g. siderite, FeCO₃). Mineralogical analyses are required to determine the distribution of sulfur between acid-producing and nonacid-producing species and the distribution of carbonate between minerals which neutralize acid and those which do not.

$$AP(S_T) = 31.2 \times \%S_T \quad (15)$$

$$NP(CO_2) = 22.7 \times \%CO_2 \quad (16)$$

$$AP(S^{2-}) = 31.2 \times \%S^{2-} \quad (17)$$

For the samples in the present study, two methods were used for quantifying both potentials for acid production and acid neutralization. In most cases the sulfide content was used to determine the potential for acid production (equation 17). This assumes all sulfide is present as iron sulfide, which for these samples was generally the case. Corrections were made and noted when trace metal sulfide content was not negligible.

The magnitude of sulfur-bearing minerals reacted was calculated as the sulfur present in sulfate released to drainage. The remnant total sulfur content was calculated by subtracting the sulfur released from the initial total sulfur content. The remnant AP was calculated using the remnant total sulfur content (S_T, equation 15), which assumes all sulfur is present as iron sulfide. It was not possible to determine the fraction of the remnant total sulfur content present as sulfide, since the analytical methods used did not permit identification of the source of sulfur from which the sulfate present in drainage was derived. However, educated guesses can often be made on these sources. For example, elevated sulfate concentrations are commonly observed over the first five to ten weeks of dissolution testing. Much of this elevation has been attributed to sulfate release from readily soluble sulfate minerals (e.g. gypsum, CaSO₄, and melanterite, FeSO₄) which accumulated during sample storage prior to testing (e.g. Lapakko et al. 2000).

For all data analyses, neutralization potential in g CaCO₃ equivalent (kg rock)⁻¹ was calculated as that present as calcium and magnesium carbonates (equation 18). The NP implied by the carbon dioxide content is presented for comparison (equation 16). As discussed in the second paragraph of this section, this calculation tends to overestimate the actual potential for acid neutralization. Net neutralization potential represents the difference between potentials to neutralize and produce acid, and was calculated as indicated in equation 19. Positive values indicate an excess of neutralization potential, while negative values indicate an excess of acid production potential.

$$\text{NP}[(\text{Ca}+\text{Mg})\text{CO}_3] = 10 \times \% \text{CaCO}_3 + 11.9 \times \% \text{MgCO}_3 \quad (18)$$

$$\text{Net NP} = \text{NP}[(\text{Ca}+\text{Mg})\text{CO}_3] - \text{AP}(\text{S}^{2-}) \quad (19)$$

4.4.2. Estimation of Minimum Mineral Availability for Reaction

Mineral availability was more difficult to quantify than mineralogical composition. The lower bound of mineral availability was approximated by the degree of liberation. The degree of liberation quantifies only grains which are removed from the rock matrix and most likely represents a minimum value for availability. “Well exposed minerals” on the rock surfaces will also be available for reaction but the extent of these minerals was not quantified.

4.4.3. Chemical Mass Release and Release Rates

The masses of sulfate, calcium, and magnesium release were calculated as the product of the observed concentration in the drainage and the drainage volume. Release rates were calculated for several periods for each cell. Cumulative sulfate release over time was graphed for each cell. Periods of linear sulfate release were selected based on visual examination of these plots, and the release rate for each period was determined by linear regression. Calcium and magnesium release rates were determined by conducting linear regression of the same periods.

5. RESULTS

5.1. Introduction

As discussed in section 2, the oxidation of iron sulfide minerals leads to acid production, and dissolution of calcium and magnesium carbonate minerals neutralizes acid. Whereas dissolution of other minerals will neutralize acid, this report assumes only calcium and magnesium carbonate contribute significantly to this reaction for drainage pH values of at least 6.0. Drainage will not acidify as long as the rate of acid neutralization (usually calcium/magnesium carbonate mineral dissolution) exceeds that of acid production (usually iron sulfide oxidation or iron sulfate dissolution). The key solid-phase variables controlling these reactions are the specific minerals present and their surface areas available for reaction. The maximum potentials for acid production and neutralization can be determined based on solid-phase analyses. However, there is presently no accurate and expedient method of determining the fractions of acid-producing and acid-neutralizing minerals in these rocks which are available for reaction. This can be determined only through dissolution testing.

A number of kinetic tests have been used for dissolution testing of mine wastes, and these tests generally accelerate weathering rates beyond those observed in the field. It has been noted that some natural conditions, such as those typical of tropical areas (e.g. surface temperatures that exceed 40°C, compounded by tropical rainfall), are more conducive to weathering than those commonly employed in kinetic tests. Under such extreme temperatures, iron sulfide mineral oxidation would increase. However, effects of weathering in kinetic tests can be observed more quickly than in the natural environment, even under extreme conditions, since virtually all of the rock mass is exposed to oxygen-saturated air and a large volume of water (per unit mass rock) is available to transport reaction products.

All eleven original samples were subjected to dissolution testing using the MN DNR method, and these data are used for comparisons. One mafic-intrusive (MS-2) and one tuffaceous-sedimentary (MS-8) sample were run in duplicate. These two samples and the USGS AML sample were also subjected to dissolution testing using ASTM Standard Method D5744-96, and results from the two methods are compared in section 5.5. Drainage quality data and rates of sulfate, calcium, and magnesium release are presented for results generated through October 2001. This represents 168 weeks of dissolution for the mafic-intrusive and tuffaceous-sedimentary samples and 158 weeks for the USGS AML sample.

The six additional tuffaceous-sedimentary samples with low neutralization potentials (see 4.1.2) were subjected to dissolution testing using the MN DNR method. Two samples were run in duplicate. Periods of record were 20 weeks for five of the samples and 40 weeks for the sixth. Results for these samples are presented in section 5.3.2.

Detailed information on solids composition, laboratory methods, drainage quality, cumulative mass release, rates of release and quality assurance are presented in appendix 7.

5.2. Mafic-Intrusive Samples

5.2.1. Solid-Phase Analyses

Particle size determinations on the seven mafic-intrusive samples indicated roughly 50% of the mass was in the -4/+20 mesh Tyler fraction ($4.75 \text{ mm} < d \leq 0.850 \text{ mm}$), 75% was coarser than 48 mesh ($0.300 \text{ mm} < d$), and 10% was in the -200 mesh fraction ($d \leq 0.074 \text{ mm}$; Table 2).

Chemical analysis of the mafic-intrusive samples revealed sulfide contents (total sulfur minus sulfur present as sulfate) of 6.20% to 8.55% and evolved CO_2 contents of 2.15% to 5.84% (Table 3). Arsenic concentrations ranged from 1200 to 2100 ppm (Table 4), while most other trace metal concentrations were below 100 ppm. Notable exceptions were barium (270 ppm average), rubidium (140 ppm average), vanadium (120 ppm average), and zirconium (260 ppm average).

Mineralogical analyses included a general description of the mafic-intrusive rocks (Appendix 1, Attachment A1.1).

The seven mafic-intrusive samples are generally similar and consist of fine- to medium-grained, highly altered rock containing fine-grained disseminated sulfides with additional sulfides in quartz and carbonate veinlets. The alteration and replacement is primarily of the host rock minerals and is probably associated with the mineralizing events. Except for tarnished pyrite and minor iron oxides, there is little direct evidence of surficial alteration.

The major minerals present in the mafic-intrusive samples were illite (some sericite may have been present also but was not identified with the methods used), quartz, pyrite, and ferroan dolomite (Table 5). Pyrite, which contained some arsenic, was the dominant sulfide mineral, although marcasite, stibnite, and arsenopyrite were reported present in trace amounts. Sulfate was present as gypsum and barite. Ferroan dolomite was the dominant carbonate in all samples and the carbonate was distributed among Ca (42%), Mg (44%), Fe (12%), Mn (1.6%), and Sr (0.1%). Therefore, 86% of the carbonate was associated with calcium or magnesium.

The chemical and mineralogical data were used to determine potentials for acid production and acid neutralization. Virtually all of the sulfide is associated with iron, and sulfide content was used to calculate acid production potentials (AP) of 193 to 267 g CaCO_3 equivalent $(\text{kg rock})^{-1}$ (equation 14). The carbonate fraction associated with calcium and magnesium (86%) and the carbon dioxide contents (Table 3), were used to calculate neutralization potential present as calcium and magnesium carbonate ($\text{NP}[(\text{Ca}+\text{Mg})\text{CO}_3]$, equation 20). This calculation yielded values of 42 to 114 g CaCO_3 equivalent $(\text{kg rock})^{-1}$. The net NP values (equation 19) ranged from -216 to -79 g CaCO_3 equivalent $(\text{kg rock})^{-1}$, indicating all samples had the potential to produce acidic drainage. However, the fairly high NP values (42-114 g CaCO_3 equivalent $(\text{kg rock})^{-1}$) indicate that the drainage may remain neutral for a fairly long time prior to acidification.

$$\text{NP}[(\text{Ca}+\text{Mg})\text{CO}_3] = 19.5 \times \% \text{CO}_2 \quad (20)$$

The liberation (separation of individual mineral grains from the rock matrix) of both pyrite and ferroan dolomite was described as poor. Both minerals were present as fine grains, relative to the coarse rock particles, and were “reasonably well liberated” for rock particle fractions finer than 100 mesh, which comprise 10 to 15 percent of the samples (Table 2). For the combined size fractions, pyrite liberation ranged from 14 to 19 percent and ferroan dolomite liberation from 16 to 22 percent (Table 6). This yielded estimated minimum values for available AP(S²⁻) of 32 to 51 g CaCO₃ equivalent (kg rock)⁻¹ and available NP[(Ca+Mg)CO₃] of 8 to 25 g CaCO₃ equivalent (kg rock)⁻¹ (Table 7). These estimates are minimums since they include only the liberated minerals and not minerals exposed on rock surfaces.

5.2.2. Drainage Quality Results for the MN DNR Method

One-kg charges of seven mafic-intrusive waste rock samples were loaded into eight MN DNR cells and subjected to initial rinsing (week 0) on 11 August 1998. One of the samples was run in duplicate. (This sample was also subjected to testing using the ASTM method.) Cells for two of the seven solids, as well as one of the duplicates for a third (and the ASTM method cell), were terminated after 102 weeks. Five cells containing five different sulfur contents (6.75, 7.05, 7.30, 8.10, 9.05% S_T) continue to operate. The text of the present report focuses on 168 weeks of data from the cells presently operating. Data for all cells are presented in tables, figures and appendices.

Drainage quality from the mafic-intrusive samples indicated that, while iron sulfides were oxidizing, pH and alkalinity were controlled by the dissolution of calcium and magnesium carbonate minerals. After week 72, drainage pH typically ranged from 7.8 to 8.3, with values for the 7.3% S_T sample at the lower end of the range and values from the 8.1% S_T sample at the upper end (Table 8). Drainage pH often increased slightly over the initial 40 weeks, but values generally remained within a fairly narrow range for the duration of the tests (Figures 2-10). Alkalinities averaged roughly 40 to 90 mg/L as CaCO₃, increasing as sulfate concentrations increased.

Average sulfate concentrations from week 72 to 168 ranged from approximately 40 to 130 mg/L, with no correlation with total solid-phase sulfur content (Table 8). Concentrations from samples containing 7.40 and 9.05 percent sulfur were on the lower end of the range. Sulfate concentrations decreased relatively rapidly over the first five weeks, reflecting the removal of oxidation products accumulated between the time of sample segregation and the inception of the experiment (see section 4.1.1). Subsequently, concentrations tended to decrease over the first 30 to 50 weeks, then remained in a fairly stable range (Figures 2-10).

The rates of sulfate release from week 72 to the end of the period of record ranged from about 0.2 to 0.6 mmol(kg rock•week)⁻¹ (Table 9). For samples with sulfur contents of 6.5 to 7.4 percent, these rates were typically 10 to 15 percent slower than those observed from week 24 to 72. For the two highest sulfur samples, rates increased slightly (Appendix 5, Table A5.1). The three lowest rates were observed for samples with sulfur contents of 7.30, 7.40 and 9.05%. Whereas these sulfur contents were at the upper end of those tested, it should be noted that the sulfur range was fairly small (6.50% to 9.05%, Table 9). When normalized for pyrite content, the rates ranged from roughly

1 to 5 mmol SO₄ (kg FeS₂•week)⁻¹, averaging 2.7 mmol SO₄ (kg FeS₂•week)⁻¹ for the MN DNR method (Table 9). (Only rates for samples with a 168-week period of record were used to calculate this average.)

The cause of variation in sulfate release rates has not been identified. The range in rates cannot be explained solely by differences in pyrite liberation, which was fairly constant and ranged from 14% to 19% (Table 6). The two samples with the lowest sulfate release rates, normalized for pyrite content (7.40% and 9.05% S_T samples), were described as fine-to-medium grained (photos A1.6. and A1.7.). The texture of these samples was coarser than that of the other five rocks, which were described as generally fine grained (Photos A1.1.- A1.5.). The coarser texture of the 7.40% and 9.05% S_T samples may have resulted in liberated pyrite grains in these samples that were coarser than liberated grains from other samples. This may have been a subtle difference because the pyrite present was described as “generally fine grained disseminated sulfides” for all samples. The texture might also affect the unliberated pyrite exposure. The relatively small range in water retained after rinsing (averaging 206 to 257 mL for individual samples on the day after rinsing; Appendix 2, Table A2.1) suggests that rinsing efficiency was fairly uniform.

From week 72 to 168, average drainage concentration ranges for calcium and magnesium were approximately 20-50 mg/L and 10-20 mg/L, respectively. As was observed for sulfate, calcium and magnesium concentrations decreased relatively rapidly over the first five weeks, more slowly for the next 25 to 45 weeks, then remained in a fairly constant range (Figures 2 -10). Calcium and magnesium concentrations also tended to increase as sulfate concentrations increased (Table 8).

The dissolution of trace amounts of calcite would explain why the rate of calcium release was 1.1 to 1.9 times that of magnesium (Table 9). Congruent dissolution of ferroan dolomite, with a 1:1 molar ratio of calcium to magnesium (see section 5.2.1), would yield a 1:1 ratio of calcium release to magnesium release. It should be noted that the ratio of calcium to magnesium release rates decreased over time, suggesting a decrease in calcite dissolution. The rates of sulfate release were 0.39 to 0.66 times the sum of calcium and magnesium release rates. This suggests neutralization of 0.78 to 1.32 moles of acid per mole of calcium plus magnesium carbonate dissolution.

During the first 72 weeks, trace metal release was limited to relatively low levels of manganese, antimony, arsenic, and zinc (Table 8). Concentrations of all these elements decreased over time. After week 72 the typical ranges for average concentrations were 0.006-0.38, 0.001-0.008, 0.001-0.01, and 0.001 to 0.003 mg/L, respectively. Manganese was likely released during dissolution of the ferroan dolomite, while zinc was probably contributed by oxidation of trace amounts of sphalerite (Appendix 1, Attachment A1.1). The high release of antimony relative to arsenic is somewhat surprising since the solid-phase concentrations of antimony were roughly three percent those of arsenic (Table 4). Apparently the antimony is present in a less stable form (stibnite) than the arsenic (pyrite, arsenopyrite).

5.2.3. Extent of Sample Dissolution

The extent of sulfur-bearing and carbonate mineral depletion during the 168 weeks of dissolution was fairly small. The initial AP(S_T) of these samples ranged from approximately 200 to 280 g CaCO₃ equivalent (kg rock)⁻¹ and these values decreased by 5 to 15 g CaCO₃ equivalent (kg rock)⁻¹ during the 168 weeks of dissolution testing (Table 10). (The rationale for using AP(S_T) rather than AP(S^{2-}) is presented in section 5.1.) The initial NP[(Ca+Mg)CO₃] values ranged from approximately 40 to 110 g CaCO₃ equivalent (kg rock)⁻¹ and decreased by 10 to 21 g CaCO₃ equivalent (kg rock)⁻¹ during dissolution testing (Table 10). Thus, even over the course of about 3.2 years, the extent of AP(S_T) depletion was roughly 2% to 7% and NP[(Ca+Mg)CO₃] depletion was 14% to 48%.

The dissolution time required to deplete the calcium and magnesium carbonate minerals is dependent on the dissolution rate and availability of these minerals. It was assumed that the dissolution rate of the minerals would remain constant at the rate observed for weeks 72 through 168. If the calcium and magnesium carbonates were 100% available, 200 to 1600 additional weeks of dissolution would be required for their depletion. This time frame would be reduced to 0 to 130 weeks if the carbonate mineral availabilities are near the minimum estimated (Table 11). For four of the samples, calcium plus magnesium release exceeded the minimum availability. This indicates that the actual availability exceeds that present in liberated carbonate grains. That is, calcium and magnesium carbonate grains on the faces of rock particles dissolve to some degree and contribute to acid neutralization.

5.3. Tuffaceous-Sedimentary Samples

5.3.1. Three Original Samples

5.3.1.1. Solid-Phase Analyses

Particle size determinations indicated the three tuffaceous-sedimentary samples were coarser than the mafic intrusive samples, with about 65 percent in the -4/+20 mesh fraction (4.75 mm < d ≤ 0.850 mm), 80 percent coarser than 48 mesh (0.300 mm < d), and 7 percent in the -200 fraction (d ≤ 0.074 mm; Table 2).

Chemical analyses revealed that the tuffaceous-sedimentary samples have lower sulfide (1.3 to 3.75 percent) and evolved CO₂ (1.92 to 4.05 percent) contents than the mafic-intrusive samples (Table 3). Arsenic concentrations in the tuffaceous sedimentary rocks range from approximately 250 to 500 ppm (Table 4). Most other trace metal concentrations are below 100 ppm. Notable exceptions are barium (120 ppm average) and chromium (170 ppm average).

Mineralogical analyses of the tuffaceous-sedimentary samples included the following description (Appendix 1, Attachment A1.1).

The three tuffaceous-sedimentary samples are generally similar and consist of very fine-grained, highly siliceous, black rock with numerous quartz and lesser carbonate veins.

Sulfides tend to occur mostly in the veins, but are also disseminated in the rock. All three of these samples contain carbonaceous material and it is most common in M-9. There is very little evidence of surficial alteration (Photos A1.8 - A1.10.).

The major minerals in the tuffaceous-sedimentary samples are quartz, illite (some sericite may have been present also but was not identified with the methods used), ferroan dolomite, and pyrite (Table 5). Although these minerals also dominated the mafic-intrusive samples, the relative amounts varied between the two rock types. Pyrite was again the dominant sulfide mineral, containing some arsenic, although contents were lower than those for the mafic-intrusive samples (roughly 2-7% vs 12-16%). Marcasite, stibnite and arsenopyrite were present in small quantities. Ferroan dolomite (see section 5.2.1 for chemical composition) was the dominant carbonate and contents were comparable to the lower half of the range for the mafic-intrusive samples. Trace amounts of calcite were present. The non-carbonate carbon present may have been the result of deposition of organic matter along with the inorganic sediments, both of which ultimately contributed to the rock composition.

The chemical and mineralogical data were used to determine potentials for acid production and acid neutralization. Virtually all of the sulfide is associated with iron, and sulfide content was used to calculate acid production potentials (AP) of 41 to 117 g CaCO₃ equivalent (kg rock)⁻¹ (equation 17). The carbonate fraction associated with calcium and magnesium (86%) and the carbon dioxide contents (Table 3), were used to calculate the NP[(Ca+Mg)CO₃] (equation 20), yielding values of 37 to 79 g CaCO₃ equivalent (kg rock)⁻¹. The net NP values (equation 19) ranged from -38 to +22 g CaCO₃ equivalent (kg rock)⁻¹, and indicated two of the three samples had the potential to produce acidic drainage. However, the fairly high NP values of these two samples, 37 and 79 g CaCO₃ equivalent (kg rock)⁻¹, suggest that drainage from these samples would remain neutral for a fairly long time prior to acidification.

Pyrite was “reasonably well liberated” in the 3.90% S sample fractions finer than 100 mesh and in the fractions finer than 150 mesh in the other two samples. The corresponding fractions for ferroan dolomite liberation were -65 and -100 mesh. The extent of liberation ranged from 12 to 17 percent for pyrite and 13 to 22 percent for the ferroan dolomite (Table 6). Using these values to determine available AP(S²⁻) and NP[(Ca+Mg)CO₃] indicates a slight excess of AP for the 1.31% S and 3.90% S samples, and a slight excess of NP for the 1.37% S sample (Table 7).

5.3.1.2. Drainage Quality Results for the MN DNR Method

One-kg charges of three tuffaceous-sedimentary waste rock samples were loaded into four MN DNR cells and subjected to initial rinsing (week 0) on 11 August 1998. One of the samples was run in duplicate. (This sample was also subjected to testing using the ASTM method.) Cells for one of the three solids (1.37% S_T), as well as one of the duplicates for a second (3.90% S_T)(and the ASTM method cell), were terminated after 102 weeks. Two cells containing rock with total sulfur contents of 1.31 and 3.90% remain in operation. The text focuses on the 168 weeks of data for these cells. Data from the terminated cells are included in tables, figures and appendices.

As with the mafic-intrusive rocks, the pH and alkalinity in drainage from the three tuffaceous-sedimentary rocks were controlled by the dissolution of ferroan dolomite in the samples (4 to 13 weight percent), despite the oxidation of iron sulfides present. Drainage pH typically ranged from 7.7 to 8.2, with values from the 1.31 percent sulfur sample at the lower end of the range (Table 8). Drainage pH values after about week 40 remained in a fairly constant range for each of the samples, with variations of 0.2 to 0.4 units (Figures 11-14). From week 72 to week 168 average alkalinities ranged from 30 to 40 mg/L as CaCO₃ (Table 8) and, as was the case with pH, fell within a fairly constant range over time (Figures 11-14).

Average sulfate concentrations in drainage from the two tuffaceous-sedimentary samples were approximately 50 and 70 mg/L (Table 8). Concentrations decreased through the first 30 to 60 weeks then remained in a fairly constant range (Figures 11-14). Rates of sulfate release for weeks 72 through 168, when normalized for pyrite content, were 10 and 5.5 mmol SO₄ (kg FeS₂•week)⁻¹ (Table 9). This suggests only slight variation of pyrite reactivity and availability among the solids. The average tuffaceous-sedimentary sulfate release rate when normalized for pyrite content was 2.3 times that for the mafic-intrusive samples (7.75 vs. 3.3 mmol SO₄ (kg FeS₂•week)⁻¹); only samples with 168 weeks of data were used to determine averages).

The average drainage concentration ranges for calcium and magnesium were 20-30 and 9-12 mg/L, respectively (Table 8). Temporal variations of both tended to parallel those for sulfate concentrations (Figures 11-14). Molar release rates for calcium were about 30-40 percent higher than those for magnesium. The sulfate release rate was approximately 0.6 times the sum of calcium and magnesium release rates, implying about 1.2 moles of acid were neutralized per mole of calcium/magnesium carbonate dissolved.

Trace metal concentrations tended to decrease over time. Manganese and zinc were elevated for an extended period, decreasing below detection (2 ppb) in drainages from both samples by week 120 (Tables 8, A3.13, A3.14). Arsenic and antimony concentrations decreased below detection (10 ppb) within the first 10 to 30 weeks. As with the mafic-intrusive rocks, aqueous antimony concentrations exceeded those of arsenic; in contrast solid-phase antimony concentrations were 5 to 10 percent those of arsenic (Table 4).

5.3.1.3. Extent of Sample Dissolution

The initial AP(S_T) values of the two active samples were 41 and 122 g CaCO₃ equivalent (kg rock)⁻¹ and these values decreased by 5 and 8 g CaCO₃ equivalent (kg rock)⁻¹, respectively, during the 168 weeks of dissolution testing (Table 10). The corresponding initial NP[(Ca+Mg)CO₃] values were 38 and 79 g CaCO₃ equivalent (kg rock)⁻¹ and decreased by 8 and 12 g CaCO₃ equivalent (kg rock)⁻¹ during dissolution testing (Table 10). Thus, over the course of about 3.2 years, the extent of depletion for AP(S_T) was 6.6% to 12%, while that for NP[(Ca+Mg)CO₃] was 15% to 21%.

Estimation of the dissolution time required to deplete the calcium and magnesium carbonate minerals is dependent on the availability of these minerals. To estimate dissolution time required for depletion

of these carbonates it was assumed that the dissolution rate of the minerals would remain constant at the rate observed over most of the experiment. If the calcium and magnesium carbonates were 100% available, 680 to 1100 additional weeks of dissolution would be required for their depletion. This time frame would be reduced to 0 to 118 weeks if the carbonate mineral availabilities are near the minimum estimated (Table 11). The fact that one sample has not acidified, despite depletion of the minimum available NP[(Ca+Mg)CO₃], suggests that calcium and magnesium carbonate grains on the faces of rock particles dissolve to some degree and contribute to acid neutralization.

5.3.2. Six Low NP Tuffaceous-Sedimentary Samples

5.3.2.1. Introduction

The objective of sample collection was to obtain samples with modest amounts of neutralization potential, for example 1 to 20 g CaCO₃ equivalent (kg rock)⁻¹. Seventeen additional samples were collected to augment experimentation on the mafic-intrusive and tuffaceous-sedimentary rock dissolution testing (Table 1). Six of these samples, all tuffaceous-sedimentary rocks, were selected for additional dissolution testing.

5.3.2.2. Results

5.3.2.2.1. Solid-phase Analyses

The six low NP tuffaceous-sedimentary samples were analyzed for particle size distribution, whole rock chemistry and trace metal content. They were coarser than the first set of tuffaceous-sedimentary samples, and the fractions finer than 10, 35 and 100 mesh were 37, 13 and 6 percent (Table 2). The corresponding values for the initial sample set were approximately 62, 23 and 12 percent (Table 2). (The coarser particles may have resulted in slightly lower water retention by the new samples. Water retention by the new samples in the humidity cells prior to rinsing ranged from 134 to 161 mL as compared to 152 to 184 mL for the original samples.)

Four of the samples collected (356, 361, 362, 363) had sulfide contents within a fairly small range (1.05% to 1.28%) and CO₂ contents of <0.05, 0.26, 0.29 and 0.95 percent (Table 3). These values were well below the range of 1.92 to 4.05% for the samples previously tested (see first paragraph). The sulfur contents were lower than the 1.31% to 3.90% values for the samples in progress, although not to the extent of the CO₂ values. This set of samples was selected to assess the NP availability.

Two additional samples with CO₂ < 0.05% were also selected (364, 370). These samples had sulfur contents of 0.26% and 1.91%. Along with the 1.09% sulfur sample mentioned in the previous paragraph, these three samples were subjected to dissolution testing to examine acid neutralization by host rock minerals alone (non carbonate acid neutralization). Since the calcium/magnesium carbonate content of these rocks is essentially zero, any neutralization observed would be the result of host rock mineral dissolution and would be reflected by the release of base metal cations.

The whole rock chemistry of the six samples was generally similar to that of the three original samples. In both cases SiO₂ constituted 75% to 90% of the whole rock chemistry. The new samples had lower CO₂, CaO and MgO contents, reflecting the lower calcium and magnesium carbonate contents (Table 3). As was the case for the original samples, barium, chromium and arsenic concentrations in the low NP solids were elevated (Table 4).

No mineralogical analyses were conducted on the unleached samples. For the original samples, the carbonate was associated with calcium and magnesium was estimated as 86% (section 5.3.1) Assuming the carbonate mineral chemistry was the same as that estimated for the original samples, the range of NP[(Ca + Mg)CO₃] was calculated as <1 to 19 g CaCO₃ equivalent (kg rock)⁻¹ using equation 20.

5.3.2.2.2. Dissolution Test Results

NP Availability. Three samples contained measurable NP[(Ca+Mg)CO₃], with values ranging from 5.1 to 19 g CaCO₃ equivalent (kg rock)⁻¹ and total sulfur contents of 1.23 to 1.47%. From 0 to 31% of the NP[(Ca+Mg)CO₃] in these samples was available to dissolve and maintain drainage pH above 6.0. The pH of the three week 0 rinses of these samples were acidic, with values ranging from 2.5 to 5.0 (Table A7.7). With the exception of the sample with the highest NP[(Ca+Mg)CO₃] (1.30% S_T) all drainages remained acidic throughout the 20-week period of record. This included samples with estimated NP[(Ca+Mg)CO₃] values of 5.1 and 5.7 g CaCO₃ equivalent (kg rock)⁻¹ and respective total sulfur contents of 1.23% and 1.47%.

Some of the calcium and magnesium carbonates dissolved from the samples with estimated NP[(Ca+Mg)CO₃] values of 5.1 and 5.7 g CaCO₃ equivalent (kg rock)⁻¹, as indicated by elevated calcium and magnesium concentrations in the drainages from these samples (Table 12). Furthermore, the drainage pH values for these samples ranged from roughly 2.5 to 3.6 and were higher than those from samples with undetectable CO₂ and similar sulfur contents (see non-carbonate mineral dissolution discussion). Nonetheless, the NP[(Ca+Mg)CO₃] present in these samples was not available to maintain pH above 6.0 because the rate of acid neutralization was less than the rate of acid generation.

The sample with the highest NP[(Ca+Mg)CO₃] produced drainage pH values above 6.0 for most of the first 20 weeks (values of 5.95 and 5.84 reported for weeks 14 and 16, respectively). With the exception of a 6.57 value reported for week 26, subsequent drainage pH values remained below 6.0, reaching a minimum of 4.21 at week 40 when the cell was terminated. Through week 20 the cumulative sulfate mass release was 59.2 millimoles and the corresponding value for calcium plus magnesium release was 59.5 millimoles (Table 9). These values both represent an NP release of approximately 5.9 g CaCO₃ equivalent (kg rock)⁻¹. This indicates 31% of the estimated NP[(Ca+Mg)CO₃] of 19 g CaCO₃ equivalent (kg rock)⁻¹ was available to dissolve and maintain a drainage pH of at least 6.0.

After dissolution testing for 40 weeks a leached sample was collected and analyzed by scanning electron microscope and energy dispersive spectrometry (SEM and EDS, respectively) and for chemistry. The SEM and EDS indicated the presence of two ferroan dolomite compositions, and that 82.5% to 87.5% of the carbonate was associated with calcium and magnesium [$\text{Ca}(\text{Mg}_{0.65}, \text{Fe}_{0.35})(\text{CO}_3)_2$, $\text{Ca}(\text{Mg}_{0.75}, \text{Fe}_{0.25})(\text{CO}_3)_2$]. Assuming the two compositions were present in equal amounts, the average of these values indicates 85% of the carbonate was associated with calcium and magnesium. This is in close agreement with the 86% estimate reported for the original samples (see section 5.3.1).

An SEM photomicrograph of a particle from the leached sample taken after test termination revealed that some of the ferroan dolomite was included in the rock matrix. The edges originally exposed had reacted and the reaction front continued along the dolomite into the interior of the particle. However, dolomite near the center of the particle was intact (Figure 16). In conjunction with the continued release of calcium and magnesium to the drainage, this suggests that the dissolution rate of dolomite near the exterior of the rock particle (possibly in conjunction with liberated ferroan dolomite grains) was fast enough to neutralize acid and maintain drainage pH near neutral. Dissolution of ferroan dolomite near the center of the rock particle was less rapid, slower than the rate of acid production, and was inadequate to maintain drainage pH above 6.0.

The solid-phase analyses indicated calcium and magnesium releases of 5.7 and 3.2 g CaCO_3 equivalent $(\text{kg rock})^{-1}$ (Table A7.25), for a total NP $[(\text{Ca}+\text{Mg})\text{CO}_3]$ loss of 8.9 g CaCO_3 equivalent $(\text{kg rock})^{-1}$. These values were in reasonable agreement with the 4.9 and 3.3 g CaCO_3 equivalent $(\text{kg rock})^{-1}$ values (8.2 g CaCO_3 equivalent $(\text{kg rock})^{-1}$ total) calculated based on respective releases of calcium and magnesium with drainage during 40 weeks of dissolution (Table A7.18). NP $[(\text{Ca}+\text{Mg})\text{CO}_3]$ losses based on respective changes in solid-phase CO_2 and LOI were calculated as 2.7 and 12 g CaCO_3 eq $(\text{kg rock})^{-1}$. These calculations assumed all LOI loss occurred as CO_2 and that, for both calculations, 86% of the CO_2 was associated with calcium and magnesium (equation 20). These values are both disparate from those determined based on solid-phase changes in calcium and magnesium, as well as calcium and magnesium release to solution. The reason for this discrepancy is unclear. Replicate analyses of initial and leached phases should be conducted to provide insight into the extent of error introduced by sampling and analysis.

The ratio of magnesium to calcium release was 0.56 based on the change in solid-phase chemistry and 0.67 based on calcium and magnesium release to drainage. Assuming all calcium and magnesium release occurred during stoichiometric carbonate mineral dissolution, these ratios represent the Mg:Ca ratio in the carbonate. This suggests that the Ca and Mg were released from a carbonate mineral closer in composition to $\text{Ca}(\text{Mg}_{0.65}, \text{Fe}_{0.35})(\text{CO}_3)_2$ than $\text{Ca}(\text{Mg}_{0.75}, \text{Fe}_{0.25})(\text{CO}_3)_2$ (see presentation in third paragraph above).

It should be noted that the new set of low NP $[(\text{Ca}+\text{Mg})\text{CO}_3]$ samples produced acid more rapidly than the original set (see rates of sulfate release section below). If the ferroan dolomite occurrence in the two sets of samples is similar, its capacity to maintain drainage pH above 6.0 for the original set of samples may be higher than the 31% maximum observed. Previous discussion suggests the

capacity of the ferroan dolomite to maintain drainage pH of at least 6.0 may be kinetically limited. Therefore, at slower rates of acid production this capacity will increase.

Non-Carbonate Mineral Neutralization. Assuming host rock mineralogy similar to the original three tuffaceous-sedimentary samples, the non-carbonate minerals capable of neutralizing acid were illite and potassium feldspar (Table 5). Drainage pH values from the samples with $\text{NP}(\text{CO}_2) < 1 \text{ g CaCO}_3 \text{ equivalent (kg rock)}^{-1}$ were generally lower than those from the samples containing measurable CO_2 . Minimum observed values decreased from 2.6 to 2.1 with increasing sulfur content. This indicates that the illite and potassium feldspar did not provide appreciable acid neutralization.

Drainage from samples with $\text{CO}_2 < 0.05\%$ exhibited lower calcium and magnesium concentrations and higher potassium concentrations than those from samples containing measurable CO_2 . Sodium concentrations from the two sets of solids were roughly equal (Table 12). The lower calcium and magnesium concentrations reflect the lower ferroan dolomite content of the low CO_2 samples. Higher sodium and potassium concentrations from the low CO_2 samples might be expected, due to the lower pH levels. At lower pH the dissolution of illite and potassium feldspar would be expected. In particular, the elevated calcium release from the 2.13% sulfur sample may have been due to accelerated illite dissolution at the low pH generated by this sample (Table 12).

Rates of sulfate release. The rates of sulfate release from the low NP tuffaceous-sedimentary samples, normalized for pyrite content, ranged from 67 to 212 $\text{mmol SO}_4 \text{ (kg FeS}_2 \cdot \text{week)}^{-1}$. These rates were roughly 7 to 40 times those observed for the original tuffaceous-sedimentary samples (Table 9). The elevated rates may be due to microbially mediated catalysis of pyrite oxidation. Drainage pH values commonly in the range of 2.2 to 3.5 support this contention. Furthermore, the low initial drainage pH observed for the highest NP samples suggests that acidic conditions may have existed in the microenvironment of the pyrite, despite higher drainage pH values during the first 20 weeks. It is also possible that the pyrite surface area in the new samples was greater than that in the original samples, although the low NP samples were coarser than the originals (see section 5.3.2.).

5.4. USGS AML Weathered Waste Rock Sample

5.4.1. Solid-Phase Analyses

Particle size determinations indicated the USGS AML sample was coarser than both the mafic-intrusive and tuffaceous-sedimentary rocks. 76 percent of the sample occurred in the -1/4-in/+20M fraction, 84 percent was coarser than 48 mesh, and 6 percent finer than 200 mesh (Table 2).

Chemical analyses of the USGS AML sample revealed a sulfide content of 13 percent as compared to an evolved CO_2 content of 20.9 percent (Table 3). Lead and zinc concentrations are highly elevated in the sample (1.7 and 4.2 percent, respectively). The respective mole percentages (percent composition divided by molecular weight) of sulfide, lead, and zinc are 0.405, 0.0082, and 0.064. Assuming these metals occur entirely as sulfides indicates that 82 percent of the sulfur (10.7 percent of rock) is associated with iron, and the resultant $\text{AP}(\text{FeS}_2)$ is $334 \text{ g CaCO}_3 \text{ equivalent (kg rock)}^{-1}$.

Copper and cadmium are also relatively high, with reported levels of 460 and 350 ppm, respectively. Concentrations of other trace metals are typically lower than 10 ppm (Table 4).

Mineralogical information on the USGS AML sample included the following description (Appendix 1, Attachment A1.1).

The sample is composed of relatively coarse grained siderite, pyrite, sphalerite, and galena plus a number of secondary sulfates, iron oxides, carbonates, and silicates (?). The crushed mineral grains available are surprisingly fresh looking considering that this material has reportedly been stockpiled for about eighty years. The secondary minerals tend to be soft/friable materials that break up easily on crushing and are relatively concentrated in the finer grained size fractions (Photos A1.11. - A1.14.).

The USGS AML sample is composed largely of siderite (52.1%), pyrite (17.3%), sphalerite (10%), and goethite (8%). Minerals present at levels of 1 to 3 percent include melanterite, quartz, kaolinite, galena, and gypsum (Table 5). Whereas the majority of sulfur was associated with pyrite, additional sulfide is associated with sphalerite and galena. It should be noted that the mineralogical balance used a 26% iron content for sphalerite. This is at the upper end of the range reported in the literature for sphalerite and indicates an iron sulfide content of 4.1% (1.5% S associated with iron), in addition to the pyrite. Sulfate minerals present included melanterite, gypsum, and anglesite.

The vast majority of the carbonate is present as siderite comprised of FeO (39.5 wt%), MnO (17.1 wt%), MgO (4.1 wt%), CaO (0.06 wt%) and CO₂ (39.3 wt%) (Mattson 2000). Although the iron and manganese carbonate fractions of the siderite do not neutralize acid under oxidizing conditions, the calcium and magnesium carbonate fractions do contribute NP. The calcite content was only 0.2 percent. The respective NP[(Ca+Mg)CO₃] of the siderite and calcite are 53 and 2 g CaCO₃ equivalent (kg rock)⁻¹, yielding a total NP[(Ca+Mg)CO₃] of 55 g CaCO₃ equivalent (kg rock)⁻¹.

The sulfides present are coarser grained than those in the mafic-intrusive and tuffaceous- sedimentary samples, and are “reasonably well liberated” in the -35 mesh fractions. Overall, 18 percent of the pyrite and 24 percent of the carbonates were reported to be liberated (Table 6). Largely due to the high pyrite content and low calcium/magnesium carbonate content, the available AP is well in excess of the available NP (Table 7).

5.4.2. Drainage Quality Results for the MN DNR Method

As with the mafic-intrusive and tuffaceous-sedimentary rocks, drainage quality data indicated that the dissolution of carbonate minerals in the USGS AML sample was adequate to neutralize the acid produced by iron sulfide mineral oxidation (Table 8). Drainage pH increased from values near 6.7 in the initial rinse to about 7.9 at about week 80 then typically remained in the range of 7.8 to 8.0 through the 158-week period of record (Figure 17). Alkalinity increased from 10 initially to 70 mg/L as CaCO₃ at about week 90, then plateaued (Figure 17).

Sulfate concentrations averaged about 100 mg/L and were at the upper end of those observed for the previously discussed rock types (Table 8). As was the case with the other rock types, concentrations decreased relatively rapidly over the first 40 weeks and more slowly subsequently (Figure 17). The rate of sulfate release ($0.53 \text{ mmol (kg rock}\cdot\text{week)}^{-1}$) was at the upper end of the samples tested (Table 9). This sample also had the highest sulfur content and, when the rate was normalized for pyrite content, it was close to the average for the mafic-intrusive rocks (3.0 vs $3.3 \text{ mmol SO}_4 \text{ (kg FeS}_2\cdot\text{week)}^{-1}$, Table 9).

The calcium concentrations in drainage from the USGS AML sample were lower than those from the mafic-intrusive and tuffaceous-sedimentary samples (Table 8). Calcium concentrations decreased rapidly over the first 16 weeks and fairly steadily until week 36 (Figure 17). The mass of calcium release over the first 16 weeks was 27 mmol or 1080 mg (Appendix 4, Table A4.15). This suggests the more rapid calcium release during this period may have been due to dissolution of the 0.2 percent calcite (802 mg Ca) present in this sample. It should be noted that this calculation assumes all calcium release was from carbonates and ignores calcium release from other minerals such as gypsum (0.9%, containing 2100 mg Ca). Reflecting the trend observed for calcium concentrations, the rate of calcium release from the USGS AML sample was lower than all rates observed for the mafic-intrusive and tuffaceous-sedimentary samples (Table 9).

Magnesium concentrations in drainage from the USGS AML sample were higher than those from the mafic-intrusive and tuffaceous-sedimentary samples. These concentrations were fairly constant after week 5 (Figure 17). After week 62, the molar ratio of calcium to magnesium release rates was 0.071:1, much lower than the range of 1.2:1 to 1.9:1 observed for the mafic-intrusive and tuffaceous-sedimentary samples (Table 9).

Manganese and zinc concentrations in drainage from the USGS AML sample were much higher than those observed for the mafic-intrusive and tuffaceous-sedimentary samples (Table 8). Although these values decreased over time, the respective concentrations were approximately 0.5 and 0.1 after 158 weeks (Table A3.17). Arsenic and antimony were below detection (0.010 mg/L) (Table 8). Cadmium and lead concentrations were detectable throughout the experiment and decreased over time. Respective concentrations at 158 weeks were approximately 0.005 and 0.01 mg/L.

5.4.3. Extent of Sample Dissolution

The initial $\text{AP(S}_T\text{)}$ and $\text{NP}[(\text{Ca}+\text{Mg})\text{CO}_3]$ of the USGS AML sample were 427 and 55 g CaCO_3 equivalent $(\text{kg rock})^{-1}$, respectively. These values each decreased by 12 and 15 g CaCO_3 equivalent $(\text{kg rock})^{-1}$ during the 158 weeks of dissolution testing (Table 10). If the calcium and magnesium carbonates were 100% available, about 450 additional weeks of dissolution would be required for their depletion. The samples would have acidified already if the carbonate mineral availabilities were near the minimum estimated (Table 11). This indicates that liberated calcium and magnesium carbonates were not the only calcium and magnesium carbonates contributing to acid neutralization.

5.5. Assessment of Dissolution Test Methods

The following summarizes assessment of the MN DNR method on mafic-intrusive and tuffaceous-sedimentary rocks and the USGS AML sample. This assessment is presented in more detail, including additional rock types, in a report comparing test methods (Lapakko et al. 2002a).

5.5.1. Comparison of MN DNR and ASTM Methods

Three samples of the original study samples were subjected to dissolution by both ASTM and MN DNR methods: the 7.05-percent sulfur mafic-intrusive sample, the 3.75-percent sulfur tuffaceous-sedimentary sample, and the USGS AML sample. For the mafic-intrusive and tuffaceous-sedimentary samples, the ASTM method produced a drainage pH value 0.07 units lower than the average value for the MN DNR cells (Table 13). In contrast, for the USGS AML sample the ASTM method produced a final pH which was 0.3 units higher than that for the MN DNR method (Table 13). For all three samples the MN DNR method produced higher alkalinities (Table 8). For the mafic-intrusive and tuffaceous-sedimentary samples this difference was substantial (106 vs 56 mg/L as CaCO₃ and 61 vs 37 mg/L as CaCO₃ averages for weeks 72-102, Table 8).

Although there were differences in the sulfate release rates produced by the two methods, there was no consistent trend. For the mafic-intrusive and USGS AML samples, sulfate release rates at the end of the test with the MN DNR method were 37% and 21% higher than those with the ASTM method. In contrast, the sulfate release rate from the tuffaceous-sedimentary rock with the ASTM method was 21% higher than that with the MN DNR method (Table 13). Based on these data, it cannot be concluded that the ASTM method enhanced acid production relative to the MN DNR method.

The dissolution of calcium and magnesium carbonate minerals is driven, in part, by the acid produced as a result of iron sulfide mineral oxidation. Consequently, the dissolution rate of calcium and magnesium carbonates tended to increase as the rate of iron sulfide oxidation increased (Table 13). To partially account for this influence, the ratio of the sum of calcium and magnesium release rates to the sulfate release rate was calculated. The calcium and magnesium carbonate dissolved per mole of sulfate released in the ASTM method was less than or, in the case of the USGS AML sample, roughly equal to that in the MN DNR method. This, in conjunction with the higher alkalinities observed for the MN DNR method, suggests that the MN DNR method enhanced dissolution of calcium and magnesium carbonates.

The MN DNR method retained more water in the rock pores and this may have affected carbonate mineral dissolution. Water retention in the MN DNR cells one day after the rinse water addition was about 25 percent greater than that in the ASTM cells (Table 14). Although the reason is unknown, the MN DNR cells started the cycle with a higher water content. The water content of the MN DNR cells was fairly constant during the cycle, with average retention decreasing by only 6 to 10 mL during the week. In contrast, the water content of the ASTM cells decreased by 68 to 89 mL during the dry air cycle and increased by roughly 4 to 13 mL during the wet air cycle (Table 14). Consequently, at the end of the seven day cycle, the average water content of the MN DNR cells was

about two to four times that of the ASTM cells. This difference was even larger at the end of the ASTM dry air cycle, since the water content in the ASTM cells increased by about 10 to 23 mL during the wet air cycle (Table 14).

The lower water content in the ASTM cells may have limited transport of acidic reaction products from the surfaces of iron sulfides to calcium and magnesium carbonates. Releases of calcium, magnesium and alkalinity were typically lower in the ASTM cells (Tables 13, 8). In practical terms the ASTM method may underestimate acid neutralization in the interior of waste rock piles where the water content is at field capacity. Similarly, the MN DNR method would overestimate acid neutralization near the surface of waste rock piles, where residual moisture is removed by evaporation. There was no apparent affect of the differences in water content on rates of sulfate release.

Drainages from the mafic-intrusive and tuffaceous-sedimentary rocks were initially elevated in manganese, antimony, arsenic and zinc concentrations. Concentrations of these solutes were not greatly disparate for the two methods (Tables A3.5-A3.7, A3.14-A3.16). The USGS AML sample yielded elevated concentrations of manganese, zinc, lead and cadmium. Concentrations of these metals tended to be higher with the MN DNR method than with the ASTM method (Tables A3.17, A3.18).

5.5.2. Replication of MN DNR Method

The MN DNR method was used in duplicate for one mafic-intrusive sample (102 weeks), one original tuffaceous-sedimentary sample (102 weeks), and two low NP tuffaceous-sedimentary samples (20 weeks). Final pH values and rates of sulfate, calcium and magnesium release were in good agreement. For the mafic-intrusive and tuffaceous-sedimentary samples with 102-week periods of record, final pH values were within 0.1 units. For the final period of rate calculations (weeks 72-102) rates of sulfate, calcium and magnesium release were within 10 percent of their respective mean values.

Duplicates of two of the new low NP[(Ca + Mg)CO₃] samples were subjected to dissolution testing for 20 weeks. The differences in minimum drainage pH for the two pairs were 0.07 and 0.13 units (Tables A7.11-A7.14). Rates of sulfate, calcium and magnesium release from week 12 to 20 also replicated well, with percent differences from the mean ranging from 1.9 to 8.7 percent (Table 9).

6. SUMMARY

The objectives of this study were as follows.

1. Describe the temporal variation of drainage quality, particularly pH, for the mafic-intrusive, tuffaceous-sedimentary, and weathered waste rock (USGS AML sample) lithologies.
2. Determine the rates of sulfate, calcium, and magnesium release from the eleven samples.
3. Relate the drainage pH and rates of release to the solid-phase composition of the eleven samples.
4. Estimate the time to acidification for drainages from the aforementioned rock samples.

Particle size distribution, chemistry, mineral content, and extent of sulfide and carbonate mineral liberation were determined for all samples. Sulfur contents for the mafic-intrusive, tuffaceous-sedimentary and USGS AML weathered waste rock samples were 6.05 - 9.05, 1.31 - 1.37, and 13.7 percent respectively. Approximately 80 to 100 percent of the sulfur was present as pyrite. The calcium and magnesium carbonate contents of the samples ranged from 37 to 114 g CaCO₃ equivalent (kg rock)⁻¹.

Samples were subjected to dissolution testing for 168 (five mafic-intrusive, two tuffaceous-sedimentary), 158 (USGS AML) or 102 (two mafic-intrusive, one tuffaceous-sedimentary) weeks. Drainage pH values for the mafic-intrusive and tuffaceous-sedimentary samples were typically in the range of 7.8 to 8.2 and tended to increase over the first 30 to 50 weeks then plateau. Drainage pH values from the USGS AML sample increased from about 7 to 7.8 over the first 80 weeks then plateaued. Concentrations of sulfate, calcium, and magnesium in drainage from all samples tended to decrease slowly over time.

The rates of sulfate release generally increased as sulfur content increased (Figure 19) and, when normalized for pyrite content, ranged from 1.1 to 10 mmol SO₄ (kg FeS₂•week)⁻¹. The average rate for the five remaining mafic-intrusive samples was 3.3 mmol SO₄ (kg FeS₂•week)⁻¹ (1.1 to 5.0), as compared to 7.8 mmol SO₄ (kg FeS₂•week)⁻¹ (5.5 and 10) for the two remaining tuffaceous-sedimentary samples and 3 mmol SO₄ (kg FeS₂•week)⁻¹ for the USGS AML weathered waste rock sample. It is interesting to note that the sulfate release rate for the USGS AML sample is not greatly dissimilar from rates for the rocks which have not been subjected to extensive weathering in the environment. One might expect that the rate would be lower for the USGS AML sample due to the accumulation of reaction products on sulfide mineral surfaces during roughly ninety years of weathering in the environment. Rates of calcium plus magnesium release tended to increase with sulfate release and were 1.4 to 2.5 times those of sulfate release. This reflected calcium and magnesium carbonate dissolution increasing with increasing acid generation resulting from pyrite oxidation.

The drainage pH values, as well as release of alkalinity, calcium and magnesium, indicated that dissolution of calcium and magnesium carbonate minerals was controlling drainage pH, despite the acid production resulting from pyrite oxidation. This is quantitatively supported by the observation

that the sum of calcium release (reflecting dissolution of calcium and magnesium carbonates) consistently exceeded the rate of sulfate release (reflecting the oxidation of pyrite and consequent acid production).

The additional dissolution time required to deplete the calcium and magnesium carbonates, assuming total carbonate availability, ranged from 200 to 1600 weeks. However, it is unlikely that all carbonates will be available. Using percent carbonate liberation to estimate minimum availability, the dissolution times for calcium/magnesium carbonate mineral depletion were estimated as 0 to 144 weeks. The zero value was calculated for six samples, and indicates that the calcium/magnesium carbonate dissolution exceeded that present in liberated carbonate minerals. Drainage from these samples have not acidified. Thus, it is reasonable to assume that calcium/magnesium carbonate availability exceeds that present in the liberated carbonates.

To gain more timely insight on the availability of calcium and magnesium carbonates in tuffaceous-sedimentary rock and, consequently better estimate the dissolution time required for drainage acidification, six low-NP tuffaceous-sedimentary samples were collected, characterized (particle size distribution, chemistry) and subjected to dissolution testing. The objectives of this experiment were as follows.

1. Determine the availability of calcium and magnesium carbonate minerals to dissolve and maintain drainage pH above 6.0.
2. Determine the ability of non-carbonate host rock minerals to neutralize acid generated by pyrite in the samples.

Testing of tuffaceous-sedimentary samples with NP[(Ca+Mg)CO₃] values ranging from 5.1 to 19 g CaCO₃ equivalent (kg rock)⁻¹ indicated that 0 to 31% of the NP[(Ca+Mg)CO₃] dissolved to maintain drainage pH of at least 6.0. SEM examination of a rock sample collected after dissolution tests were terminated indicated that some of the unavailable ferroan dolomite was largely included within rock particles. Portions exposed to drainage dissolved over the course of 40 weeks of testing, and it appeared this dissolution extended along the dolomite into the interior of the rock particle over time. It suggests that the dissolution of the ferroan dolomite slowed over time, as a result of decreased accessibility of acid to the carbonate mineral (as the reaction front progressed into the rock particle interior).

The original set of tuffaceous-sedimentary samples produced acid roughly 7 to 40 times slower than the new samples. Consequently, assuming similar modes of ferroan dolomite occurrence, availability of the ferroan dolomite in the original samples to maintain pH of at least 6.0 would be expected to exceed that observed for the new samples. The finer particle size of the original samples would also tend to increase this availability.

For the MN DNR method, drainage from the mafic-intrusive and tuffaceous-sedimentary samples initially contained elevated concentrations of manganese, antimony, arsenic and zinc. These concentrations generally decreased below detection over time. The USGS AML weathered waste

rock sample produced drainage with detectable concentrations of manganese, zinc, cadmium and lead throughout the 158-week period of record.

7. ACKNOWLEDGMENTS

Bill White of the US BLM Salt Lake City Office was largely responsible for segregating the original mafic-intrusive and tuffaceous-sedimentary rock samples, providing initial mineralogical descriptions of the samples, and collecting the low NP samples. John Folman conducted laboratory dissolution experiments, with assistance from Anne Jagunich and Patrick Geiselman. Mr. Folman was responsible for data input and, with Andrea Johnson, producing appendix tables and generating figures throughout the report.

8. REFERENCES

- Alpers, C.N. 2000. Email communication from Charles Alpers, USGS, 12 May 2000.
- Alpers, C. N., Blowes, D. W., Nordstrom, D. K., Jambor, J. L. 1994. Secondary minerals and acid-mine water chemistry. In Short Course Handbook on Environmental Geochemistry of Sulfide Mine Wastes, Waterloo, Ontario, May 1994. Mineralogical Association of Canada. pp. 247-270.
- American Public Health Association (APHA), American Water Works Association, Water Environment Federation. 1992. Standard Methods for the Examination of Water and Waste water, 18th edition. American Public Health Association, Washington, D.C.
- ASTM. 2000. D5744-96, Standard test method for accelerated weathering of solid materials using a modified humidity cell. Annual Book of ASTM Standards, 11.04. American Society for Testing and Materials, West Conshohocken, PA. p. 257-269.
- Biggs, F.R. 1989. Telephone conversation with Fred Biggs, Mining Engineer, Spokane Research Center, U.S. Bureau of Mines.
- Brown, R. 1989. Water management at Brenda Mines. In Proc. of the Thirteenth Annual British Columbia Mine Reclamation Symposium. June 7-9, 1989, Vernon, British Columbia. p. 8-17.
- Busenberg, E., Clemency, C. 1976. The dissolution kinetics of feldspars at 25° C and 1 atmosphere CO₂ partial pressure. *Geochim. Cosmochim. Acta* 40: 41-49.
- Busenberg, E., Plummer, L.N. 1986. A comparative study of the dissolution and crystal growth kinetics of calcite and aragonite. *U.S. Geol. Surv. Bull.* 1578. pp. 139-168.
- Cravotta, C. A. 1994. Secondary iron-sulfate minerals as sources of sulfate and acidity: Geochemical evolution of acidic ground water at a reclaimed surface coal mine in Pennsylvania. In Environmental Geochemistry of Sulfide Oxidation; ACS Symposium Series 550; American Chemical Society: Washington, DC, 1993. pp. 343-364.
- Crock, J.G., Lichte, F.E., Briggs, P.H. 1983. Determination of elements in National Bureau of Standards' geological reference materials SRM 278 obsidian and SRM 688 basalt by inductively coupled argon plasma-atomic emission spectrometry: *Geostandards Newsletter*, 7. p. 335-340.
- Drever, J.I. 1988. *The geochemistry of natural waters*: Prentice Hall, Englewood Cliffs, New Jersey, 437 p.
- Guard, G. 1997. Humidity cell testing - an experimental and theoretical approach. University of Utah, Department of Chemical and Fuels Engineering, MS Thesis, June 1997. 105 p.

Hem, J.D. 1970. Study and interpretation of the chemical characteristics of natural water. Geological Survey Water-Supply Paper 1473, Washington, D.C. 363 p.

Hoffman, E.L. 1992. Instrumental neutron activation in geoanalysis. Jour. Geochem. Explor., 44. p. 297-319.

Iversen, I.R., Johannessen, M. 1987. Water pollution from abandoned mines in Norway. Report to the Norwegian State Pollution Control Authority and The Ministry of Industry by the Norwegian Institute for Water Research. 60 p.

Jambor, J.L. 1994. Mineralogy of sulfide-rich tailings and their oxidation products. In Environmental Geochemistry of Sulfide Mine-Wastes. Mineralogical Association of Canada, Short Course Handbook, Volume 22. p. 59-102.

Kleinmann, R.L.P., Crerar, D.A., Pacelli, R.R. 1981. Biogeochemistry of acid mine drainage and a method to control acid formation. Mining Eng. March 1981.

Kwong, Y.T.J., Ferguson, K.D. 1990. Water chemistry and mineralogy at Mt. Washington: Implications to acid generation and metal leaching. In Acid Mine Drainage: Designing for Closure. (J.W. Gadsby, J.A. Malick & S.J. Day, eds). Bitech Publishers, Vancouver, British Columbia. p. 217-230.

Lapakko, K. A. 1988. Prediction of acid mine drainage from Duluth Complex mining wastes in northeastern Minnesota. In Mine Drainage and Surface Mine Reclamation. v. 1. Mine Water and Mine Waste. Proceedings of the 1988 Mine Drainage and Surface Mine Reclamation Conference. BuMines IC 9183. pp. 180-190.

Lapakko, K.A. 1990. Regulatory mine waste characterization: A parallel to economic resource evaluation. In Mining and Mineral Processing Wastes, Proceedings of the Western Regional Symposium on Mining and Mineral Processing Wastes. Fiona Doyle, ed. Berkeley, California, May 30 - June 1, 1990. p. 31-39.

Lapakko, K.A. 1991. Non-ferrous mine waste characterization project. MN Dept. Nat. Resour., Div. of Minerals. St. Paul, MN. 68 p. plus appendices.

Lapakko, K.A. 1993. Field dissolution of test piles of Duluth Complex rock. Report to the US Bureau of Mines Salt Lake City Research Center. 41 p. plus appendices.

Lapakko, K.A. 1994. Comparison of Duluth Complex rock dissolution in the laboratory and field. In Proceedings of the International Land Reclamation and Mine Drainage Conference on the Abatement of Acidic Drainage, Pittsburgh, PA, April 24-29, 1994. pp. 419-428.

Lapakko, K.A. 1998a. Laboratory drainage quality from siltite-argillite rock. Progress report on Contract BLM JP10P72015 to the U.S. Bureau of Land Management, Salt Lake City Office. 11 February 1998. 41 p. plus appendices.

Lapakko, K.A. 1998b. Laboratory drainage quality from Duluth Complex rock and assessment of test methods for waste rock dissolution. Final report on Contract BLM JP910P72015 to the U.S. Bureau of Land Management, Salt Lake City Office. 30 April 1998. 18 p. plus appendices.

Lapakko, K.A. 1998c. Laboratory drainage quality from mafic-intrusive, tuffaceous-sedimentary, and weathered waste rocks. Progress report on Contract BLM JP910C82009 to the U.S. Bureau of Land Management, Salt Lake City Office. 30 November 1998. 20 p. plus appendices.

Lapakko, K.A. 1999a. Laboratory drainage quality from siltite-argillite rock. Final Appendices for Contract BLM JP10P82009, U.S. Bureau of Land Management, Salt Lake City Office. 1 March 1999.

Lapakko, K.A. 1999b. Laboratory drainage quality from Duluth Complex rock and assessment of test methods for waste rock dissolution. Progress report on Contract BLM JP910C82009 to the U.S. Bureau of Land Management, Salt Lake City Office. 30 June 1999. 32 p. plus appendices.

Lapakko, K.A. 1999c. Laboratory drainage quality from mafic-intrusive, tuffaceous-sedimentary, and weathered waste rocks. Final report on Contract BLM JP910C82009 to the U.S. Bureau of Land Management, Salt Lake City Office. 30 June 1999. 32 p. plus appendices.

Lapakko, K.A. 2000. Laboratory drainage quality from siltite-argillite rock. Final Appendices for Contract BLM JP910P82018 for the U.S. Bureau of Land Management, Salt Lake City Office. August 2000.

Lapakko, K. A., Antonson, D. A. 1994. Oxidation of sulfide minerals present in Duluth Complex rock: A laboratory study. In Environmental Geochemistry of Sulfide Oxidation; ACS Symposium Series 550; American Chemical Society: Washington, DC, 1993. pp. 593-607.

Lapakko, K.A., Antonson, D.A. 2000a. Laboratory drainage quality from mafic-intrusive, tuffaceous-sedimentary, and weathered waste rocks. Final Report on Contract J910P82018 to the U.S. Bureau of Land Management Utah State Office. 64 p. plus appendices.

Lapakko, K.A., Antonson, D.A. 2000b. Laboratory drainage quality from Duluth Complex rock and assessment of test methods for waste rock dissolution. Final report on Contract BLM JP910C82018 to the U.S. Bureau of Land Management, Salt Lake City Office. 54 p. plus appendices.

Lapakko, K.A., Antonson, D.A., Folman, J.T., Johnson, A.M. 2002a. Laboratory drainage quality from Duluth Complex rock and assessment of test methods for waste rock dissolution. Final report on Contract BLM JSP012002 to the U.S. Bureau of Land Management, Salt Lake City Office.

Lapakko, K.A., Antonson, D.A., Folman, J.T., Johnson, A.M. 2002b. Laboratory drainage quality from Archean greenstone rock. Final report on Contract BLM JSP012002 to the U.S. Bureau of Land Management, Salt Lake City Office.

Lapakko, K.A., Antonson, D.A., Wagner, J.R. 2000. Mixing of rotary kiln fines with finely-crushed acid-producing rock. In Proc. Fifth International Conference on Acid Rock Drainage. SME, Littleton, CO. p. 901-910.

Lapakko, K.A., Antonson, D.A., Wagner, J.R. 1997. Mixing of limestone with finely-crushed acid-producing rock. In Proc. Fourth Intl. Conf. On Acid Rock Drainage. Vol. 3, Vancouver, British Columbia, Canada, May 31 - June 6, 1997. p. 1345-1360.

Lapakko, K.A., White, W.W. III. 2000. Modification of the ASTM D5744-96 kinetic test. In Proc. from the Fifth International Conference on Acid Rock Drainage. SME, Littleton, CO. p. 631-639.

Lin, C.K. 1996. Modeling Acid Mine Drainage. Ph.D. dissertation, U of Utah, Salt Lake City, UT.

Lin, C.K., Trujillo, E.M., White, W.W. III. 1997. A three-dimensional, three-phase geochemical kinetic model for acid rock drainage. In Proceedings of the Fourth International Conference on Acid Rock Drainage. Vancouver, B.C., Canada. May 31-June 6, 1997. p. 479-495.

Mattson, L. 2000. Personal conversation with Louis Mattson of Mineralogical Consulting Service, Pengilly, MN.

Morin, K. A. and Hutt, N. M. 1994. Observed preferential depletion of neutralization potential over sulfide minerals in kinetic tests: Site specific criteria for safe NP/AP ratios. In Proceedings of the International Land Reclamation and Mine Drainage Conference on the Abatement of Acidic Drainage, Pittsburgh, PA, April 24-29, 1994. p. 148-156.

Nelson, M.B. 1978. Kinetics and mechanisms of the oxidation of ferrous sulfide. Ph.D. Thesis, Stanford University, Palo Alto, CA. 286 p.

Nesbitt, H.W., Jambor, J.L. 1998. Role of mafic minerals in neutralizing ARD, demonstrated using a chemical weathering methodology. In Cabri, L.J. and Vaughan, D.J. (eds.), Modern Approaches to Ore and Environmental Mineralogy. Mineralogical Association of Canada Short Course Series, v. 27. p. 403-421.

- Nordstrom, D. K. 1982. Aqueous pyrite oxidation and the consequent formation of secondary iron minerals. *In* Acid Sulfate Weathering. J.A. Kittrick, D.S. Fanning, and L.R. Hossner (eds.), Soil Sci. Soc. America Spec. Pub. 10. p. 37-56.
- Nordstrom, D.K. 1999. Some fundamentals of aqueous geochemistry. *In* The Environmental Geochemistry of Mineral Deposits. Part A: Processes, Techniques, and Health Issues. Vol. 6A, Chapter 4. Reviews in Economic Geology. Society of Economic Geologists, Inc., Chelsea, MI. p. 117-123.
- Nordstrom, D.K., Alpers, C.N. 1999. Geochemistry of acid mine waters. *In* The Environmental Geochemistry of Mineral Deposits. Part A: Processes, Techniques, and Health Issues. Vol. 6A, Chapter 4. Reviews in Economic Geology. Society of Economic Geologists, Inc., Chelsea, MI. p. 133-160.
- Plumlee, G. 1999. The environmental geology of mineral deposits. *In* The Environmental Geochemistry of Mineral Deposits. Part A: Processes, Techniques, and Health Issues. Vol. 6A, Chapter 3. Reviews in Economic Geology. Society of Economic Geologists, Inc., Chelsea, MI. p. 71-116.
- Rauch, H.W., White, W. B. 1977. Dissolution kinetics of carbonate rocks 1. Effects of lithology on dissolution rate. *Wat. Resour. Res.*, v. 13, no. 2, pp. 381-394.
- Singer, P.C., Stumm, W. 1970. Acid mine drainage: The rate determining step. *Science*, 167. p. 1121-1123.
- Smith, K.S. 1998. Conversation with Kathleen Smith of the USGS, Denver, CO.
- Smith, K.S. 1999. Metal sorption on mineral surfaces: An overview with examples relating to mineral deposits. *In* The Environmental Geochemistry of Mineral Deposits. Part B: Case Studies and Research Topics. Vol. 6B, Chapter 7. Filipek, L., Plumlee, G. (Volume Eds). Reviews in Economic Geology. Society of Economic Geologists, Inc., Chelsea, MI. p. 161-182.
- Smith, K.S., Huyck, H.L.O. 1999. An overview of the abundance, relative mobility, bio-availability, and human toxicity of metals. *In* The Environmental Geochemistry of Mineral Deposits. Part A: Vol. 6A, Chapter 2. Plumlee, G., Logsdon, M. (Volume eds.). Reviews in Economic Geology. Society of Economic Geologists, Inc., Chelsea, MI. p. 29-70.
- Stumm, W., Morgan, J.J. 1981. Aquatic chemistry - An introduction emphasizing chemical equilibria in natural waters. John Wiley & Sons, Inc. 470 p.
- U.S. Bureau of Mines. 1985. Control of acid mine drainage. Proceedings of a Technology Transfer Seminar, U.S. Department of the Interior, BuMines IC 9027.

White III, W.W., Lapakko, K.A. 2000. Preliminary indications of repeatability and reproducibility of the ASTM D5744-96 kinetic test for drainage pH and sulfate release rate. In Proceedings from the Fifth International Conference on Acid Rock Drainage. SME, Littleton, CO. p. 621-630.

White, W. W. III, Jeffers, T. H. 1994. Chemical predictive modeling of acid mine drainage from metallic sulfide-bearing rock. In Environmental Geochemistry of Sulfide Oxidation; ACS Symposium Series 550; American Chemical Society: Washington, DC, 1993. p. 608-630.

White, W.W.III, Trujillo, E.M., Lin, C.K. 1994. Chemical predictive modeling of acid mine drainage from waste rock: Model development and comparison of modeled output to experimental data. In Proc. Int Land Reclamation and Mine Drainage Conf. And the Third Int. Conf. On Abatement of Acidic Drainage. Pittsburgh, PA, 1, 157.

Table 1. Acid producing and neutralizing potentials of mafic-intrusive and tuffaceous-sedimentary samples collected in 2000. Acid producing potential (AP) and neutralization potential (NP) expressed as g CaCO₃ equivalent (kg rock)⁻¹. Samples used for dissolution testing in **bold**. Analyses by Newmont Metallurgical Services, Englewood, CO.

Sample	Rock Type ¹	%S ²⁻	AP(S ²⁻)	NP(CO ₂)
control ²	NA	0.8	25	430
356	TS	1.09	34	0
357	TS	4.35	135	88
358	TS	4.09	127	100
359	TS	1.94	60	98
360	TS	2.50	78	49
361	TS	1.05	33	22
362	TS	1.28	40	4
363	TS	1.10	34	4.8
364	TS	0.26	7.9	0
365	TS	0.72	22	594
366	MI	0	0	79
367	MI	0	0	67
368	MI	1.18	37	137
369	MI	2.58	80	45
370	TS	1.91	59	0
371	TS	1.91	59	0
372	TS	1.80	56	0

¹ TS: tuffaceous-sedimentary; MI: mafic-intrusive

² Control: reference standard for analysis

Table 2. Particle size distribution of mafic-intrusive and Tuffaceous-sedimentary samples. (Analysis by Lerch Brothers, Inc.). Page 1 of 2.

SAMPLE	MS-1	MS-2	MS-3	MS-4	MS-5	MS-6	MS-7	MS-8	MS-9	MS-10
S _T	7.30%	7.05%	8.10%	6.75%	6.50%	9.05%	7.40%	3.90%	1.37%	1.31%
FRACTION	% Passing									
1/4"	100.0	100.0	100.0	100.0	100.0	100.0	100.0	100.0	100.0	100.0
4M	100.0	100.0	100.0	99.9	99.9	100.0	100.0	99.9	99.4	99.6
10M	80.2	82.5	79.2	80.9	81.6	81.5	77.0	65.5	63.6	58.5
20M	46.1	49.1	47.7	48.9	47.4	45.4	39.4	37.2	37.0	31.7
28M	38.3	41.2	40.3	41.5	39.9	37.7	32.1	30.2	29.5	24.8
35M	32.3	34.8	34.4	35.7	34.2	32.0	27.0	25.2	24.0	20.0
48M	25.2	26.4	27.2	29.5	28.1	25.9	21.8	20.5	19.0	15.7
65M	21.3	23.5	22.7	24.8	23.4	21.7	18.5	18.6	15.4	12.6
100M	16.0	17.6	17.0	10.9	18.1	16.9	13.9	13.7	11.6	9.9
150M	13.0	13.8	14.2	15.7	15.0	13.7	11.7	10.6	8.8	7.5
200M	9.5	10.8	10.2	12.2	12.0	10.4	9.1	8.8	7.0	5.8

Wet vs. dry sieving of MS-3 and MS-9, percent retained.

FRACTION	MS - 3		MS-9	
	DRY	WET	DRY	WET
-100M+150	2.8	1.2	2.8	1.9
-150M+200	4.0	2.0	1.8	1.4
-200M	10.2	13.8	7.0	8.3

Table 2. Particle size distribution of low NP tuffaceous-sedimentary and USGS AML samples. (Analysis by Lerch Brothers, Inc.). Page 2 of 2.

SAMPLE	356	361	362	363	364	370	USGS
S _T	1.16%	1.30%	1.47%	1.23%	0.33%	2.13%	13.70%
FRACTION	% Passing						
1/4"	99.4	98.6	99.3	100.0	100.0	99.1	100.0
4M	83.3	86.0	84.5	89.6	85.7	85.7	80.8
10M	34.0	35.2	32.8	42.6	35.5	39.6	38.2
20M	18.5	18.5	17.8	25.8	19.8	23.6	24.1
28M	13.6	13.6	13.3	19.6	14.7	18.1	19.8
35M	10.9	11.0	10.7	16.2	11.8	15.0	16.7
48M	8.2	8.4	8.1	12.4	8.9	11.8	13.8
65M	6.3	6.7	6.3	9.7	6.8	9.4	11.7
100M	4.8	5.3	4.9	7.6	5.2	7.5	9.7
150M							7.9
200M	2.7	3.3	2.8	4.5	2.9	4.6	6.4

Note: There was no 150 mesh screen used for the low NP tuffaceous-sedimentary samples.

Table 3. Whole rock chemistry of mafic-intrusive and tuffaceous-sedimentary samples (percent)
 (analysis by Actlabs, Inc.). Page 1 of 2.

	Mafic-intrusive							Tuffaceous-sedimentary		
	MS-5	MS-4	MS-2	MS-1	MS-7	MS-3	MS-6	MS-10	MS-9	MS-8
S _T	6.50	6.75 ⁵	7.05 ³	7.30 ²	7.40	8.10 ¹	9.05 ⁴	1.31	1.37	3.90
SO ₄	0.90	0.90	0.45	<0.05	<0.05	0.15	1.50	<0.05	<0.05	0.45
S ²⁻	6.20	6.45	6.90	7.29	7.39	8.05	8.55	1.30	1.36	3.75
CO ₂	5.85	4.45	4.10	4.45	2.84	2.15	2.62	1.92	3.35	4.05
CaO	6.01	4.92	4.29	3.04	4.33	3.76	4.17	1.69	2.45	3.34
MgO	2.02	1.72	1.40	1.21	1.23	1.04	1.13	0.80	1.34	1.68
Na ₂ O	0.09	0.08	0.07	0.07	0.09	0.09	0.09	0.03	0.04	0.05
K ₂ O	4.62	4.01	4.52	4.45	5.24	4.86	5.48	0.87	1.05	1.56
Fe ₂ O ₃	10.31	9.71	11.95	14.98	10.49	11.24	12.43	2.28	2.29	4.52
MnO	0.12	0.10	0.15	0.27	0.07	0.05	0.06	0.04	0.06	0.08
TiO ₂	2.81	2.55	3.08	3.04	3.38	3.31	3.39	0.14	0.14	0.60
P ₂ O ₅	1.47	1.38	1.38	1.52	1.77	1.67	1.73	0.35	0.15	0.49
Al ₂ O ₃	12.99	11.87	14.50	14.39	15.66	15.21	15.68	2.20	2.66	3.97
SiO ₂	47.66	52.89	47.08	44.28	46.64	47.60	44.06	88.81	85.50	76.16

NOTE: SO₄ reported as SO₄ as opposed to sulfur. Sulfide content calculated as S_T - SO₄/3. For sulfate concentrations reported as less than detection, 0.5 x the detection limit was used for the calculation.

Table 3. Whole rock chemistry of low NP tuffaceous-sedimentary and USGS samples (percent) (analysis by Actlabs, Inc.). Page 2 of 2.

Low NP tuffaceous-sedimentary							USGS
	356	361	362	363	364	370	
S _T	1.16	1.30	1.47	1.23	0.33	2.13	13.7
SO ₄	0.13	0.25	0.31	0.15	0.07	0.20	2.15
S ²⁻	1.03	1.05	1.16	1.08	0.26	1.93	12.98
CO ₂	<.05	0.95	0.29	0.26	<.05	<.05	20.90
CaO	0.38	0.93	0.50	0.60	0.15	0.37	0.45
MgO	0.20	0.47	0.26	0.30	0.14	0.79	2.12
Na ₂ O	0.05	0.04	0.03	0.03	0.02	0.06	<0.01
K ₂ O	1.00	0.70	0.90	0.96	0.69	3.92	0.04
Fe ₂ O ₃	2.00	2.21	2.42	2.23	0.89	3.92	43.68
MnO	0.006	0.028	0.011	0.015	0.006	0.011	9.53
TiO ₂	0.190	0.118	0.207	0.181	0.105	0.651	0.04
P ₂ O ₅	0.25	0.19	0.19	0.25	0.10	0.27	0.05
Al ₂ O ₃	2.81	2.00	2.43	2.46	1.74	9.68	0.84
SiO ₂	90.48	89.48	89.88	90.15	94.73	75.96	3.45

NOTE: SO₄ reported as SO₄ as opposed to sulfur. Sulfide content calculated as S_T - SO₄/3.

45

Table 4. Trace metal analysis (analysis by Actlabs, Inc., concentrations in ppm unless otherwise noted). Page 1 of 4.

	Mafic-intrusive							Tuffaceous-sedimentary		
	MS-5	MS-4	MS-2	MS-1	MS-7	MS-3	MS-6	MS-10	MS-9	MS-8
Ag	2.3	2.2	1.9	0.7	2.6	1.5	2.8	1.3	1.1	2.1
As	1330	1230	1530	1350	1850	1820	2070	245	260	494
Au (ppb)	1470	1930	1420	1120	1590	1370	1400	451	489	1230
Ba	268	244	256	233	314	290	311	87	104	156
Be	2	2	2	3	2	2	2	<1	<1	-1
Bi	<5	<5	<5	<5	<5	<5	<5	<5	<5	<5
Br	<1	<1	<1	<1	<1	<1	<1	<1	<1	<1
Cd	<0.5	<0.5	<0.5	<0.5	<0.5	<0.5	<0.5	<0.5	<0.5	<0.5
Co	16	16	19	20	17	20	19	4	3	7
Cr	38	58	38	21	27	38	32	229	141	137
Cs	15.6	14.0	20.2	21.6	22.1	20.9	22.3	2.3	2.9	4.1
Cu	15	17	19	23	16	20	17	10	11	14
Hf	6.0	5.6	6.6	6.6	6.7	6.8	6.2	0.7	0.9	1.6
Ir (ppb)	<5	<5	<5	<5	<5	<5	<5	<5	<5	<5
Mo	<5	<5	<5	<5	<5	<5	<5	<5	5	7
Ni	14	13	19	23	20	19	21	10	12	15
Pb	<5	<5	<5	<5	5	7	<5	<5	<5	5
Rb	117	115	138	161	145	139	145	<20	23	43
Sb	38.7	40.8	43.9	48.5	41.0	50.3	43.7	22.3	24.8	24.3
Se	<3	4	<3	<3	<3	<3	<3	<3	<3	<3

Table 4. Trace metal analysis (analysis by Actlabs, Inc., concentrations in ppm unless otherwise noted). Page 2 of 4.

	Mafic-intrusive							Tuffaceous-sedimentary		
	MS-5	MS-4	MS-2	MS-1	MS-7	MS-3	MS-6	MS-10	MS-9	MS-8
Sr	67	59	61	54	67	59	67	25	25	38
Ta	<1	<1	1	1	<1	<1	1	<1	<1	<1
V	109	112	116	107	120	128	127	53	75	60
W	26	23	36	50	28	29	29	5	7	7
Y	50	47	58	58	62	59	65	10	9	15
Zn	23	23	65	118	23	27	23	28	24	25
Zr	274	251	245	287	273	262	255	38	37	79
Ce	107	96	120	122	147	124	132	25	24	39
Eu	4.0	3.7	4.3	4.1	4.3	4.3	4.1	0.9	0.7	1.4
La	51.3	45.3	57.0	59.3	72.0	59.7	68.9	13.6	14.4	21.2
Lu	0.57	0.48	0.63	0.63	0.68	0.61	0.62	0.07	0.08	0.18
Nd	54	52	67	71	86	70	77	11	11	21
Sc	16.4	14.5	20.6	22.0	19.0	18.2	18.2	1.7	2.3	5.9
Sm	12.0	11.0	13.4	13.6	14.9	14.0	14.0	2.2	2.2	4.0
Tb	1.4	1.5	1.8	1.6	2.0	1.7	1.9	<0.5	<0.5	<0.5
Th	4.6	4.3	5.2	5.4	5.7	5.4	5.3	1.4	1.6	2.0
U	2.2	<0.5	<0.5	<0.5	<0.5	<0.5	1.3	1.1	1.6	0.9
Yb	3.4	3.3	4.2	4.6	4.5	4.3	4.7	0.5	0.5	1.1

Table 4. Trace metal analysis (analysis by Actlabs, Inc., concentrations in ppm unless otherwise noted). Page 3 of 4.

Low NP tuffaceous-sedimentary							USGS
	356	361	362	363	364	370	
Ag	9.6	5.1	8.0	11.0	5.6	3.1	20.0
As	120	297	390	230	53	284	94
Au (ppb)	905	1020	1840	1570	706	496	18
Ba	707	140	238	405	148	1060	7
Be	<1	<1	<1	<1	<1	2	<2
Bi	<2	<2	<2	<2	<2	<2	7
Br	<1	<1	<1	<1	<1	<1	<1
Cd	<0.3	1.5	9.3	1.2	<0.3	0.5	351.7
Co	9	6	8	6	2	10	2
Cr	463	549	552	543	468	167	43
Cs	5.3	4.4	4.3	5.0	4.1	8.9	<0.5
Cu	63	39	38	44	23	73	464
Hf	<0.5	<0.5	<0.5	<0.5	<0.5	4.1	<0.5
Ir (ppb)	<5	<5	<5	<5	<5	<5	<5
Mo	7	8	<5	5	<5	<5	<2
Ni	30	22	26	27	23	34	4
Pb	12	<3	6	9	<3	3	17117
Rb	35	<20	50	58	<20	113	<20
Sb	36.2	1250	2190	165	224	54.2	5.7
Se	<3	11	<3	<3	<3	<3	<3

Table 4. Trace metal analysis (analysis by Actlabs, Inc., concentrations in ppm unless otherwise noted). Page 4 of 4.

Low NP tuffaceous-sedimentary							USGS
	356	361	362	363	364	370	
Sr	na	na	na	na	na	na	4
Ta	<1	<1	<1	<1	<1	1	<1
V	na	na	na	na	na	na	4
W	na	na	na	na	na	na	4
Y	na	na	na	na	na	na	6
Zn	68	144	840	66	43	130	42070
Zr	50	41	45	53	31	192	9
Ce	28	26	18	26	10	42	5
Eu	0.7	<0.1	<0.1	0.9	0.4	0.7	0.2
La	17.4	14.7	14.3	16.1	6	25.4	2.7
Lu	0.11	<0.05	0.09	0.11	<0.05	0.34	0.09
Nd	11	10	<5	14	<5	20	<5
Sc	2.3	1.6	1.9	2	1	7.5	1
Sm	2.4	2.3	1.8	2.7	0.8	4.1	0.5
Tb	<0.5	<0.5	<0.5	<0.5	<0.5	<0.5	<0.5
Th	2.5	1.3	<0.05	1.8	1.2	7.5	1.3
U	2.9	2.5	<0.5	<0.5	<0.5	2.6	0.8
Yb	0.7	<0.05	0.09	0.11	<0.05	0.34	0.4

na - not analyzed

Table 5. Mineralogic composition. Page 1 of 2.

Mineral	Mafic-intrusive							Tuffaceous-sedimentary			USGS
	MS-1	MS-2	MS-3	MS-4	MS-5	MS-6	MS-7	MS-8	MS-9	MS-10	
	Weight Percent										
Pyrite	13.7	13.0	15.1	12.1	11.7	16.1	13.9	7.0	2.6	2.5	17.3
Marcasite	Tr	Tr	Tr	Tr	Tr	Tr	Tr	Tr	Tr	Tr	NR
Spalerite	NR	NR	NR	NR	NR	NR	NR	NR	NR	NR	9.6
Galena	NR	NR	NR	NR	NR	NR	NR	NR	NR	NR	1.9
Chalcopyrite	NR	NR	NR	NR	NR	NR	NR	NR	NR	NR	<0.1 ¹
Argentite	NR	NR	NR	NR	NR	NR	NR	NR	NR	NR	<0.1 ¹
Arsenopyrite	Tr	Tr	Tr	Tr	Tr	Tr	Tr	Tr	Tr	Tr	NR
Stibnite	<0.1	<0.1	<0.1	<0.1	<0.1	<0.1	<0.1	<0.1	<0.1	<0.1	NR
Melanterite	NR	NR	NR	NR	NR	NR	NR	NR	NR	NR	4.6 ²
Anglesite	NR	NR	NR	NR	NR	NR	NR	NR	NR	NR	<0.1
Gypsum	<0.1	0.2	0.1	1.6	0.5	0.9	<0.1	0.3	<0.1	<0.1	0.9
Barite	<0.1	<0.1	0.1	<0.1	0.1	0.1	0.1	<0.1	<0.1	<0.1	NR
Dolomite	10.5	9.0	4.4	9.7	12.7	5.6	6.0	8.6	7.1	4.1	NR
Calcite	Tr	Tr	Tr	Tr	Tr	Tr	Tr	Tr	Tr	Tr	0.2
Siderite	NR	NR	NR	NR	NR	NR	NR	NR	NR	NR	52.1
Cerussite	NR	NR	NR	NR	NR	NR	NR	NR	NR	NR	<0.1

¹ Not positively identified but probably present.

² May be mixed Fe-sulfates, exact compositions not determined.

³ Secondary iron oxides+goethite>>>>hematite>>akaganeite.

NR: Not reported

Tr: Trace

Table 5. Mineralogic composition. Page 2 of 2.

Mineral	Mafic-intrusive							Tuffaceous-sedimentary			USGS
	MS-1	MS-2	MS-3	MS-4	MS-5	MS-6	MS-7	MS-8	MS-9	MS-10	
	Weight Percent										
Fe Oxides	1.9	2.2	1.6	0.8	1.6	1.6	1.4	<0.1	0.4	0.5	NR
Magnetite	NR	NR	NR	NR	NR	NR	NR	NR	NR	NR	0.7
Hematite	NR	NR	NR	NR	NR	NR	NR	NR	NR	NR	NR ³
Goethite	NR	NR	NR	NR	NR	NR	NR	NR	NR	NR	8.0 ³
Akaganeite	NR	NR	NR	NR	NR	NR	NR	NR	NR	NR	NR ³
Rutile	3.0	3.1	3.3	2.6	2.8	3.4	3.4	0.6	0.1	0.1	NR
Quartz	15.7	18.0	16.4	27.5	19.8	10.7	14.0	67.4	79.6	83.9	2.4
K-Feldspar	<0.1	<0.1	<0.1	0.8	3.8	4.0	2.3	2.8	1.8	1.5	NR
Illite	50.2	50.1	54.7	41.4	43.2	53.2	54.2	11.8	7.8	6.4	NR
Kaolinite	1.1	0.8	<0.1	<0.1	<0.1	<0.1	0.2	0.3	0.2	0.1	2.1
Zircon	0.1	0.1	0.1	0.1	0.1	0.1	0.1	<0.1	<0.1	<0.1	NR
Apatite	3.8	3.5	4.2	3.4	3.7	4.3	4.4	1.2	0.4	0.9	NR
Carbon	?	?	?	?	?	?	?	<1 ?	1+/-	<1 ?	NR
Gold	<0.1	<0.1	<0.1	<0.1	<0.1	<0.1	<0.1	<0.1	<0.1	<0.1	NR

¹ Not positively identified but probably present.

² May be mixed Fe-sulfates, exact compositions not determined.

³ Secondary iron oxides+goethite>>>>hematite>>akaganeite.

NR: Not reported.

Table 6. Sulfide and carbonate mineral liberation.

Percent of Minerals Liberated from Rock Matrix

S _T Percent	Sample Number	Carbonate	Pyrite	Sphalerite	Galena	Total Sulfide
Mafic-intrusive						
6.50	MS-5	22	18	-	-	-
6.75	MS-4	22	18	-	-	-
7.05	MS-2	20	17	-	-	-
7.30	MS-1	16	15	-	-	-
7.40	MS-7	16	14	-	-	-
8.10	MS-3	20	17	-	-	-
9.05	MS-6	20	19	-	-	-
Tuffaceous-sedimentary						
1.31	MS-10	14	14	-	-	-
1.37	MS-9	13	12	-	-	-
3.90	MS-8	22	17	-	-	-
USGS						
13.7	USGS	24	18	18	16	34 ¹

¹ The total sulfide mineral liberation exceeded that of individual sulfide minerals since aggregates of sulfide minerals were observed. Whereas the individual minerals were not liberated, the aggregates were.

Table 7. Estimation of minimum available AP (S^{2-}) and NP $[(Ca+Mg)CO_3]$.

Parameter	Mafic-intrusive							Tuffaceous-sedimentary			USGS
	MS-5	MS-4	MS-2	MS-1	MS-7	MS-3	MS-6	MS-10	MS-9	MS-8	
S_{TOT} , pct	6.50	6.75	7.05	7.30	7.40	8.10	9.05	1.31	1.37	3.90	13.7
S^{2-} , pct ¹	6.20	6.45	6.90	7.30	7.40	8.05	8.55	1.31	1.37	3.75	13.0
FeS ₂ , pct	11.6	12.1	13.0	13.6	13.9	15.1	16.0	2.4	2.5	7.0	17.3
FeS ₂ liberated, pct	18	18	17	15	14	17	19	14	13	17	18
AP (S^{2-}) ²	193	201	215	228	231	251	267	41	43	117	334 ²
Available AP (S^{2-}) ^{2,3}	35	36	37	34	32	43	51	5.7	5.6	20	60

CO ₂ , pct	5.85	4.45	4.10	4.45	2.84	2.15	2.62	1.92	3.35	4.05	20.90
Ferroan dolomite, pct	12.7	9.7	9.0	10.5	6.0	4.4	5.6	4.1	7.1	8.6	5.5 ⁵
Dolomite liberated, pct	22	22	20	16	16	20	20	14	12	22	24 ⁵
NP (CO ₂) ²	133	101	93	101	65	49	60	44	76	92	475
NP $[(Ca+Mg) CO_3]$ ^{2,4}	114	87	80	87	55	42	51	37	65	79	55 ⁵
Available NP $[(Ca+Mg) CO_3]$ ^{2,3}	25	19	16	14	8.8	8.4	10	5.2	7.8	17	13

¹ Determined as difference between total sulfur and sulfur present as sulfate.

² AP and NP values expressed as g CaCO₃ equivalent (kg rock)⁻¹. AP(S^{2-}) = 31.2 x (percent S^{2-} with Fe), for the USGS sample this includes 1.44% S with Fe in sphalerite; NP(CO₂) = 22.7x (percent CO₂).

³ Available AP (or NP) determined as product of AP (or NP) and the percent liberated FeS₂ (or ferroan dolomite) divided by 100. Note that for the USGS sample the liberation of sphalerite, and the contained FeS, is also 18%.

⁴ NP $[(Ca+Mg)]$ = 19.5x (%CO₂) based on chemistry of ferroan dolomite.

⁵ Using 0.2% calcite (Table 4), 0.06% CaO in siderite and assuming all magnesium is present as MgCO₃ in siderite [2.12% MgO (Table 2) = 1.28% Mg implies 52.7g/kg CaCO₃ equivalent]

Table 8. Drainage quality summary statistics (average/rate period): Concentrations reported in mg/L, pH in standard units, and specific conductance (SC) in $\mu\text{S}/\text{cm}$ (excluding anomalous values from Table A3.2). Page 1 of 2.

S _T (%)	Rate Period	pH	SC	Net ¹ Alkalinity	SO ₄	Ca	Mg	Ca/Mg ²	As	Mn	Sb	Zn	Cell #
Mafic-intrusive													
6.50	6-72	8.16	406	105	108	59	17.4	2.1	0.004	0.286	0.025	0.012	m-34
	72-102*	8.18	311	100	75	49	15.9	1.8	<0.010 ⁵	0.006	0.004	<0.002	
6.75	6-72	8.13	451	79	154	62	19.7	1.9	0.004	0.174	0.024	0.012	m-35
	72-168	8.10	336	58	117	49	15.7	1.9	<0.010 ⁵	0.017	0.003	<0.002	
7.05	6-72	8.02	517	87	196	73	25.5	1.7	0.013	0.317	0.029	0.012	m-36
	72-168	8.02	375	83	125	49	21.8	1.4	<0.010 ⁵	0.085	0.001	<0.002	
7.05 ³	6-72	8.03	495	98	156	66	23.0	1.7	0.018	0.356	0.027	0.012	m-37
	72-102*	8.05	351	106	104	51	19.4	1.6	<0.010 ⁵	0.225	0.004	<0.002	
7.05 ⁴	6-72	7.94	396	38	151	47	17.6	1.6	0.008	0.212	0.023	0.011	n-2
	72-102*	8.05	299	56	112	40	20.0	1.2	0.002	0.142	0.006	<0.002	
7.30	6-72	7.87	330	63	114	44	15.8	1.7	0.030	1.700	0.013	0.011	m-33
	72-168	7.95	177	51	40	19	10.8	1.1	0.012	0.377	0.002	<0.002 ⁶	
7.40	6-72	8.14	224	70	45	31	9.4	2.0	0.027	0.132	0.052	0.013	m-38
	72-102*	8.18	165	47	34	23	7.6	1.8	0.015	0.008	0.008	<0.002	
8.10	6-72	8.19	409	89	116	53	18.7	1.7	0.068	0.327	0.050	0.012	m-39
	72-168	8.25	405	94	131	58	21.9	1.6	0.005	0.048	0.008	<0.002	
9.05	6-72	8.15	212	62	50	30	9.2	2.0	0.007	0.181	0.027	0.012	m-40
	72-168	8.13	156	41	37	21	7.2	1.7	0.005	0.129	0.007	<0.002	

¹ Net alkalinity = alkalinity - acidity in mg/L as CaCO₃.

² Molar ratio

³ Duplicate

⁴ ASTM Method (changed to MN DNR method after week 90)

⁵ Values after week 10 were <0.010.

⁶ One value during this period appeared anomalous (week 128)

* Cell terminated after week 102

Table 8. Drainage quality summary statistics (average/rate period). Concentrations reported in mg/L, pH in standard units, and specific conductance (SC) in $\mu\text{S}/\text{cm}$ (excluding anomalous values from Table A3.2). Page 2 of 2.

S _T (%)	Rate Period	pH	SC	Net ¹ Alkalinity	SO ₄	Ca	Mg	Ca/Mg ²	As	Mn	Sb	Zn	Cell #
Tuffaceous-sedimentary													
1.31	6-72	7.87	185	34	54	21	8.9	1.4	<0.010 ⁵	0.115	0.009	0.012	m-29
	72-168	7.90	167	32	49	20	9.0	1.3	NA	0.002	NA	<0.002	
1.37	6-72	8.05	208	46	53	25	9.3	1.7	<0.010 ⁵	0.053	0.013	0.012	m-30
	72-102*	8.09	182	38	51	25	9.3	1.6	NA	0.011	NA	<0.002	
3.90	6-72	8.03	297	50	101	36	15.0	1.5	<0.010 ⁵	0.242	0.008	0.010	m-31
	72-168	8.01	226	38	73	28	11.9	1.4	NA	0.017	NA	<0.002	
3.90 ³	6-72	8.07	317	64	103	39	16.4	1.5	<0.010 ⁵	0.300	0.006	0.011	m-32
	72-102*	8.16	243	61	67	32	13.0	1.5	NA	0.134	NA	<0.002	
3.90 ⁴	6-72	7.98	311	37	115	35	15.8	1.4	<0.010 ⁵	0.126	0.009	0.013	n-1
	72-102*	8.14	245	37	86	32	13.2	1.4	NA	0.026	NA	<0.002	
USGS													
13.7	6-62	7.39	411	29	176	19	34.8	0.3	<0.010	11.2	<0.010	1.842	m-41
	62-158	7.89	305	65	103	5	39.2	0.1	NA	1.4	NA	0.153	
13.7 ⁴	6-62	7.58	517	19	240	31	48.8	0.4	<0.010 ⁶	1.36	<0.010 ⁶	0.421	n-3
	62-158	7.88	325	59	110	5	40.1	0.1	NA	1.07	NA	0.134	

¹ Net alkalinity = alkalinity - acidity in mg/L as CaCO₃

² Molar ratio

³ Duplicate

⁴ ASTM Method (changed to MN DNR method after week 90 for tuffaceous-sedimentary, after week 80 for USGS)

⁵ Values after week 10 were <0.010.

⁶ One value during this period appeared anomalous (week 28)

* Cell terminated after week 102

Table 9. Sulfate, calcium, and magnesium release rates for most recent rate period.

S _T Pct	S ⁻² Pct	FeS ₂ Pct	SO ₄	Ca	Mg	SO ₄ / (Ca + Mg)	SO ₄ mmol SO ₄ (kg FeS ₂ •week) ⁻¹	Sample	Cell
			mmol(kg rock•week) ⁻¹						
Mafic-intrusive (72-102* or 168 weeks)									
6.50*	6.20	11.6	0.369	0.606	0.328	0.40	3.2	MS-5	m-34
6.75	6.45	12.1	0.603	0.602	0.317	0.66	5.0	MS-4	m-35
7.05	6.90	13.0	0.644	0.609	0.450	0.61	5.0	MS-2	m-36
7.05*	6.90	13.0	0.498	0.617	0.385	0.50	3.8	MS-2	m-37
7.05* ¹	6.90	13.0	0.505	0.422	0.353	0.65	3.9	MS-2	n-2
7.30	7.29	13.6	0.195	0.234	0.221	0.43	1.4	MS-1	m-33
7.40*	7.40	13.9	0.162	0.265	0.147	0.39	1.2	MS-7	m-38
8.10	8.05	15.1	0.637	0.694	0.431	0.57	4.2	MS-3	m-39
9.05	8.55	16.0	0.180	0.244	0.140	0.47	1.1	MS-6	m-40
Tuffaceous-sedimentary (72-102* or 168 weeks)									
1.31	1.30	2.4	0.253	0.248	0.185	0.58	10.1	MS-10	m-29
1.37*	1.36	2.5	0.242	0.290	0.179	0.52	9.3	MS-9	m-30
3.90	3.75	7.0	0.382	0.343	0.241	0.65	5.5	MS-8	m-31
3.90*	3.75	7.0	0.324	0.384	0.268	0.50	4.6	MS-8	m-32
3.90* ¹	3.75	7.0	0.422	0.360	0.250	0.69	6.0	MS-8	n-1
Low NP Tuffaceous-sedimentary (20 weeks)									
0.33	0.26	0.49	1.03	0.021	0.001	45.78	211.7	364	m-42
1.16	1.03	1.9	3.07	0.076	0.004	38.04	159.3	356	m-43
1.3	1.05	2.0	1.32	0.862	0.568	0.92	67.2	361	m-49 ³
1.23	1.08	2.0	2.20	0.764	0.482	1.77	109.0	363	m-47
1.23	1.08	2.0	2.05	0.807	0.501	1.57	101.4	363	m-48
1.47	1.16	2.2	2.40	0.537	0.311	2.83	110.7	362	m-45
1.47	1.16	2.2	2.23	0.639	0.368	2.21	102.7	362	m-46
2.13	1.93	3.6	4.84	0.319	0.005	14.95	133.9	370	m-44
USGS (62-158 weeks)									
13.70	12.99	17.3 ²	0.528	0.057	0.799	0.62	3.0	USGS	m-41
13.70 ¹	12.99	17.3 ²	0.551	0.065	0.831	0.61	3.2	USGS	n-3

* Cell terminated after week 102

¹ ASTM method (changed to MN DNR method after week 90 for mafic-intrusive and tuffaceous-sedimentary, and after week 80 for USGS)

² Also contained 9.6% sphalerite, 1.9% gypsum, and 4.6% melanterite

³ cell 49 release rates for weeks 20-40 are (SO₄= 1.01, Ca = 0.617, Mg = 0.439)

Table 10. Initial and final AP and NP [(Ca+Mg)CO₃]. Page 1 of 2.

Initial Composition						Mass Release, millimoles			Leached Composition				
S _T	AP	NP			Net NP ⁵				AP	NP			Net NP ⁵
	S _T ¹	CaCO ₃ ²	MgCO ₃ ³	(Ca+Mg)CO ₃		ST ¹	CaCO ₃	MgCO ₃	(Ca+Mg)CO ₃				
PCT	g CaCO ₃ equivalent (kg rock) ⁻¹					S	Ca	Mg	g CaCO ₃ equivalent (kg rock) ⁻¹				
Mafic-intrusive (102 or 168 weeks of dissolution)													
6.50*	203	56	59	114	-88	68.7	80.7	45.6	196	48	54	102	-94
6.75	211	42	45	87	-124	136.5	125.0	70.6	197	30	38	68	-129
7.05	220	39	41	80	-140	153.8	127.9	95.5	205	27	32	59	-146
7.05*	220	39	41	80	-140	84.7	80.4	53.5	212	31	36	67	-145
7.05*.4	220	39	41	80	-140	83.1	60.1	44.3	212	33	37	70	-142
7.30	228	42	45	87	-14	75.0	69.7	51.7	221	36	40	75	-145
7.40*	231	27	28	56	-175	38.8	42.8	28.2	227	23	26	49	-178
8.10	253	21	22	42	-211	123.7	123.5	80.3	241	9	14	22	-218
9.05	282	25	26	51	-231	59.9	62.6	40.8	277	19	22	41	-235

*Cell terminated after week 102

¹ AP(S_T) = 31.2 (PCT S_T)

² NP [CaCO₃] = 9.55 (PCT CO₂) for mafic-intrusive and tuffaceous-sedimentary samples

³ NP [MgCO₃] = 10.0 (PCT CO₂) for mafic-intrusive and tuffaceous-sedimentary samples

⁴ ASTM method (changed to MN DNR method after week 90)

⁵ Net NP = NP[(Ca+Mg)CO₃] - AP(S_T)

Visual
oxid

5

3

57

2

1

4

Table 10. Initial and final AP and NP [(Ca+Mg)CO₃]. Page 2 of 2.

Initial Composition						Mass Release, millimoles			Leached Composition				
S _T	AP	NP			Net NP ⁵				AP	NP	NP	NP	Net NP ⁵
	S _T ¹	CaCO ₃ ²	MgCO ₃ ³	(Ca+Mg)CO ₃		S _T	CaCO ₃	MgCO ₃	(Ca+Mg)CO ₃				
PCT	g CaCO ₃ equivalent (kg rock) ⁻¹					S	Ca	Mg	g CaCO ₃ equivalent (kg rock) ⁻¹				
Tuffaceous-sedimentary (102 or 168 weeks of dissolution)													
1.31	41	18	19	38	-3	51.1	47.1	34.0	36	14	16	30	-6
1.37*	43	32	34	65	23	37.5	37.2	24.8	39	28	31	60	20
3.90	122	39	41	79	-43	83.0	73.9	51.3	114	32	36	67	-47
3.90*	122	39	41	79	-43	56.6	55.0	38.2	116	33	37	70	-46
3.90* ⁴	122	39	41	79	-43	63.9	47.5	34.6	116	34	37	71	-44
USGS (158 weeks of dissolution)													
13.70	427	2.6 ⁶	53 ⁶	55 ⁶	-372	131.0	37.0	127.0	415	0	40	40 ⁷	-374
13.70 ⁴	427	2.6 ⁶	53 ⁶	55 ⁶	-372	142.2	40.3	139.3	414	0	39	39 ⁷	-375

*Cell terminated after week 102

¹ AP(S_T) = 31.2 (PCT S_T)

² NP [CaCO₃] = 9.55 (PCT CO₂) for mafic-intrusive and tuffaceous-sedimentary samples

³ NP [MgCO₃] = 10.0 (PCT CO₂) for mafic-intrusive and tuffaceous-sedimentary samples

⁴ ASTM method (changed to MN DNR method after week 90 for tuffaceous-sedimentary, after week 80 for USGS)

⁵ Net NP = NP[(Ca+Mg)CO₃] - AP(S_T)

⁶ Using 0.2% calcite (Table 4), 0.06% CaO in siderite and assuming all Mg is present in siderite (2.12% MgO from Table 2 implies an MgCO₃ content of 52.7 g/kg CaCO₃ equivalent)

⁷ Assuming 100% dissolution of CaCO₃

Table 11. Estimated additional dissolution time to deplete carbonate minerals.

%S _T	Cell	%CO ₂ ¹	NP[(Ca+Mg)CO ₃], g CaCO ₃ equivalent (kg rock) ⁻¹			Ca+Mg release rate ³ mmol/wk	Weeks to NP Depletion	
			t = 0		Dissolved at t = 102, 168, or 158 weeks		Total ⁴	Available ⁵
			Total ⁸	Minimum ⁹ A available				
Mafic-intrusive (102 or 168 weeks of dissolution)								
6.50 ¹⁰	m-34	5.85	114	25	13	0.934	1100	132
6.75	m-35	4.45	87	19	20	0.919	730	0
7.05	m-36	4.10	80	16	22	1.059	550	0
7.05 ¹⁰	m-37	4.10	80	16	13	1.002	670	26
7.05 ^{6,10}	n-2	4.10	80	16	10	0.775	900	72
7.30	m-33	4.45	87	14	12	0.455	1600	41
7.40 ¹⁰	m-38	2.84	55	8.8	7	0.412	1200	41
8.10	m-39	2.15	41	8.4	20	1.125	200	0
9.05	m-40	2.62	51	10	10	0.384	1100	0
Tuffaceous-sedimentary (102 or 168 weeks of dissolution)								
1.31	m-29	1.92	37	5.2	8	0.433	680	0
1.37 ¹⁰	m-30	3.35	64	7.8	6	0.469	1300	34
3.90	m-31	4.05	77	17	13	0.584	1100	77
3.90 ¹⁰	m-32	4.05	77	17	9	0.652	1100	118
3.90 ^{6,10}	n-1	4.05	77	17	8	0.610	1200	144
USGS (158 weeks of dissolution)								
13.70	m-41	20.90	55 ⁷	13	16	0.856	450	0
13.70 ⁶	n-3	20.90	55 ⁷	13	18	0.896	420	0

¹ Values from Table 2

² NP [(Ca+Mg) CO₃] = 19.5 CO₂ for mafic-intrusive and tuffaceous-sedimentary samples.

³ Values from Table 8

⁴ Additional time to deplete NP[(Ca+Mg) CO₃] = 10xNP[(Ca+Mg)CO₃]_r / [d(Ca+Mg)/dt], where NP[(Ca+Mg)CO₃]_r = initial NP[(Ca+Mg) CO₃] - NP[(Ca+Mg)CO₃] dissolved

⁵ Additional time to deplete minimum available NP[(Ca+Mg) CO₃] = 10 x available NP[(Ca+Mg)CO₃]_r / [d(Ca+Mg)/dt], where available NP[(Ca+Mg)CO₃]_r = initial minimum available NP[(Ca+Mg)CO₃] - NP[(Ca+Mg)CO₃] dissolved.

⁶ ASTM method (changed to MN DNR method after week 90 for mafic-intrusive and tuffaceous-sedimentary, and after week 80 for USGS)

⁷ Using 0.2% calcite (Table 4), 0.06% CaO in siderite and assuming all magnesium is present as MgCO₃ in siderite [2.12% MgO (Table 2) = 1.28% Mg implies 52.7 g CaCO₃ equivalent (kg rock)⁻¹]

⁸ Values from Table 9

⁹ Values from Table 6

¹⁰ Cell terminated after 102 weeks

Table 12. Summary of drainage from low NP tuffaceous-sedimentary samples at week 20. Concentrations in mg/L, NP[(Ca+Mg)CO₃] in g CaCO₃ equivalent/kg rock based on CO₂ content and assumed calcium and magnesium content of ferroan dolomite (equation 20).

S _T , %	NP[(Ca+Mg)CO ₃]	Ca	Mg	Na	K	pH _{min}
Samples with measurable CO ₂						
1.23	5.1	63.4	23.9	0.18	0.550	2.90
1.23	5.1	57.2	21.5	0.17	0.610	3.00
1.47	5.9	37.2	12.9	0.11	0.470	2.64
1.47	5.9	45.4	15.4	0.13	0.480	2.76
1.30	19	73	29.7	0.13	0.440	5.84
Samples with CO ₂ < 0.05%						
0.33	<1	6.70	<0.1	0.10	0.850	2.57
1.16	<1	6.22	0.15	0.14	0.530	2.35
2.13	<1	28.2	0.22	0.19	2.84	2.16

Table 13. Comparison of release rates for MN DNR and ASTM methods.

S _T (%)	S ⁻² (%)	pH ¹	Sulfate	Calcium	Magnesium	Rate ratio			Cell
			Rate, mmol(kg rock•week) ⁻¹			Ca/SO ₄	Mg/SO ₄	(Ca+Mg)/SO ₄	
Mafic-intrusive (24-72 weeks)									
7.05	6.90	8.04	0.698	0.700	0.418	1.00	0.60	1.60	m-36
7.05	6.90	8.00	0.655	0.695	0.449	1.06	0.69	1.75	m-37
7.05 ²	6.90	8.00	0.594	0.450	0.296	0.76	0.50	1.26	n-2
(72-90 weeks)									
7.05	6.90	8.11	0.573	0.608	0.396	1.06	0.69	1.75	m-36
7.05	6.90	8.08	0.547	0.647	0.400	1.18	0.73	1.91	m-37
7.05 ²	6.90	8.02	0.408	0.307	0.260	0.75	0.64	1.39	n-2
Tuffaceous-sedimentary (24-72 weeks)									
3.90	3.75	8.02	0.429	0.375	0.264	0.87	0.62	1.49	m-31
3.90	3.75	8.11	0.411	0.408	0.291	0.99	0.71	1.70	m-32
3.90 ²	3.75	8.04	0.435	0.328	0.248	0.75	0.57	1.32	n-1
(72-90 weeks)									
3.90	3.75	8.10	0.353	0.343	0.238	0.97	0.67	1.65	m-31
3.90	3.75	8.19	0.281	0.337	0.235	1.20	0.84	2.04	m-32
3.90 ²	3.75	8.07	0.384	0.309	0.221	0.80	0.58	1.38	n-1
USGS (30-62 weeks)									
13.70	12.99	7.73	0.672	0.069	0.729	0.10	1.08	1.19	m-41
13.70 ²	12.99	8.01	0.878	0.092	0.927	0.10	1.06	1.16	n-3
(62-80 weeks)									
13.70	12.99	7.90	0.556	0.055	0.752	0.10	1.35	1.45	m-41
13.70 ²	12.99	8.21	0.462	0.052	0.585	0.11	1.27	1.38	n-3

¹ Drainage pH reported for week 72 and 88 (mafic-intrusive, tuffaceous-sedimentary) or week 62 and 78 (USGS).

² ASTM method (changed to MN DNR method after week 90 for mafic-intrusive and tuffaceous-sedimentary, and after week 80 for USGS)

Table 14. Comparison of ASTM and MN DNR method water retention (grams).

	One day after leach (Tuesday)				Before leach (Monday)				Dry weight (Friday)			
	MN DNR	ASTM	ASTM/ DNR ¹		MN DNR	ASTM	ASTM/ DNR ¹		MN DNR	ASTM	ASTM/D NR ¹	
Mafic-intrusive, 7.05% S_T, 89 week period of record												
Mean	232	230	182	0.79	225	224	117	0.52	229	227	107	0.47
S.D.	8.6	8.2	12.5	1.49	8.7	7.6	42.1	2.58	9.2	9.4	29.1	3.13
Range	43	36	77	1.95	50	35	198	4.66	51	58	181	3.32
Tuffaceous-sedimentary, 3.90% S_T, 89 week period of record												
Mean	188	191	153	0.81	178	185	77	0.42	183	187	64	0.35
S.D.	13.6	8.0	12.0	1.11	13.2	6.9	45.2	4.41	13.4	7.4	37.1	3.57
Range	66	37	75	1.46	72	31	180	3.50	59	35	169	3.60
USGS, 13.70% S_T, 79 week period of record												
Mean	108		90.8	0.84	101		25.7	0.25	104		22.1	0.21
S.D.	6.8		8.3	1.22	5.8		23.2	4.0	6.2		23.1	3.72
Range	36		52	1.44	28		96	3.43	30		102	3.4

¹ Ratio of values from ASTM method to those from MN DNR method. For the mafic-intrusive and the tuffaceous-sedimentary samples, the average of duplicate MN DNR cells was used.

Figure 1. Schematic of humidity cell for ASTM and MN DNR method

All humidity cell materials are acrylic except the perforated plate (polyvinyl chloride) and the outlet pipe (high density polyethylene).

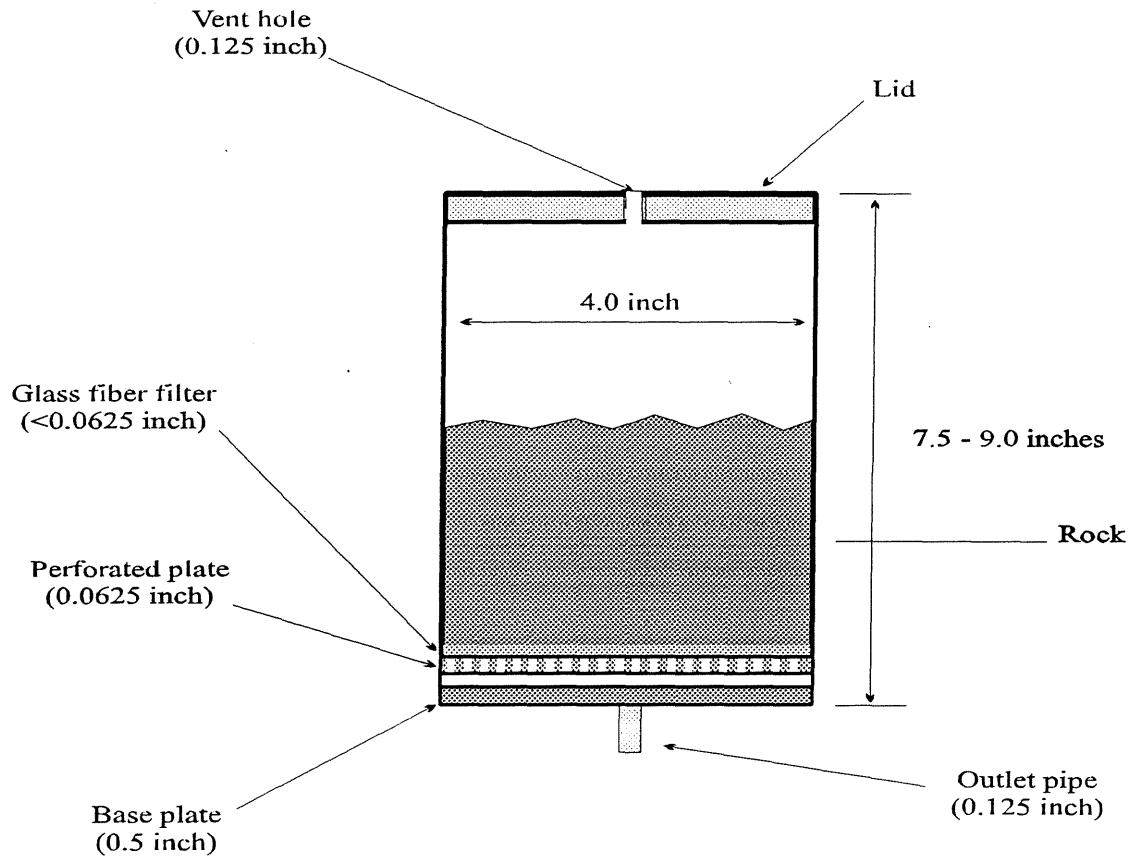


Figure 2. Drainage quality from 6.20% sulfide mafic-intrusive sample (6.50% S_T , 5.85% CO_2 , cell m-34), for weeks 5-102 (terminated). Weeks 0-5 were eliminated to improve subsequent resolution.

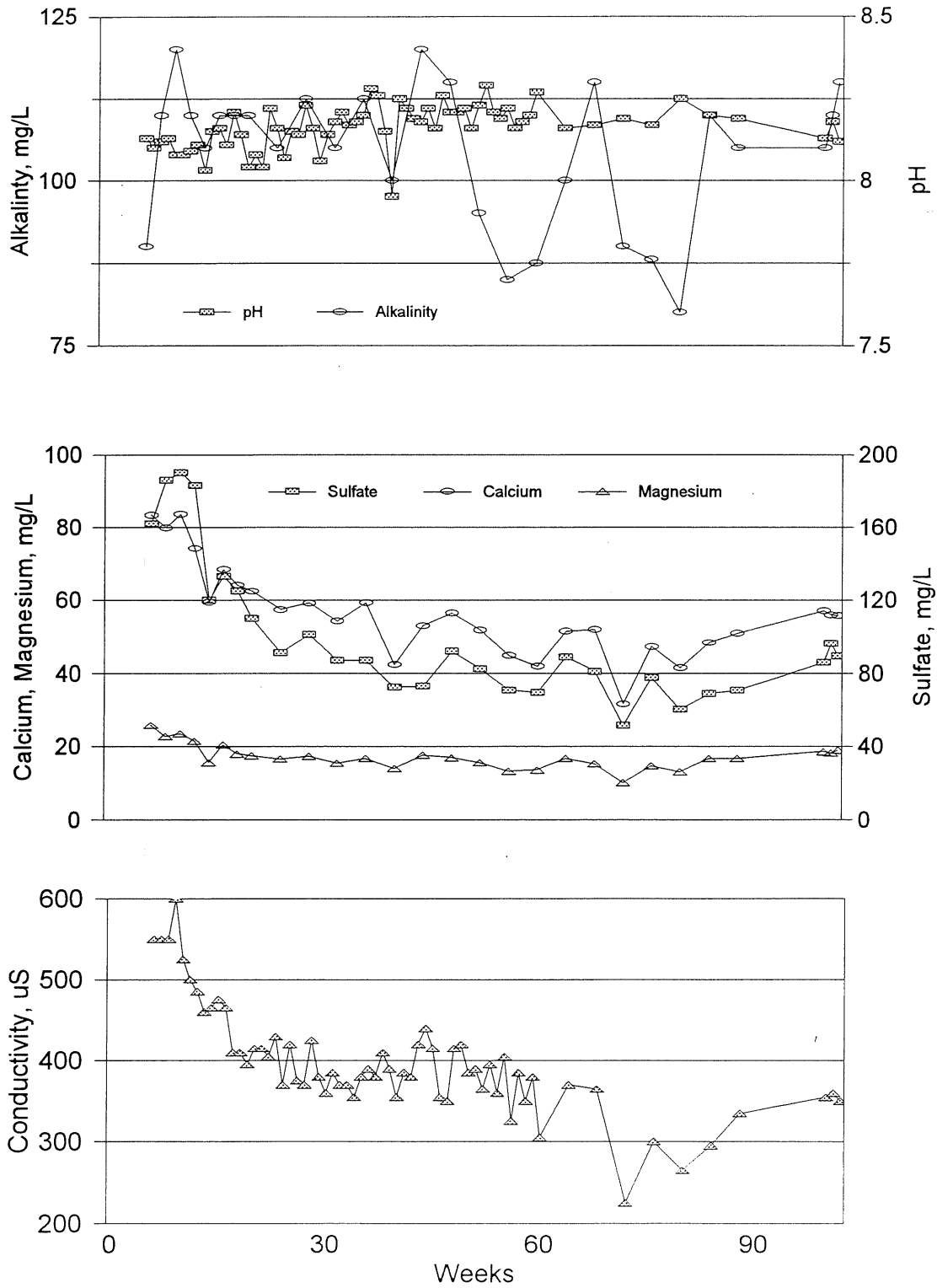


Figure 3. Drainage quality from 6.45% sulfide mafic-intrusive sample (6.75% S_T , 4.45% CO_2 , cell m-35), for weeks 5-168. Weeks 0-5 were eliminated to improve subsequent resolution.

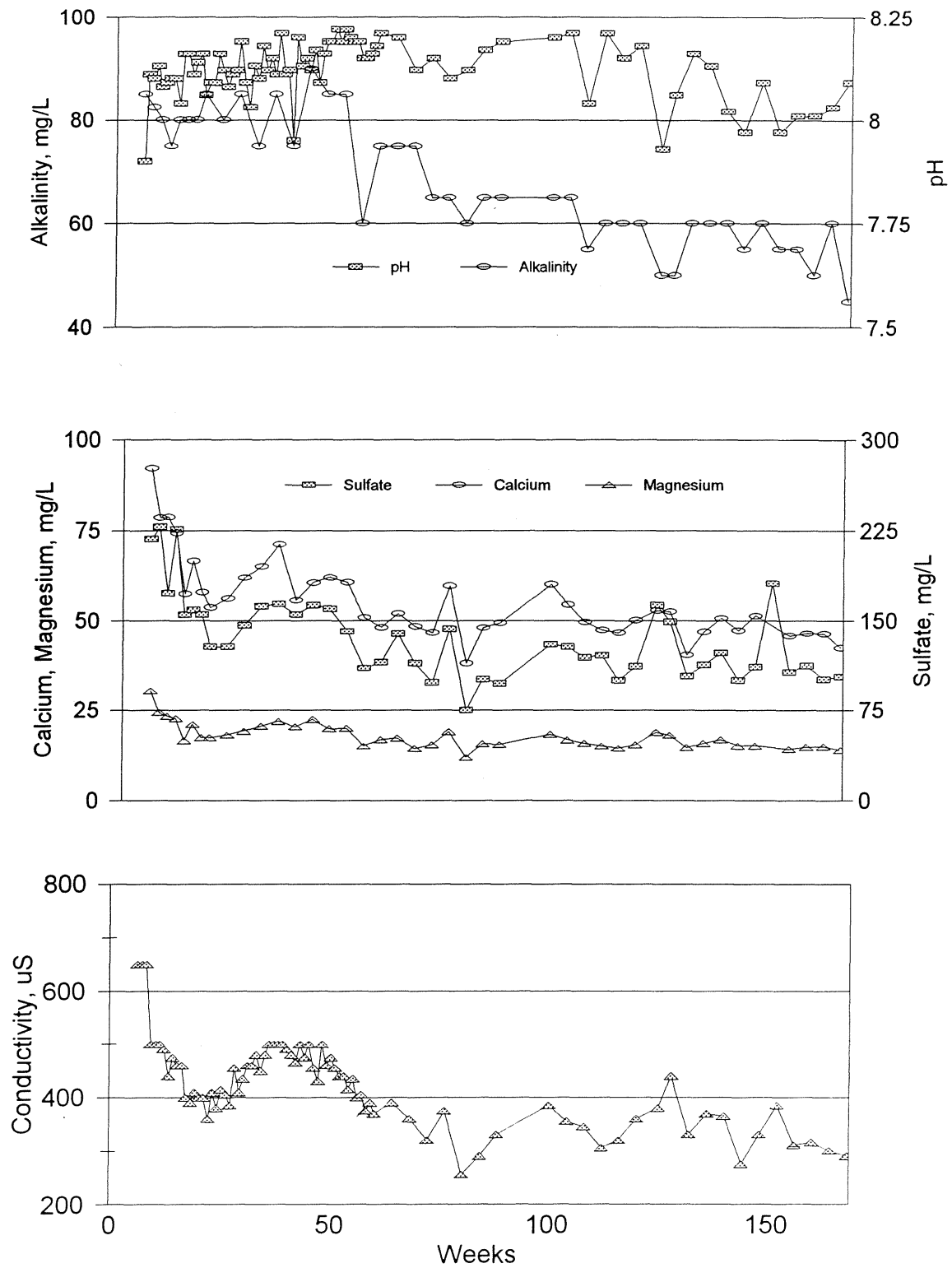


Figure 4. Drainage quality from 6.90% sulfide mafic-intrusive sample (7.05% S_T , 4.10% CO_2 , cell m-36), for weeks 5-168. Weeks 0-5 were eliminated to improve subsequent resolution.

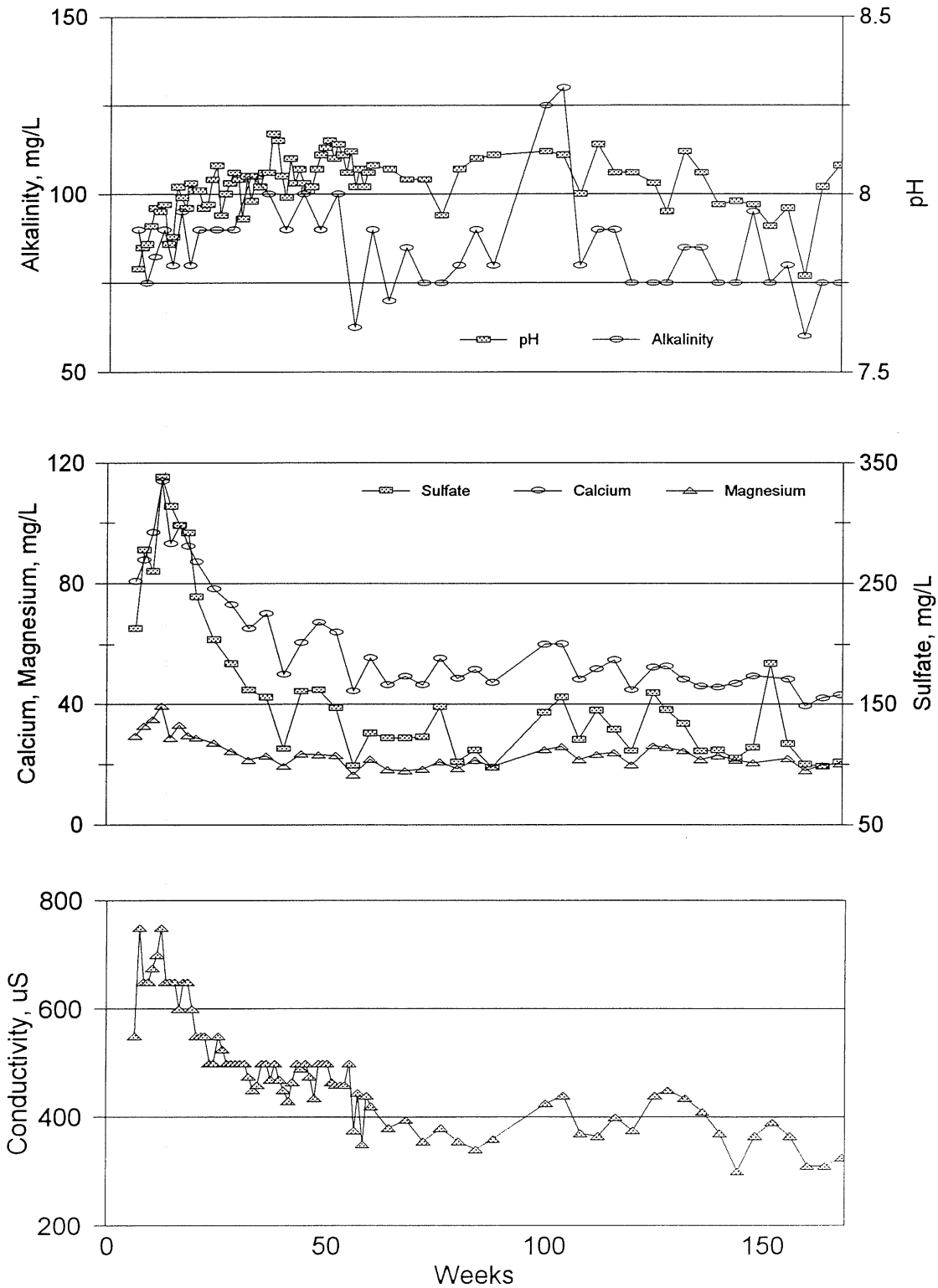


Figure 5. Drainage quality from 6.90% sulfide mafic-intrusive sample (7.05% ST, 4.10% CO₂, cell m-37), for weeks 5-102 (terminated). Weeks 0-5 were eliminated to improve subsequent resolution.

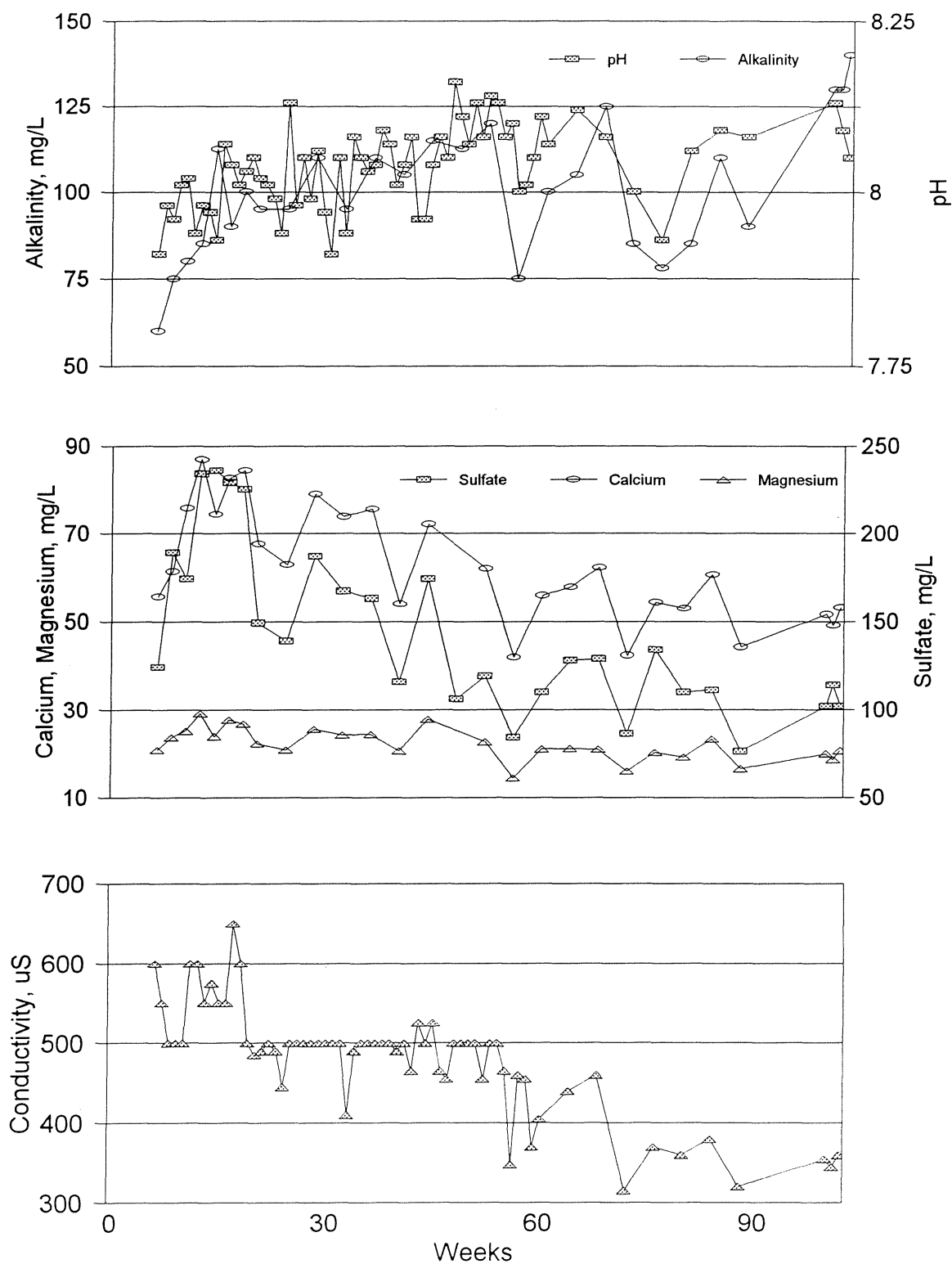


Figure 6. Drainage quality from 6.90% sulfide mafic-intrusive sample (7.05% S_T , 4.10% CO_2 , cell n-2), for weeks 5-102 (terminated). Weeks 0-5 were eliminated to improve subsequent resolution. Method changed from ASTM to MN DNR after week 90.

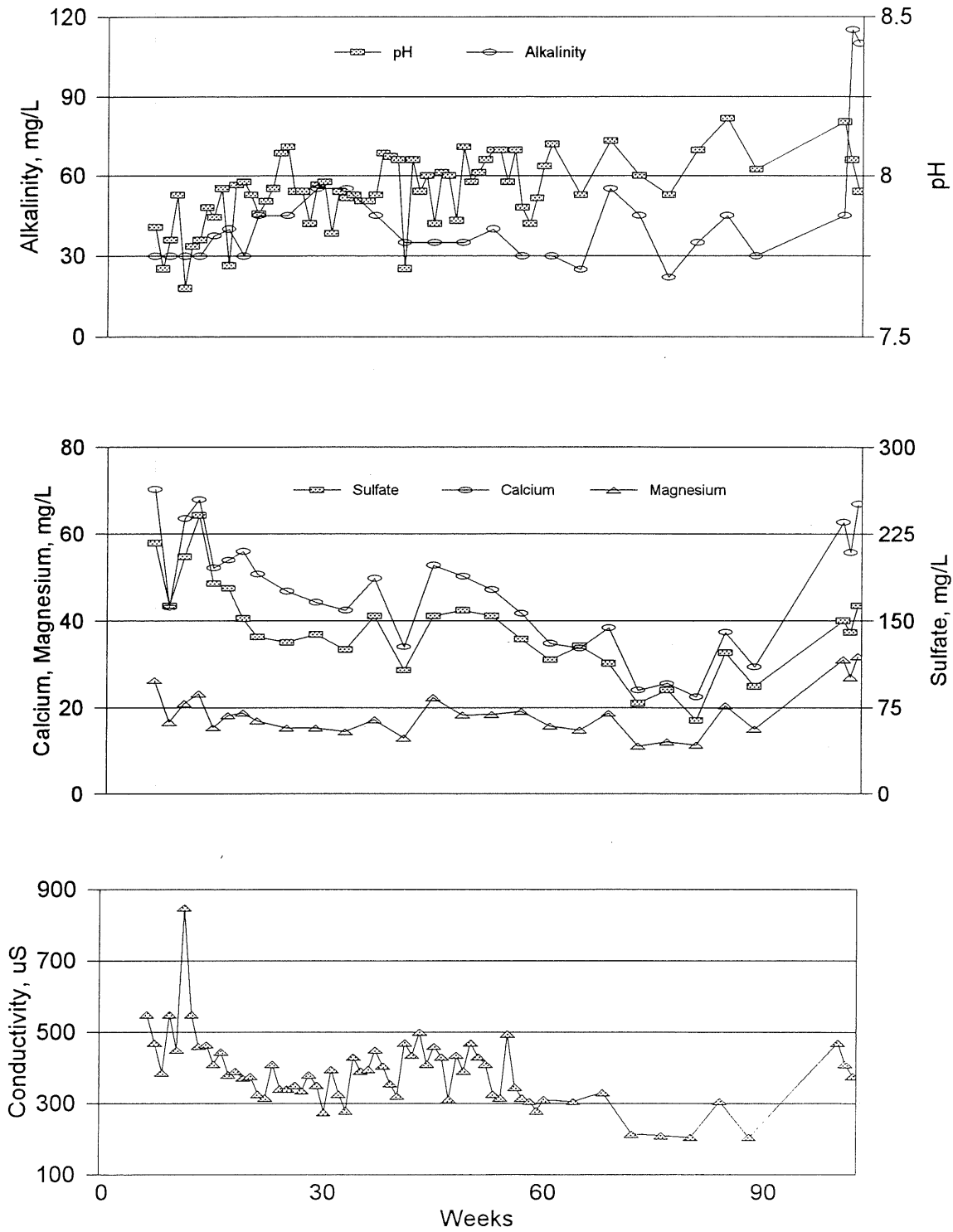


Figure 7. Drainage quality from 7.29% sulfide mafic-intrusive sample (7.30% ST, 4.45% CO₂, cell m-33), for weeks 5-168. Weeks 0-5 were eliminated to improve subsequent resolution.

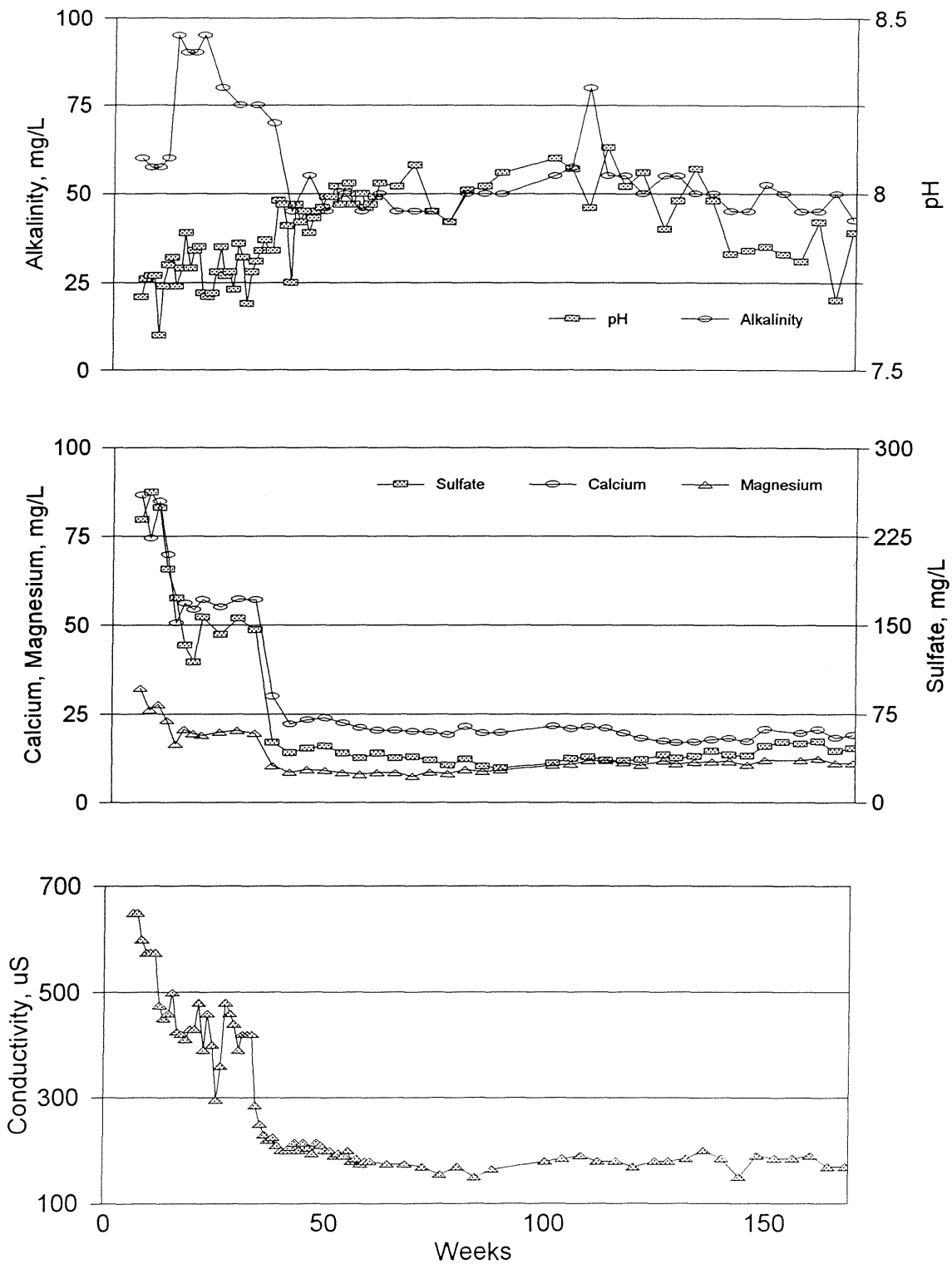


Figure 8. Drainage quality from 7.39% sulfide mafic-intrusive sample (7.40% S_T, 2.84% CO₂, cell m-38), for weeks 5-102 (terminated). Weeks 0-5 were eliminated to improve subsequent resolution.

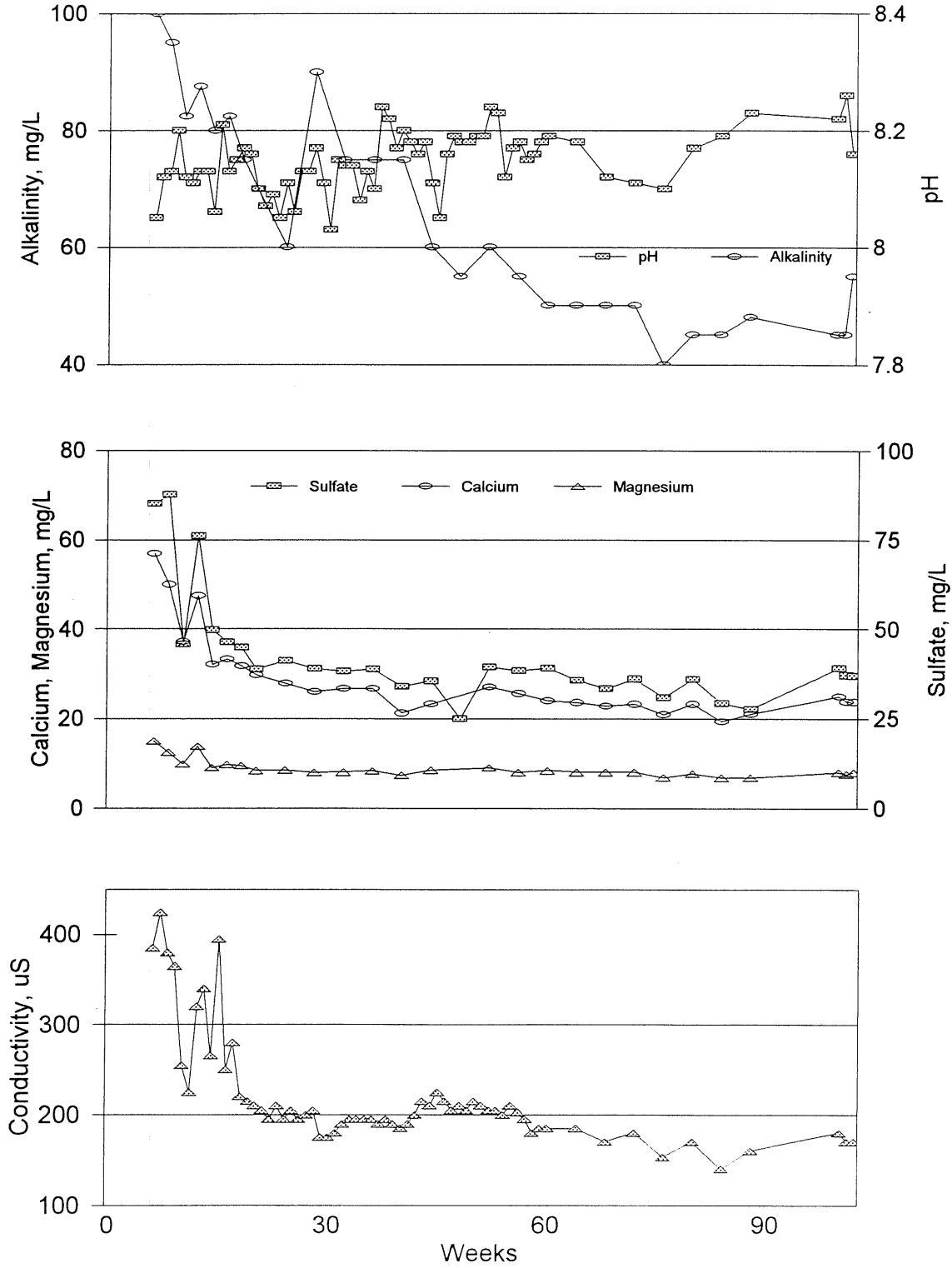


Figure 9. Drainage quality from 8.05% sulfide mafic-intrusive sample (8.10% ST, 2.15% CO₂, cell m-39), for weeks 5-168. Weeks 0-5 were eliminated to improve subsequent resolution.

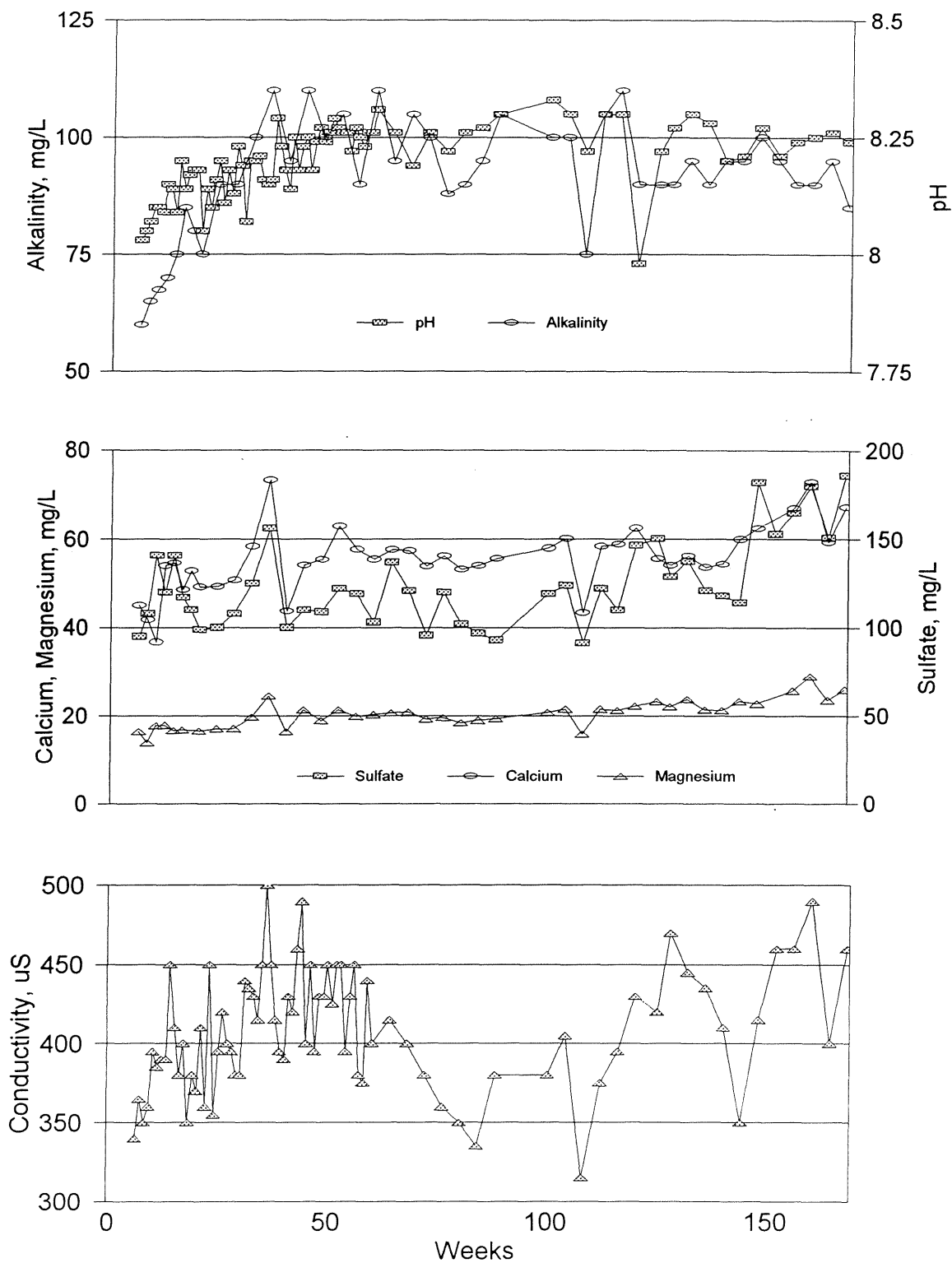


Figure 10. Drainage quality from 8.55% sulfide mafic-intrusive sample (9.05% ST, 2.62% CO₂, cell m-40), for weeks 5-168. Weeks 0-5 were eliminated to improve subsequent resolution.

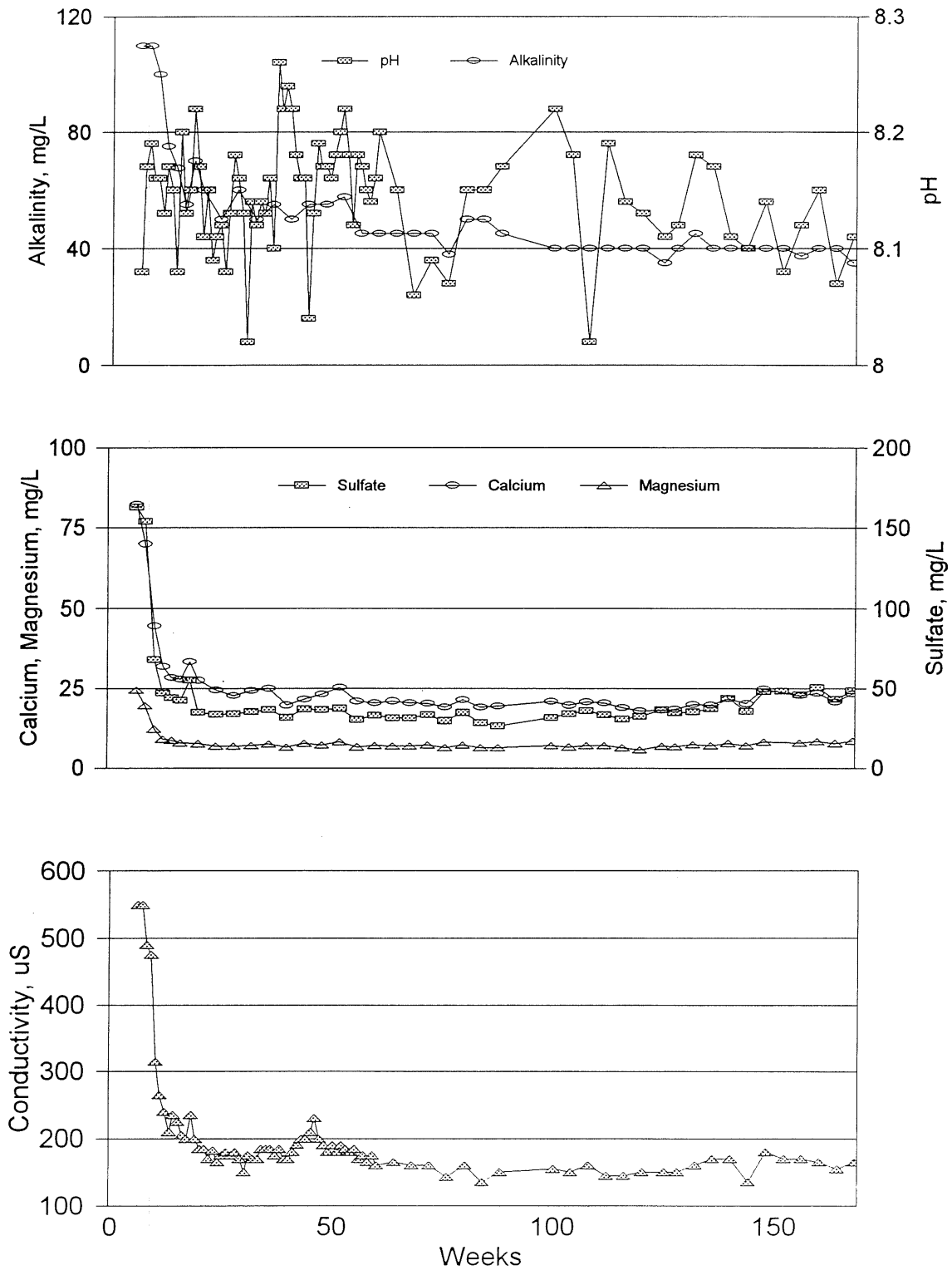


Figure 11. Drainage quality from 1.30% sulfide tuffaceous-sedimentary sample (1.31% ST, 1.92% CO₂, cell m-29), for weeks 5-168. Weeks 0-5 were eliminated to improve subsequent resolution.

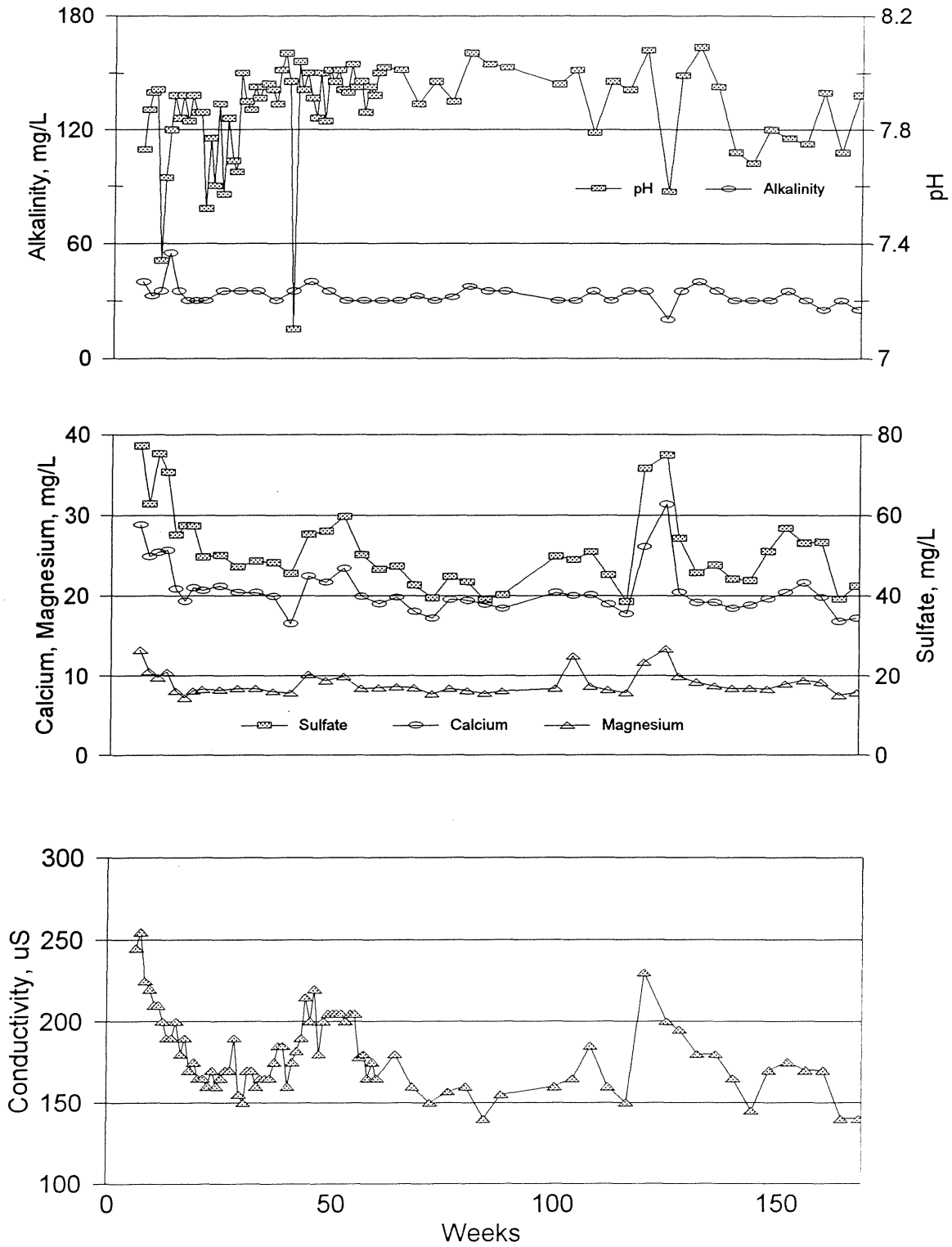


Figure 12. Drainage quality from 1.36% sulfide tuffaceous-sedimentary sample (1.37% S_T , 3.35% CO_2 , cell m-30), for weeks 5-102 (terminated). Weeks 0-5 were eliminated to improve subsequent resolution.

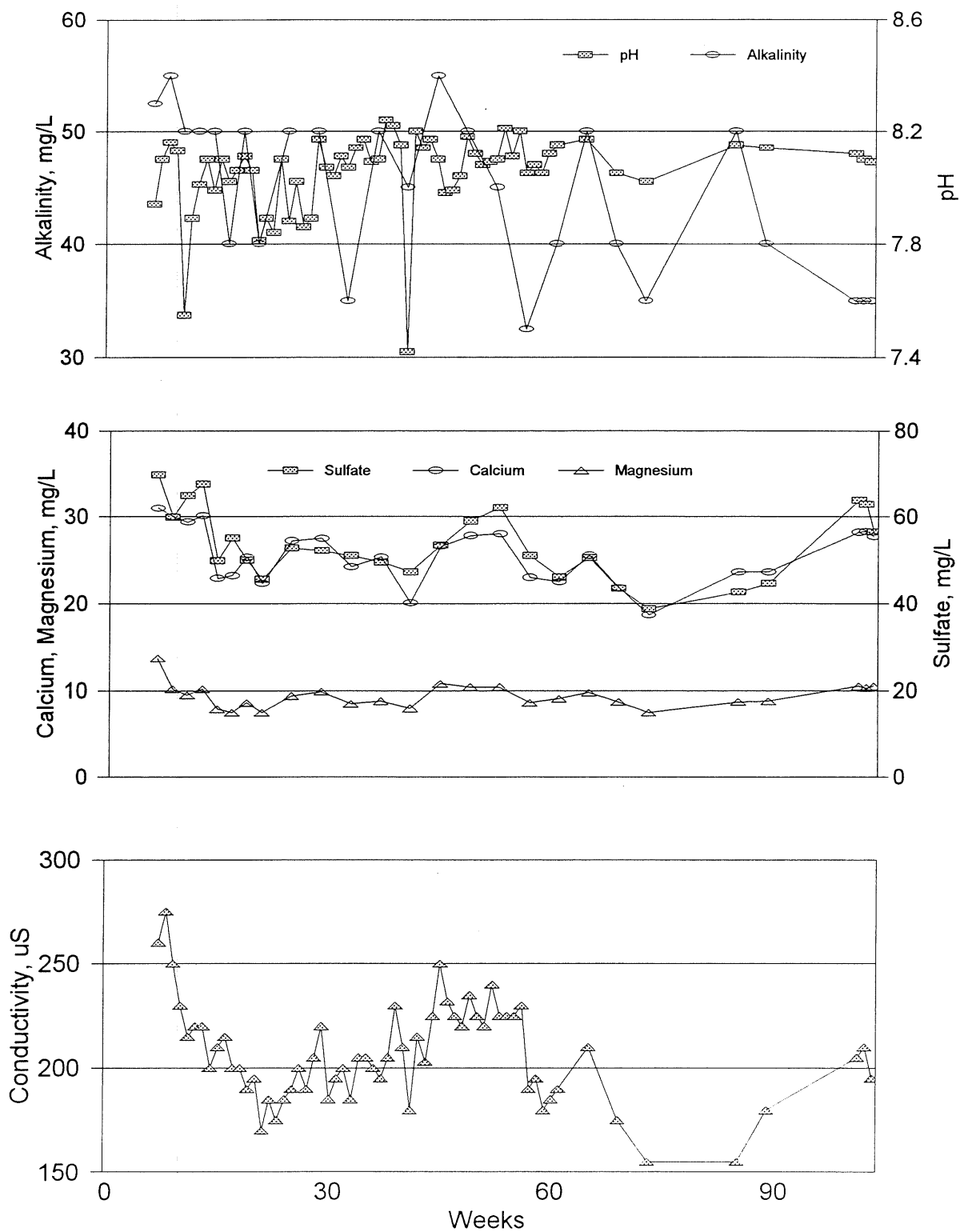


Figure 13. Drainage quality from 3.75% sulfide tuffaceous-sedimentary sample (3.90% ST, 4.05% CO₂, cell m-31), for weeks 5-168. Weeks 0-5 were eliminated to improve subsequent resolution.

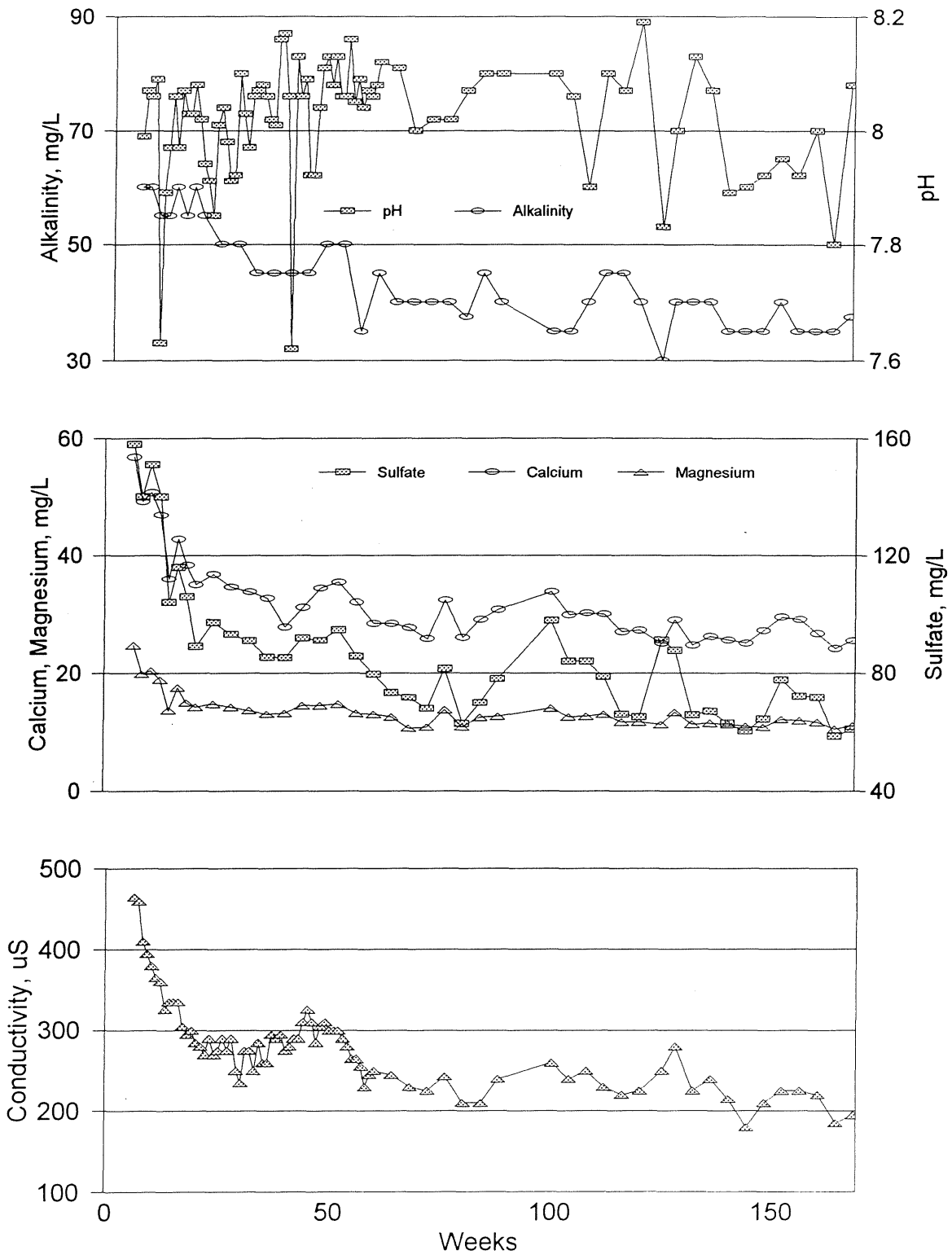


Figure 14. Drainage quality from 3.75% sulfide tuffaceous-sedimentary sample (3.90% S_T , 4.05% CO_2 , cell m-32) for weeks 5-102 (terminated). Weeks 0-5 were eliminated to improve subsequent resolution.

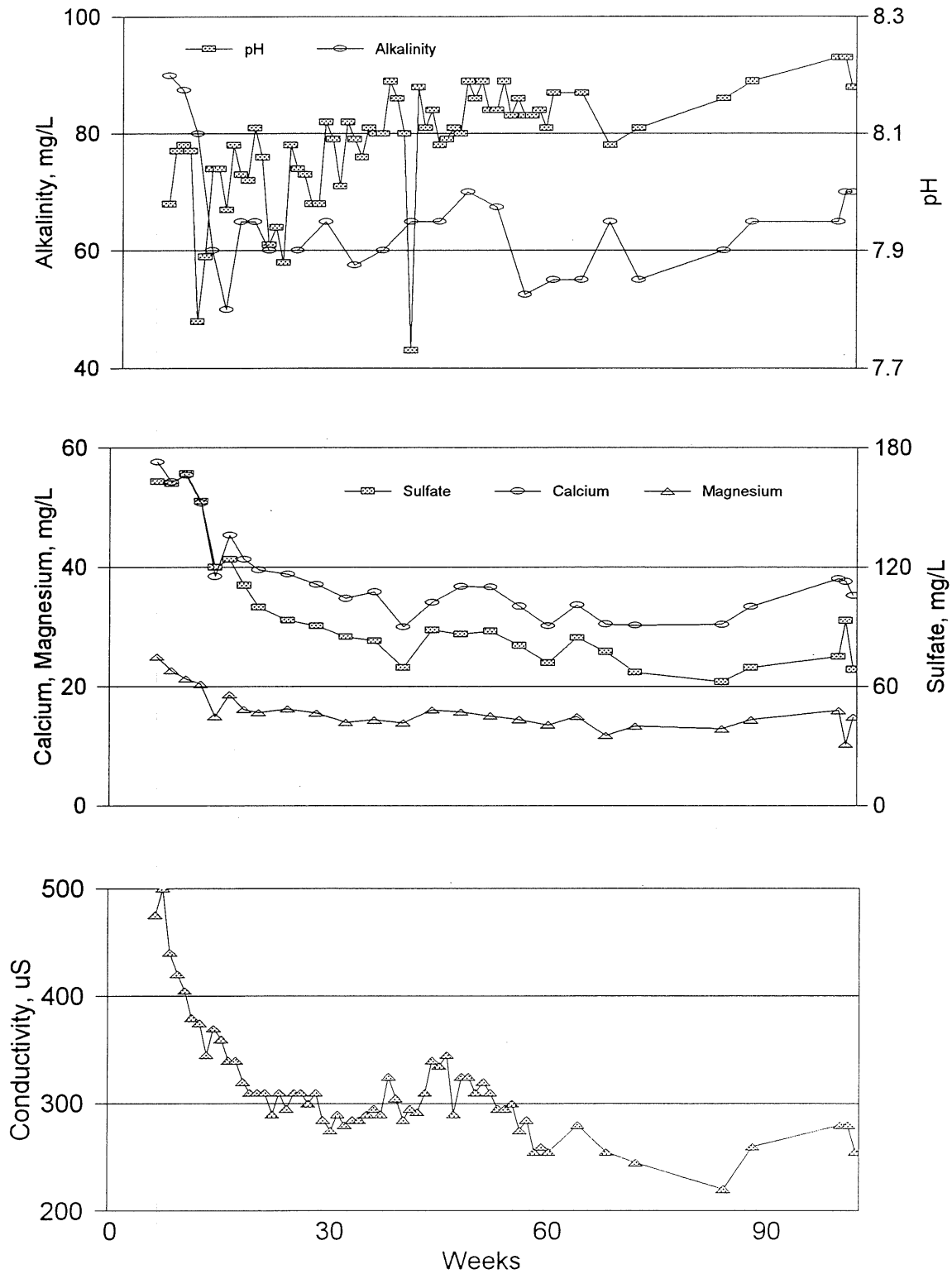


Figure 15. Drainage quality from 3.75% sulfide tufaceous-sedimentary sample (3.90% S_T, 4.05% CO₂, cell n-1), for weeks 5-102 (terminated). Weeks 0-5 were eliminated to increase subsequent resolution. Method changed from ASTM to MN DNR after week 90.

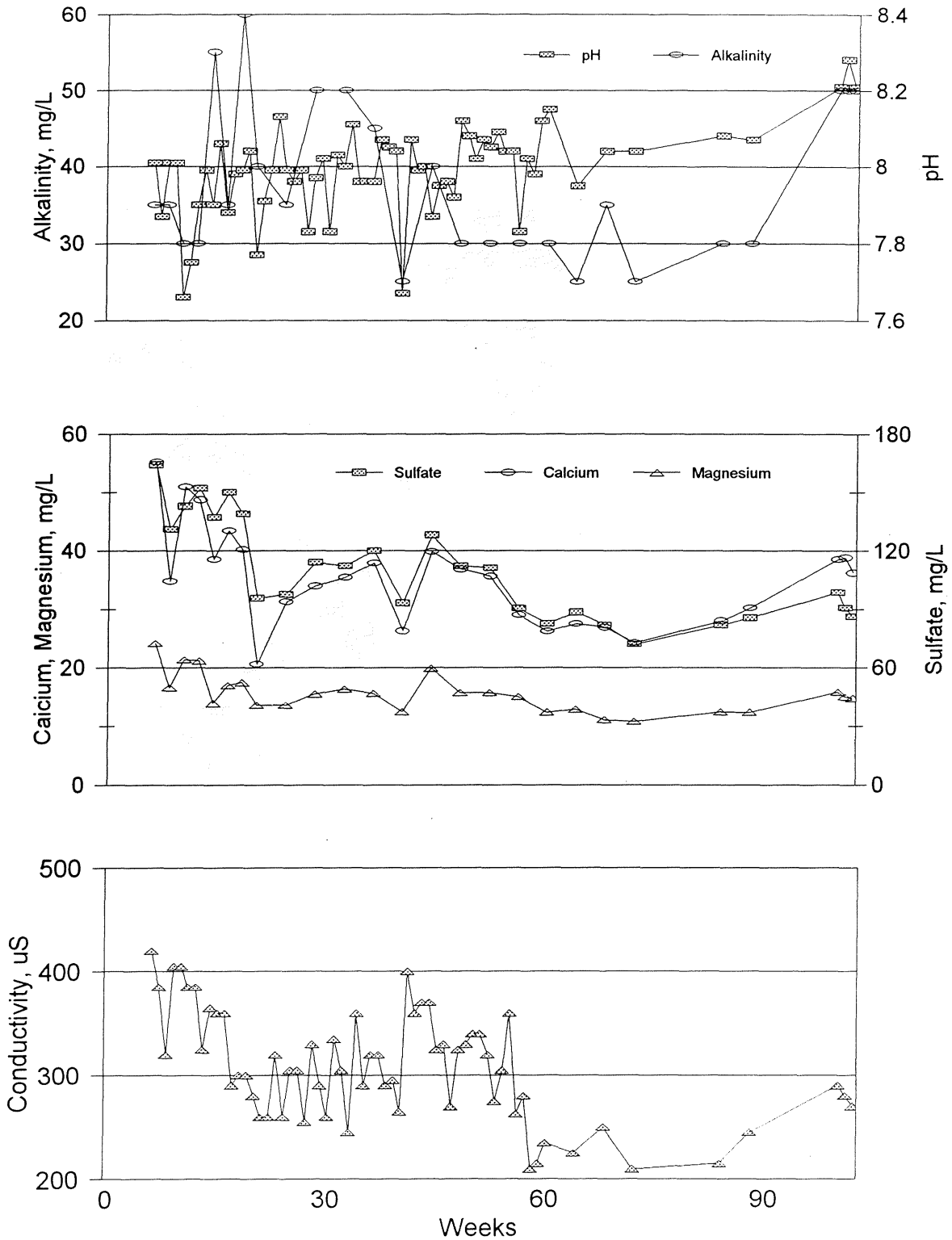


Figure 16. Particle of the 1.30 % S_T sample (0.95% CO_2) after 40 weeks of dissolution testing. The lighter rhombohedral grains in the interior of the particle are ferroan dolomite, the gray mineral is quartz and the small white mineral is pyrite. The black is the epoxy used in sample preparation. The ferroan dolomite near the middle of the grain is virtually intact and grains closer to the edge are partially dissolved. The rhombohedral voids at the particle boundary represent zones from which ferroan dolomite dissolved during the experiment.

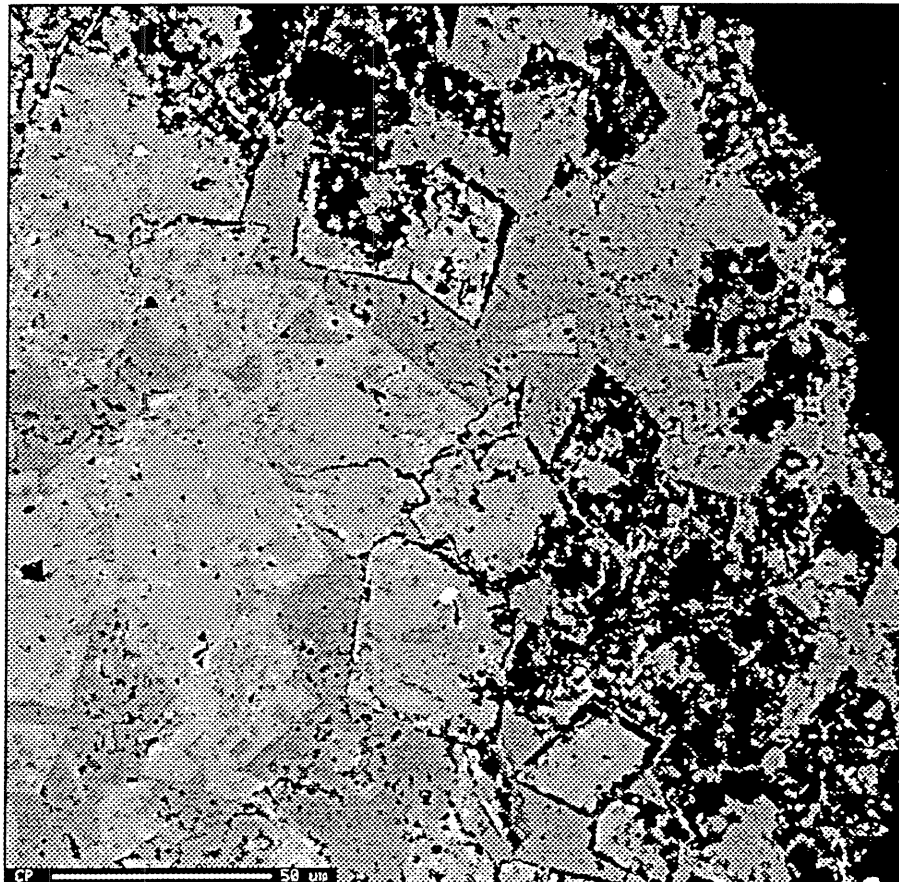


Figure 17. Drainage quality from 12.99% sulfide USGS sample (13.70% S_T , 13.70% CO_2 , cell m-41), for weeks 5-158. Weeks 0-5 were eliminated to improve subsequent resolution.

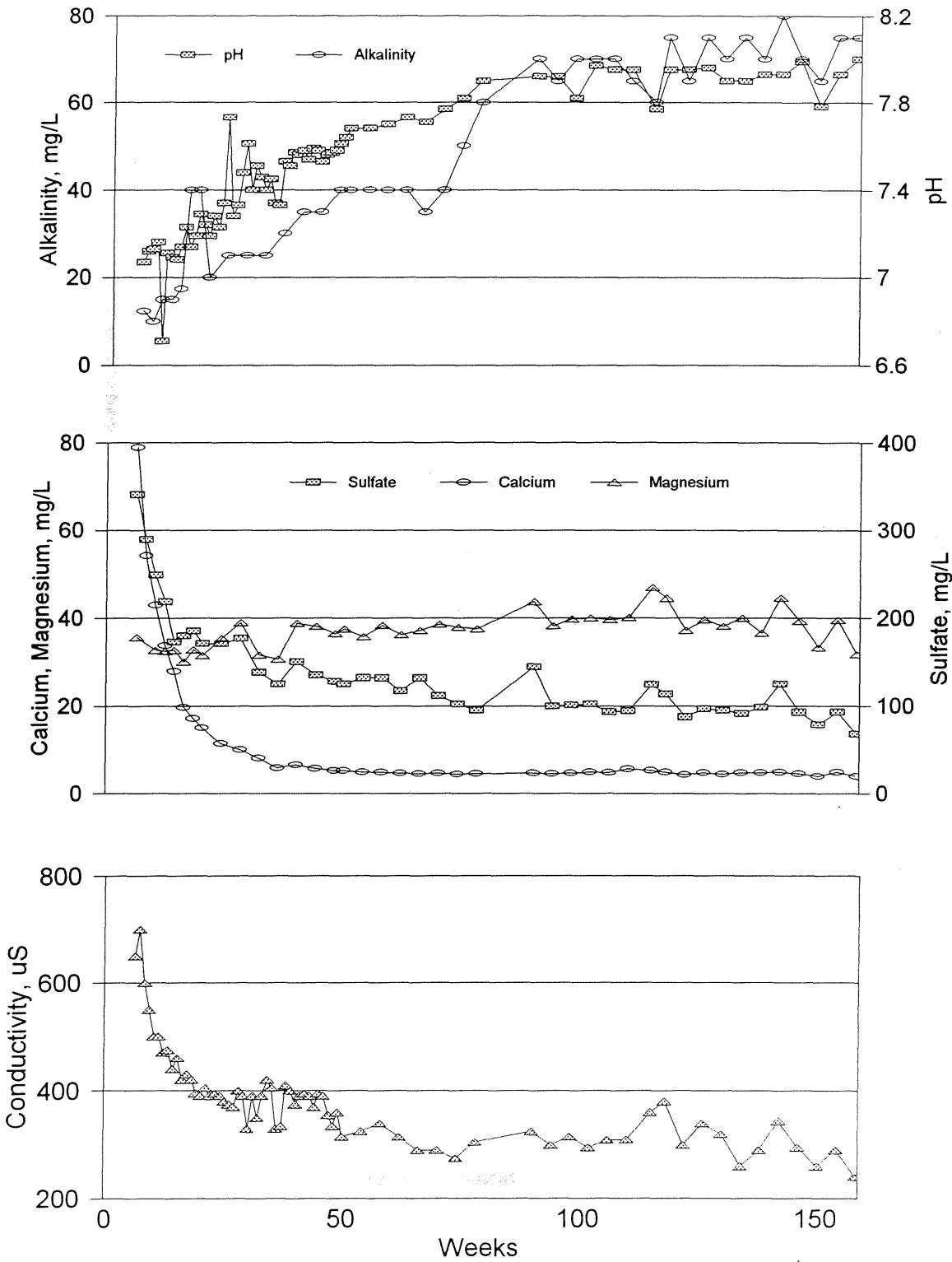


Figure 18. Drainage quality from 12.99% sulfide USGS sample (13.70% ST, 13.70% CO₂, cell n-3), for weeks 5-158. Weeks 0-5 were eliminated to improve subsequent resolution. Method changed from ASTM to MN DNR after week 80.

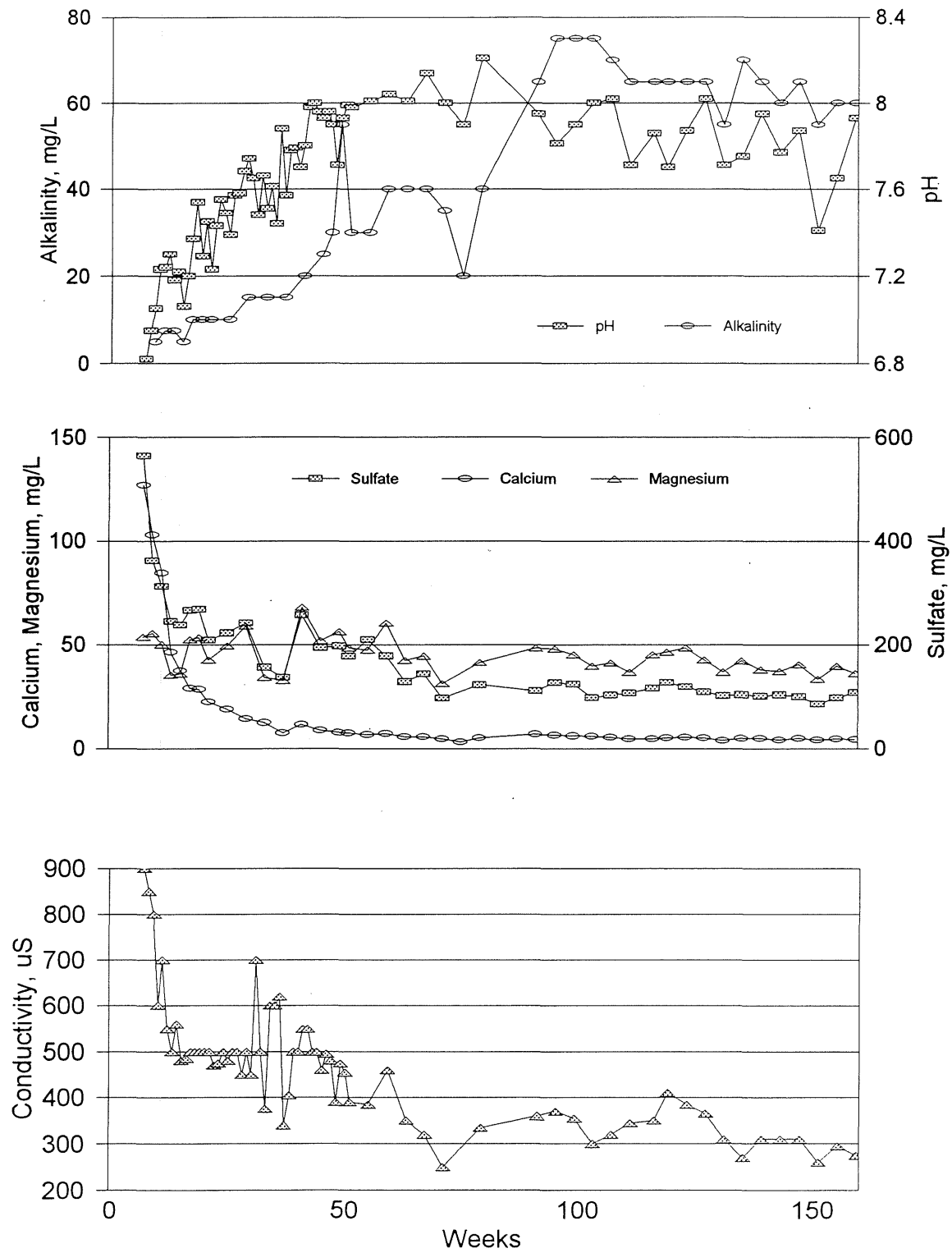


Figure 19. Observed sulfate release rate ($\text{mmol SO}_4 (\text{kg rock})^{-1} \text{ week}^{-1}$) vs. Solid-phase percent sulfur.
 Release rates for weeks 72-102 (terminated cells), 72-168, and 62-158 (USGS).
 Regression conducted for sulfate release vs. solid-phase sulfur for 7 samples (6.5, 6.75, 7.05, 8.1, 1.31, 1.37, 3.9 % S_T).
 Averages were used for replicate percent sulfur samples.

